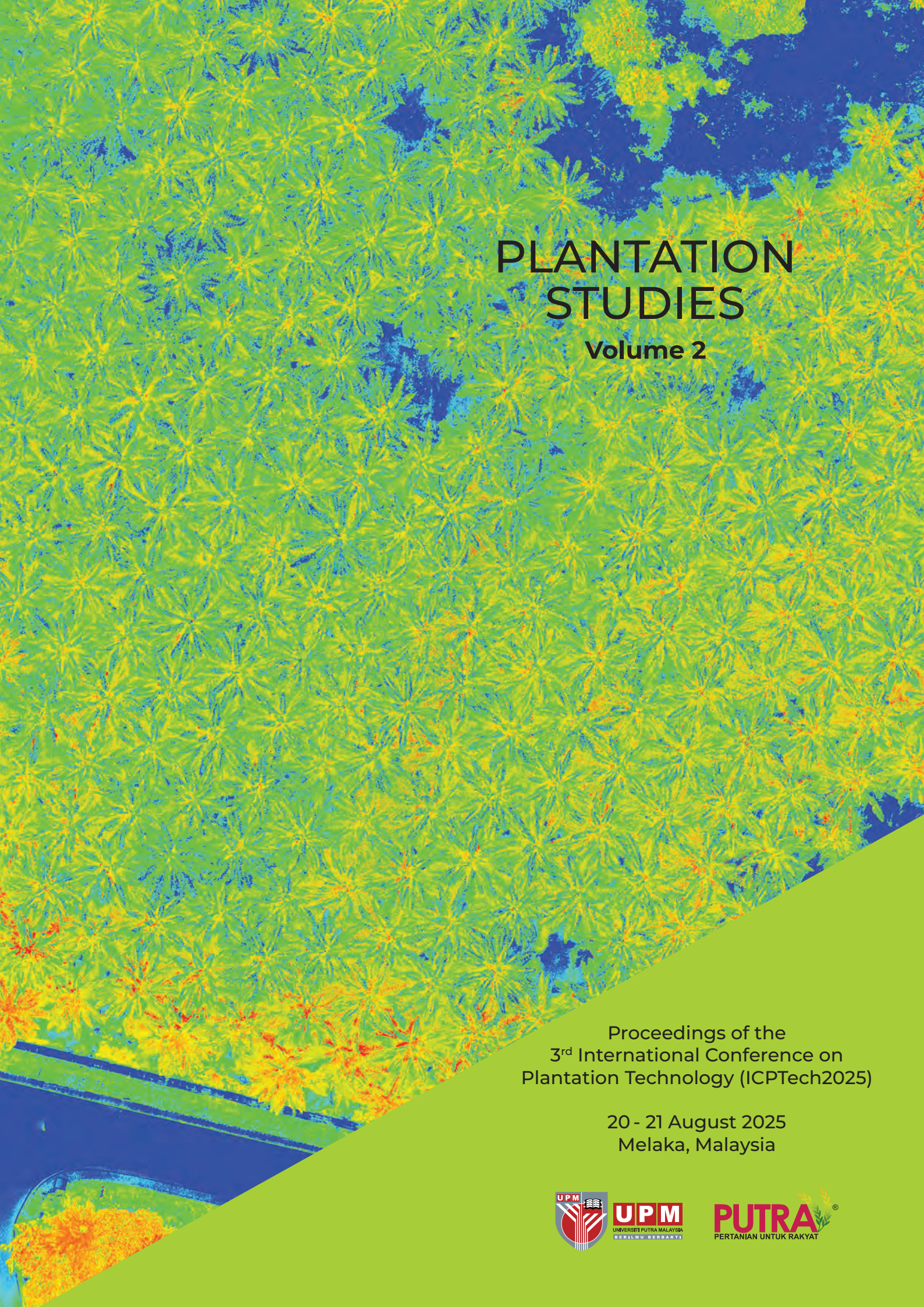

PLANTATION STUDIES

Volume 2

Proceedings of the
3rd International Conference on
Plantation Technology (ICPTech2025)

20 - 21 August 2025
Melaka, Malaysia

UPM
UNIVERSITI PUTRA MALAYSIA
BERILMU BERBAKTI

PUTRA
PERTANIAN UNTUK RAKYAT

PLANTATION STUDIES
Volume 2

Proceedings of the
3rd International Conference on Plantation Technology
(ICPTech2025)

20-21 August 2025
Melaka, Malaysia

Published by
Institut Kajian Perladangan (IKP)
Universiti Putra Malaysia
43400 UPM Serdang
Selangor Darul Ehsan

First Print 2025.

9 786299 525318

EDITORIAL BOARD

PREFACE

Welcome to the second volume of Plantation Studies. This volume, Plantation Studies Vol. 2, 2025—Proceedings of the 3rd International Conference on Plantation Technology (ICPTech2025), presents selected papers from ICPTech2025, a biennial plantation conference that brings together the latest advancements in research, innovation, and knowledge from scholars and industry practitioners in the plantation sector. ICPTech2025 serves as a dynamic platform for researchers and industry players to showcase research outcomes, exchange ideas, and share appropriate technologies that will shape the future of plantation industries.

Plantation Studies is published by the Institute of Plantation Studies (Institut Kajian Perladangan (IKP)) at Universiti Putra Malaysia, which continues to be at the forefront of agricultural research and development. Through this volume, we reinforce our commitment to providing a platform for the dissemination of knowledge that can influence policy, inform best practices, and inspire future research in plantation science and technology.

With the theme "Resilience in Industrial Crop Production through Climate-Friendly Production Systems", the 3rd ICPTech2025 and this volume focus on modern agricultural approaches that are critical for sustaining and strengthening plantation industries in an era of climate uncertainty. The contributions gathered here highlight advances in agronomy and crop protection, biotechnology, mechanization and automation, digital and smart farming technologies, bio-based products and bioenergy, as well as environmental and bioeconomy-related policies. Collectively, they explore resilient agricultural practices, efficient resource management, climate-friendly production systems, circular bioeconomy strategies, and data-informed decision-making to enhance the sustainability, productivity, and resilience of industrial crop production.

The research presented in this volume underscores the importance of integrating technological innovation with sustainable management practices and supportive policy frameworks. The findings highlight how climate-friendly production systems and circular bioeconomy approaches can enhance the resilience of plantation crops while addressing environmental, social, and governance considerations. By bridging the perspectives of scientists, engineers, policymakers, and industry practitioners, this volume offers a comprehensive overview of current challenges and forward-looking solutions in resilient and sustainable industrial crop production.

The editorial team has worked diligently to ensure a rigorous peer-review process, upholding high academic standards for all accepted contributions. We extend our sincere appreciation to the authors for their valuable work, and to the reviewers and members of the scientific and organizing committees for their thoughtful evaluations and dedication to the success of ICPTech2025.

As we continue this journey with the second volume of Plantation Studies, we invite readers to engage deeply with the research presented here. It is our hope that the insights, methods, and innovations documented in this volume will not only advance academic knowledge but also foster stronger collaboration between academia and industry toward more resilient, sustainable, and climate-friendly plantation systems.

TABLE OF CONTENTS

True Matag Coconut Seedlings Variety Identification Using RGB Images and YOLOv11 Model

N.A.M. Nordin[1], N.N. Che'Ya[2], S.D. Chen[3], N. Man[4] and M. Jahari[5]

[1]Institute of Plantation Studies, University Putra Malaysia, Malaysia
[2]Department of Agricultural Technology, Faculty of Agriculture, University Putra Malaysia
[3]Universiti Tenaga Nasional, Malaysia
[4]Faculty of Agriculture, University Putra Malaysia, Malaysia
[5]Faculty of Engineering, University Putra Malaysia, Malaysia
*Corresponding author: niknorasma@upm.edu.my

***Keywords**: Coconut, crop variety, identification, RGB, computer vision*

INTRODUCTION

Coconut (*Cocos nucifera L.*) is a member of the *Arecaceae* family, which was once called the *Palmaceae*. In Malaysia, coconut is the fourth most productive crop grown after oil palm and rubber [1]. MATAG coconut is a hybrid that has high yields and high market demand, as it was produced by crossing the Malayan Yellow Dwarf (MYD) and Tagnanan Tall (TNG) [2]. Unfortunately, coconut farmers still find it challenging to verify the authenticity of MATAG seedling progeny and are currently using only visual color analysis. Molecular markers provide accurate varietal identification, but it is costly, invasive, and impractical for use on a large scale in most nurseries [3]. Therefore, there is an increasing need for fast, non-invasive, and reliable methods to identify and distinguish seed varieties, including MATAG coconut seedlings.

By contrast, other agricultural products such as grains, rice, corn, maize, and sugarcane have used image-based deep learning analysis techniques successfully for accurate early varietal identification [4]-[10]. Yet, no prior work has applied such techniques to identify early nursery-stage coconut seedlings. Therefore, this study explores a fast, non-invasive YOLOv11 approach using RGB images to identify MATAG from non-MATAG seedlings, providing a cost-effective means for quality assurance in coconut nurseries.

MATERIALS AND METHODS

The study was located at Lekir Agriculture Centre, Perak performed testing with four-to-five-month-old coconut seedlings in the nursery stage. Four commercial varieties used in the study such as MATAG Gold, MATAG Green, Malayan Yellow Dwarf (MYD), and Malayan Red Dwarf (MRD). The RGB images of each seedling were captured indoors with controlled lights to avoid inconsistencies and enable easy identification of individuals across different seedlings while reducing background variation (Figure 1).

To evaluate the effect of image processing on model performance, three dataset versions were developed with different preprocessing techniques, including resizing, auto-orientation, contrast enhancement, and data augmentation (rotation, shear, exposure adjustment) to increase dataset variability and reduce overfitting.

Seedlings were manually annotated with bounding boxes and varietal labels. The dataset was then divided into approximately 80/20 training-validation/testing ratio. YOLOv11 was trained and evaluated using Roboflow to perform object detection and classification for over 300 epochs, and evaluated using mAP@50, precision, and recall. Model outputs were compared across datasets to analyze generalization ability.

(a) (b)

Figure 1. Image acquisition. (a) First data collection and (b) second data collection.

RESULTS AND DISCUSSSIONS

The YOLOv11 model identified MATAG and non-MATAG coconut seedlings based on the model's performance across the three dataset versions. Table 1 shows the performance evaluation for all datasets. All three datasets produced good results, but Dataset 3 produced the best results with an mAP@50 of 98.1%, precision of 91.7%, and recall of 97.1%. The other two datasets (Dataset 1 and Dataset 2) produced lower performance than Dataset 3 across most performance metrics, by around 3%–8%. The results show that training on augmented images with well-balanced samples improved the ability of the models to detect subtle color differences in the plant stems between hybrids and their parent species.

Table 1. Performance evaluation for all datasets

Dataset	mAP@50	Precision	Recall
1	95.40%	90.30%	88.00%
2	90.20%	80.80%	93.10%
3	98.10%	91.70%	97.10%

However, the evaluation showed generalization challenges, particularly for minority classes. For example, test performance of the MRD class dropped dramatically from 100% during validation to 48% during testing which indicates an issue of class imbalance and overfitting to specific

conditions within the controlled image used for training. These results also indicate that there are certain varieties of MATAG Gold that have insufficient diverse representation within the training data set and require more diverse representation of MATAG Gold seedlings for reliable detection of those varieties.

There are three major limitations must be addressed before operational deployment: (1) seasonal bias (data was collected only through November-December), which limits the environmental variability; (2) class imbalance (the lack of representative samples for MRD and MATAG Gold causes the learning model to be biased toward dominant classes); and (3) performance drop in real-world conditions (influenced by inconsistent lighting conditions, leaf occlusion, and angle variance). Future work will aim to expand training data across seasons, better balance class representation with sampling strategies, explore weight loss function methods, and investigate the use of domain adaptation to improve robustness against variability under field conditions.

CONCLUSIONS

The study demonstrates that, with a carefully selected RGB dataset and appropriate preprocessing techniques, YOLOv11 can effectively distinguish between MATAG and non-MATAG coconut seedlings, supporting quality control at the nursery level. This approach provides a rapid and reliable method for enhancing quality control standard for nurseries involved in coconut cultivation, contributing to the modernization of the coconut industry in Malaysia.

ACKNOWLEDGEMENT

The authors gratefully acknowledge Lekir Agriculture Centre and Universiti Putra Malaysia for their support. This work was supported by the Ministry of Higher Education Malaysia through the LRGS project (LRGS/1/2020/UPM/01/2).

REFERENCES

[1] Mohd, H., Zakaria, M., Zaffrie, M., Amin, M., Faireal, A., Syafiq, M., Dani, A., & Ahmad, M. (2022). Market potential and competitiveness assessment of Malaysian coconut-based products (Potensi pasaran dan penilaian daya saing produk berasaskan kelapa di Malaysia). *Economic and Technology Management Review*, *18*, 11–22. http://etmr.mardi.gov.my/Content/ETMR%20Vol.18(2022)/2.%20ETMR%20Vol.%2018%20Hafizudin.pdf

[2] Raj, D. M., Perumal, K., Balakrishnan, K., & Subramaniam, S. (2024). Revitalizing *Cocos nucifera* L. var. Matag: Unravelling new horizons in clonal propagation through organogenesis and LED illumination. *Plant Cell, Tissue and Organ Culture (PCTOC), 158*(2). https://doi.org/10.1007/s11240-024-02834-1

[3] Che'Ya, N. N., Mohidem, N. A., Tarmidi, Z., Sarifudin, M. S. A., & Shah, J. A. (2022). Mobile application devices for MATAG coconut variety detection based on spectral signature analysis: A

review. *IOP Conference Series: Earth and Environmental Science, 1064*(1), 012039. https://doi.org/10.1088/1755-1315/1064/1/012039

[4] Begum, M., Kiruthiga, S., Subhashree, B., Sathya, N., & Sarojini, B. (2024). Cereal crop variety classification using deep learning. *International Journal of Multidisciplinary Research Transactions, 5*(6), 2663–2381. https://doi.org/10.5281/zenodo.11180999

[5] Sharma, K., Sethi, G. K., & Bawa, R. K. (2024). A comparative analysis of deep learning and deep transfer learning approaches for identification of rice varieties. *Multimedia Tools and Applications*. https://doi.org/10.1007/s11042-024-19126-7

[6] A wheat grain variety recognition based on deep learning. (2024). In *2024 11th International Conference on Electrical Engineering* (pp. 454–457). https://doi.org/10.1109/eecsi63442.2024.10776197

[7] Sable, A., Singh, P., Kaur, A., Driss, M., & Boulila, W. (2024). Quantifying soybean defects: A computational approach to seed classification using deep learning techniques. *Agronomy, 14*(6), 1098. https://doi.org/10.3390/agronomy14061098

[8] Cao, Y., Luo, H., Ye, R., Li, L., Wu, Z., Tian, D., & Song, S. (2025). Img2variety: Image-based intraspecific varieties identification using spatiotemporal mixed augmentation and transfer learning. *SSRN*. https://doi.org/10.2139/ssrn.5223227

[9] Bi, C., Bi, X., Liu, J., Chen, H., Wang, M., Yu, H., & Song, S. (2024). Identification of maize kernel varieties using LF-NMR combined with image data: An explainable approach based on machine learning. *Plants, 14*(1), 37. https://doi.org/10.3390/plants14010037

[10] Veerasakulwat, S., Sitorus, A., & Udompetaikul, V. (2024). Rapid classification of sugarcane nodes and internodes using near-infrared spectroscopy and machine learning techniques. *Sensors, 24*(22), 7102. https://doi.org/10.3390/s24227102

Soil Microbial Communities in Oil Palm-Based Agroforestry Systems

W.Y. Yeong[1], N.A.J. Jagananthan[1], M.F. Sulaiman[1], A.M. Amin[1], K.B. Mahmud[1], R. Robert[2] and A. Rival[3]

[1]Department of Land Management, Faculty of Agriculture, Universiti Putra Malaysia, Malaysia
[2]Phytochemistry Lab, Sabah Forestry Department, Malaysia
[3]The French Agricultural Research Centre for International Development, CIRAD, Montpellier, France
*Corresponding author: muhdfirdaus@upm.edu.my

***Keywords**: Oil palm agroforestry, soil microbial diversity*

INTRODUCTION

In Malaysia, oil palm is predominantly cultivated in large-scale, uniform monocultures. In other regions, alternative management strategies such as oil palm agroforestry are increasingly used, particularly among smallholders to improve farmer's income and mitigate ecological degradation [1].

Agroforestry systems can enhance biodiversity in monocultural systems and modify below ground environments, influencing soil microbial community composition through edaphic factors [2]. In contrast, conventional monoculture plantations often rely heavily on inorganic fertilizers, causing soil acidification [3]. These edaphic changes can create distinct environmental niches across the soil horizons, which dictates the assembly of soil microbial communities [4].

Many oil palm plantations encapsulate rivers and natural streams. In recent years, the restoration of ecologically sensitive areas like riparian zones within agricultural landscapes has been prioritized to reintroduce ecosystem biodiversity [5]. The provision of different carbon substrates from litter fall and root exudates from more diverse tree species can create habitats which favor distinct microbial communities of different life history strategies [6]. More importantly, richness in soil biodiversity is an ecosystem indicator for climate resilience [7].

Currently, there is limited understanding of how soil microbial communities differ among monoculture, agroforestry and reforested riparian within oil palm landscapes. In this study, land use enabled us to differentiate cultivated from non-cultivated landscapes. The cultivated landscapes consist of monoculture and oil palm agroforestry, while the non-cultivated landscape was represented by the riparian zone.

Due to the significance of soil microbial roles in enhancing long term agricultural sustainability, the objective of this study is to decipher the differences in soil microbial compositions between the cultivated site and the non-cultivated site. This study hypothesizes that (1) microbial diversity and richness will be higher in the non-cultivated site, with oil palm agroforestry showing intermediary traits, and (2) variations in soil microbial community structure will be driven by soil properties such as soil nutrient content and soil pH.

MATERIALS AND METHODS

Study site

At Melangking Oil Palm Plantation (MOPP) in Kinabatangan, Sabah, 38 hectares of second-generation oil palms were set aside for the present oil palm agroforestry research and development [8]. Oil palms and native forest trees at the trial site were planted in 2022. The area is relatively flat, with a gentle slope (~ 8 m) towards the riparian site. The distance from the riparian zone to the trial site ranges from 600 meters to 1 kilometer (Figure 1). The right side of Figure 1 illustrates the aerial view of the trial site. Monoculture and agroforestry plots were established in blocks separated by trenches approximately 1.5 m deep and 1.5 m wide. Each block consists of two rows of trees.

For the monoculture, oil palm trees were planted in a standard triangular spacing with 9 m between each palm (Figure 2). In the agroforestry blocks, two native trees (*Nauclea subdita*) were planted between the oil palm trees, resulting in 3 meters between trees. The monoculture and agroforestry plots were arranged in a random format. Each design has five replicates. Adjacent to the trial site is a riparian buffer zone which was afforested by a local NGO [9] (Figure 1). A total of 10,000 trees, belonging to 12 native tree species were planted along a 7.69 ha riparian zone with old unproductive oil palm trees, creating a diverse and dense canopy (1443 trees/ ha). The native trees (3 - 5 m) are significantly shorter than the unproductive oil palm trees in the riparian zone. In comparison, the monoculture (143 palms/ ha) and agroforestry (1283 trees/ ha) plots at trial sites are less diverse and less dense, with palms and trees growing at a similar average height. The riparian zone was formerly used for timber harvesting and subsequently for oil palm cultivation before being reforested in 2020.

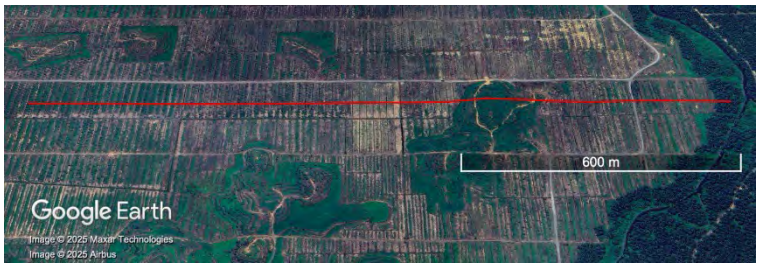

Figure 1. A red transect line is drawn across the TRAILS agroforestry trial site, showing its position relative to the riparian buffer zone, which is located on the far right (shown in darker green)

At the time of sampling, the 4-year-old oil palm trees in the cultivated zone ranged from 3-4 m. In the riparian zone, the unproductive oil palm trees were older than 25 years old, and ranged from 10 to 15 m.

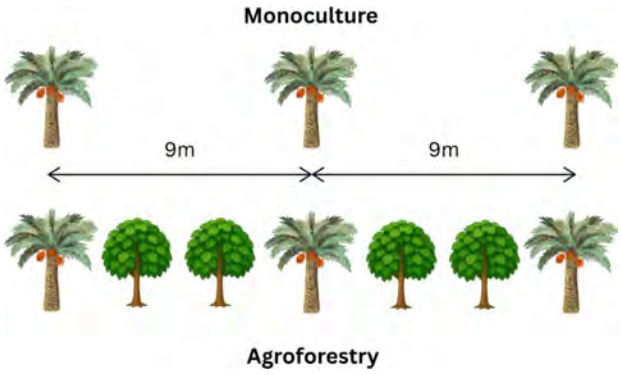

Figure 2. In monoculture plots, oil palm trees were planted in the 9m by 9m standard triangular spacing. In agroforestry, two native trees (*Nauclea subdita*) were planted in between oil palm trees

Soil sampling

Soil was collected in August 2025, no rainfall occurred throughout the duration of field sampling. At every sampling location, one soil composite was prepared from three soil cores taken using an auger [10]. For each location, samples were taken at two different depths: 0 to 15 cm, and 15 to 30 cm. For each landscape, i.e., agroforestry, monoculture and riparian, five replicates were sampled from five randomly assigned blocks. Soil was sampled between the trees, within the tree crown where foot traffic is minimal. The soil samples were split into two batches, one batch for the study of soil physicochemical property and a second one for soil DNA extraction. The samples for soil test were air dried then sieved through a 2 mm mesh. The samples for soil DNA extraction were temporarily stored in an iced cooler after field sampling, then transferred into a fridge at the camp base, and later stored in an - 80 °C freezer at the lab [11]. The process from field sampling to storage in the Sabah Forestry Department lab at Sepilok took four days.

Soil chemical properties

Total carbon was determined using the CN928 Dumas analyzer (Leco, USA) after combustion at 1,100°C. Total phosphorus (P) and potassium (K) were determined using microwave-assisted digestion on a Multiwave 5000 microwave digester (Anton-Paar, Austria). The acid mixture comprised HNO3 and HF as per US EPA method 3052. Total elements in the digestate were determined by atomic emission spectrometry on a SpectroArcos FHM22 spectrometer (Spectro Analytical Instruments, Germany). Active acidity (pH) was prepared in water suspension (soil to water ratio 1:2.5; Anderson & Ingram, 1993) that was shaken overnight. The pH was determined on SI Analytical Lab 845 pH Meter with pH-Elektrode BlueLine 29 (Xylem, USA).

16s rRNA amplicon sequencing

Soil DNA samples were extracted using the Zymobiomics DNA/RNA Miniprep Kit. Agarose gel electrophoresis was used to evaluate the integrity of the total soil DNA, spectrometric assay was used for purity (A260/A280) on the NanoDrop One Microvolum UV-Vis spectrophotometer (Scientific, MA, USA) and fluorometric assay using the Qubit High Sensitivity dsDNA Quantization kit on a Qubit 2.0 Fluorometer (Thermo Fisher Scientific) to quantify the amount of DNA. The concentration of soil DNA was normalized to 20 ng/uL. Two 50 uL aliquots were prepared for targeted-amplicon sequencing and shotgun metagenome, each containing around 1000 ng of DNA. The DNA samples were sent to a dedicated laboratory (Patriot Biotech Sdn. Bhd.) for sequencing analyses. The 16S rRNA V4-V5 hypervariables regions was amplified from gDNA using the primer pair 515F GT-GYCAGCMGCCGCGGTAA and 926R CCGYCAATTYMTTTRAGTTT [12].

RESULTS AND DISCUSSION

Soil chemical properties

Cultivated and non-cultivated sites exhibited significantly different soil chemical properties, reflecting their distinct management history (Table 1).

Table 1. Soil parameters of different land use. ANOVA was used for soil pH, Kruskal-wallis was used for soil nutrient tests

Soil test	AFS	Mono	Riparian	p	FDR
pH	4.15	4.46 **	4.8***	< 0.001	< 0.001
Total P (%)	0.035	0.038	0.018***	0.001	0.007
Av. P (mg/ kg)	4.429	8.169	1.62**	0.004	0.013
Total K (%)	0.965	1.009	0.792**	0.003	0.013
Total N (%)	0.14	0.17	0.09**	0.021	0.046

Note: AFS = agroforestry; Mono = Monoculture; Riparian = Riparian zone

The cultivated landscapes (both monoculture and agroforestry) showed a significantly lower soil pH and higher concentrations of total nitrogen, total phosphorus, available phosphorus, and total potassium compared to the reforested riparian zone ($p < 0.05$), likely due to the application of inorganic fertilizer at the cultivated sites. In contrast, the legacy effect of fertilizer use on the riparian zone was subtle, despite research showing lasting effects for years [13].

Linking soil chemistry to overall community structure

To determine the relationship between edaphic properties and soil bacterial communities, distance-based redundancy analysis (dbRDA) was performed. This analysis showed a clear separation of microbial communities based on land use (Figure 5). The microbial communities originating from the monoculture and agroforestry sites were more strongly influenced by soil nutrient levels (N, P, K). This preliminary result suggested that management-induced shifts in soil chemistry were the

primary drivers of bacterial community assembly in this landscape. In contrast, soil pH was more strongly correlated with the microbial phyla of riparian zone.

At the cultivated sites, higher soil nutrient levels may have resulted in the assembly of copiotrophic taxa [14] and thus explains the positive correlation of bacterial communities in the cultivated zone with soil nutrient levels. However, the strong correlation of soil pH with riparian microbial phyla may be due to the lack of environmental filtering from soil nutrients. Although the soil pH of riparian is significantly less acidic than the cultivated zone, it is still considered acidic. Hence, we can still assume acidophilic behavior, but the lack of nutrients creates an oligotrophic environment which favors slow growing phenotype. The effect of inorganic soil amendments has been found to be more important than soil pH in influencing microbial assembly [15], especially in acidic soil [16].

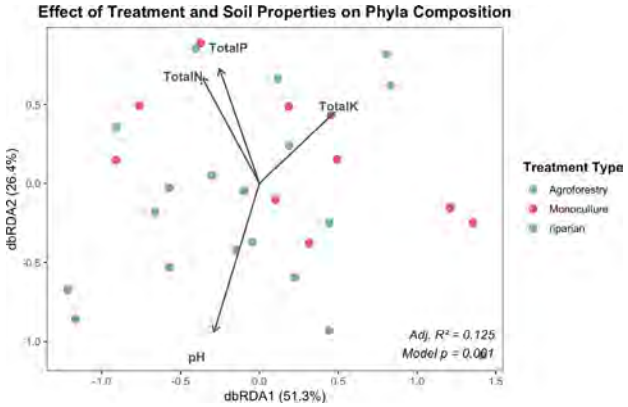

Figure 5. Distance-based redundancy analysis (dbRDA) plot showed the relationship of soil bacterial communities with soil pH, total nitrogen, total phosphorus, total potassium for agroforestry, monoculture and riparian land use. Only variables with VIF < 2 and $p < 0.05$ were plotted. The length of the lines indicated the strength of correlation between the treatment type and the soil properties

LefSe biomarker analysis

At a finer taxonomic resolution, LefSe analysis (Figure 6) revealed an apparent increase in unique bacterial biomarkers corresponding with vegetation complexity. The riparian zone hosted the highest number of biomarkers (27 genera), followed by agroforestry (7 genera), with only one single biomarker genus identified in the monoculture. This trend indicates that as aboveground plant diversity increases, so does the diversity of distinct microbial niches, likely driven by a greater variety of root exudates and litter inputs. Previous studies have suggested that aboveground heterogeneity and fertilizer inputs can significantly alter metaphonome which significantly changes the fate of microbial survival [17].

Given the minuscule scale of bacterial cells relative to the environment, small changes in soil conditions can significantly influence the metabolic functions of soil microbial communities [18]. Hence, changes in soil properties may also result in the growth or suppression of certain

communities. In the riparian zone, the association of diverse tree species has likely created distinct microhabitats, favoring the accumulation of more unique genera.

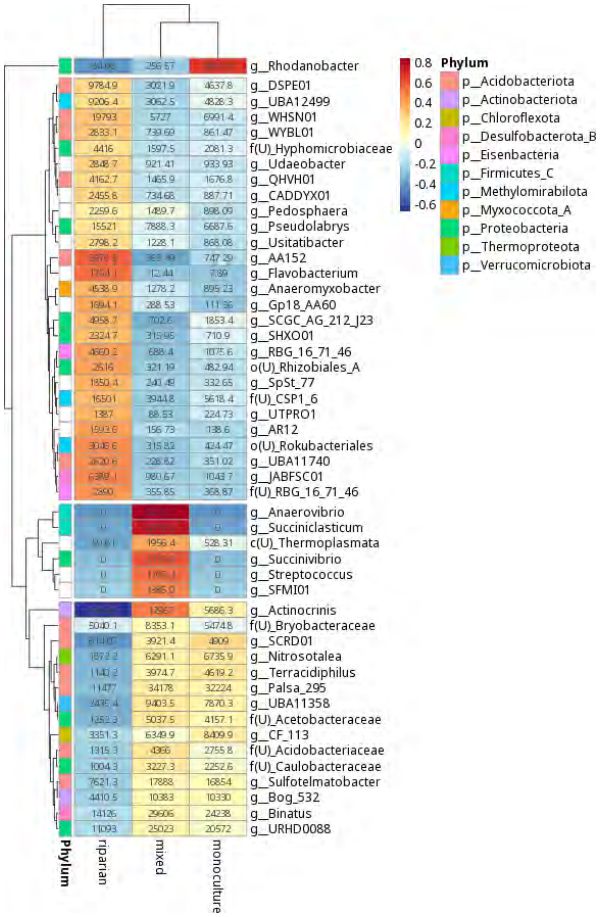

Figure 6. LefSe biomarker analyses for top 50 genera. (LDA 2.81 - 4.06, FDR: $p < 0.05$)

Moreover, the genera *Anaerobivrio*, *Succiniclasticum*, *Succinivibro*, *Streptococcus* and SFMI01 which were not found in monoculture and riparian suggest that the introduction of just one other tree species (*Nauclea subdita*) was sufficient to create conditions for specific microbial associations. In comparison to riparian, the addition of fertilizer in the topsoil of the cultivated zone might have induced filtering effects which reduced the survivability of rare and common taxa [19]. Consistent with [20], results suggest that high nutrient inputs in the cultivated zone imposed strong deterministic selection. Although the acidic conditions theoretically favor acidophilic oligotrophs, the intense competition from copiotrophs fueled by nutrient loading has likely masked the effect of soil pH in soil microbial community assembly.

Relative abundance of soil bacterial communities

In contrast to the clear distinctions observed in soil chemistry and biomarker taxa, the relative abundances of the dominant bacterial phyla did not differ significantly across the three land uses at either soil depth ($p > 0.05$, Figure 7). The communities in all samples were dominated by

Acidobacteriota, *Proteobacteria*, *Actinobacteriota*, and *Chloroflexota*, which collectively comprised 72-84% of the community, consistent with the findings of [21]. This highlights the occurrence of major ecological shifts occurring at a finer taxonomic scale (genus-level).

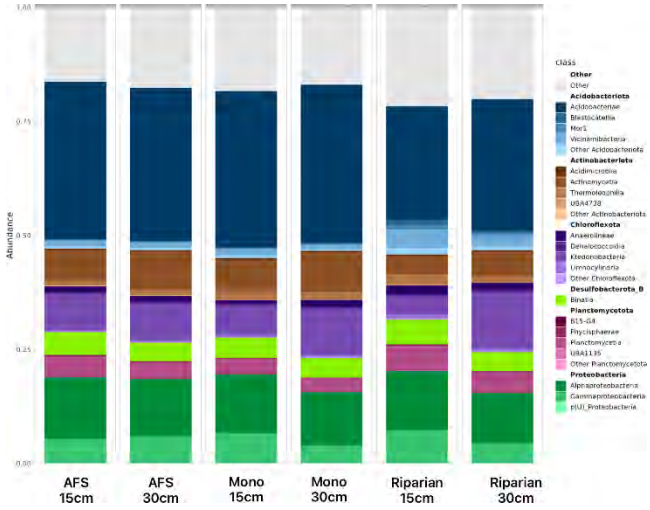

Figure 7. The relative abundance of agroforestry (AFS), monoculture (Mono), and riparian (Riparian) zones at two depths, 0 to 15 cm, and 15 to 30 cm

These results are reflective of the juvenile period of oil palm plantation, where deterministic selection is still ongoing and does not reflect the ultimate state of the full cycle of oil palm land use [22].

CONCLUSIONS

The number of unique taxa increased with increased plant diversity, as shown in the riparian and agroforestry zones, despite no differences in relative abundance between the different sites. Moreover, the results demonstrated a strong correlation between soil pH and soil nutrient contents with the soil microbial composition, which could be driven using inorganic fertilizer. Given that soils of mature oil palm plantations will experience prolonged nutrient amendment and increased shading, along with increased soil compaction which alters soil hydrology, future work should include the significance of other soil physical factors such as bulk density and soil hydraulic conductivity. Overall, this study provides the baseline results into the potential of oil palm agroforestry as an alternative land use management.

ACKNOWLEDGEMENTS

We would like to thank the TRAILS project (https:// www.trails-project.org/)for the financial support of this research work. The Melangking Oil Palm Plantation (MOPP) is gratefully thanked for providing access and maintenance to the research site. We are also grateful to the Sabah Forestry Department for providing lab access and expertise in soil analyses.

REFERENCES

[1] Susanti, A., Marhaento, H., Permadi, D. B., Hermudananto, Budiadi, Imron, M. A., et al. (2020). Smallholder farmers' perception on oil palm agroforestry. *IOP Conference Series: Earth and Environmental Science, 449*(1), 012056.

[2] Fahad, S., Chavan, S. B., Chichaghare, A. R., Uthappa, A. R., Kumar, M., Kakade, V., et al. (2022). Agroforestry systems for soil health improvement and maintenance. *Sustainability, 14*(22), 14877.

[3] Hernández-Cáceres, D., Stokes, A., Angeles-Alvarez, G., Abadie, J., Anthelme, F., Bounous, M., et al. (2022). Vegetation creates microenvironments that influence soil microbial activity and functional diversity along an elevation gradient. *Soil Biology and Biochemistry, 165*, 108485.

[4] Kee, K. K., Goh, K. J., & Chew, P. S. (1995). Effects of NK fertiliser on soil pH and exchangeable K status on acid soils in an oil palm plantation in Malaysia. In *Proceedings of the Third International Symposium on Plant–Soil Interactions at Low pH, Brisbane, Queensland, Australia, 12–16 September 1993* (pp. 809–815). Springer Netherlands. https://doi.org/10.1007/978-94-011-0221-6_130

[5] Lind, L., Hasselquist, E. M., & Laudon, H. (2019). Towards ecologically functional riparian zones: A meta-analysis to develop guidelines for protecting ecosystem functions and biodiversity in agricultural landscapes. *Journal of Environmental Management, 249*, 109391.

[6] Cappelli, S. L., Domeignoz-Horta, L. A., Loaiza, V., & Laine, A.-L. (2022). Plant biodiversity promotes sustainable agriculture directly and via belowground effects. *Trends in Plant Science, 27*(7), 674–687.

[7] Vasiliev, D. (2022). The role of biodiversity in ecosystem resilience. *IOP Conference Series: Earth and Environmental Science, 1072*(1), 012012.

[8] Rival, A., Ancrenaz, M., Guizol, P., Lackman, I., Burhan, S., Zemp, C., et al. (2025). Innovative planting designs for oil palm-based agroforestry. *Agroforestry Systems, 99*(1), 27.

[9] HUTAN. (n.d.). *Our work.* Retrieved December 2025, from https://hutan.earth/our-work

[10] Carter, M. R., & Gregorich, E. G. (Eds.). (2007). *Soil sampling and methods of analysis*. CRC Press.

[11] Wallenius, K., Rita, H., Simpanen, S., Mikkonen, A., & Niemi, R. M. (2010). Sample storage for soil enzyme activity and bacterial community profiles. *Journal of Microbiological Methods, 81*(1), 48–55.

[12] Parada, A. E., Needham, D. M., & Fuhrman, J. A. (2016). Every base matters: Assessing small subunit rRNA primers for marine microbiomes with mock communities, time series and global field samples. *Environmental Microbiology, 18*(5), 1403–1414.

[13] Lei, S., Raza, S., Irshad, A., Jiang, Y., Elrys, A. S., Chen, Z., et al. (2025). Long-term legacy impacts of nitrogen fertilization on crop yield, nitrate accumulation, and nitrogen recovery efficiency. *European Journal of Agronomy, 164*, 127513.

[14] Lladó, S., & Baldrian, P. (2017). Community-level physiological profiling analyses show potential to identify the copiotrophic bacteria present in soil environments. *PLOS ONE, 12*(2), e0171638.

[15] Zhang, H., Jiang, N., Zhang, S., Zhu, X., Wang, H., Xiu, W., Zhao, J., Liu, H., Zhang, H., & Yang, D. (2024). Soil bacterial community composition is altered more by soil nutrient availability than pH following long-term nutrient addition in a temperate steppe. *Frontiers in Microbiology, 15*, 1455891.

[16] Mombrikotb, S. B., Van Agtmaal, M., Johnstone, E., Crawley, M. J., Gweon, H. S., Griffiths, R. I., & Bell, T. (2022). The interactions and hierarchical effects of long-term agricultural stressors on soil bacterial communities. *Environmental Microbiology Reports, 14*(5), 711–718.

[17] Fierer, N., Lauber, C. L., Ramirez, K. S., Zaneveld, J., Bradford, M. A., & Knight, R. (2012). Comparative metagenomic, phylogenetic and physiological analyses of soil microbial communities across nitrogen gradients. *The ISME Journal, 6*(5), 1007–1017.

[18] Tecon, R., & Or, D. (2017). Biophysical processes supporting the diversity of microbial life in soil. *FEMS Microbiology Reviews, 41*(5), 599–623.

[19] Coolon, J. D., Jones, K. L., Todd, T. C., Blair, J. M., & Herman, M. A. (2013). Long-term nitrogen amendment alters the diversity and assemblage of soil bacterial communities in tallgrass prairie. *PLOS ONE, 8*(6), e67884.

[20] Xun, W., Zhao, J., Xue, C., Zhang, G., Ran, W., Wang, B., Shen, Q., & Zhang, R. (2016). Significant alteration of soil bacterial communities and organic carbon decomposition by different long-term fertilization management conditions of extremely low-productivity arable soil in South China. *Environmental Microbiology, 18*(6), 1907–1917.

[21] Salamat, S. S., Hassan, M. A., Shirai, Y., Hanif, A. H., Norizan, M. S., Zainudin, M. M., Mustapha, N. A., Isa, M. M., & Bakar, M. A. (2021). Effect of inorganic fertilizer application on soil microbial diversity in an oil palm plantation. *BioResources, 16*(2), 2279–2302.

[22] Söllinger, A., Séneca, J., Borg Dahl, M., Motleleng, L. L., Prommer, J., Verbruggen, E., Sigurdsson, B. D., Janssens, I., Peñuelas, J., Urich, T., & Richter, A. (2022). Down-regulation of the bacterial protein biosynthesis machinery in response to weeks, years, and decades of soil warming. *Science Advances*, *8*(12), eabm3230.

Biogas Slurry-Driven Soil Enzyme Activity for Sustainable Agronomy

Xihuan Zhang[1,2], Ngai Paing Tan[2], Hao Yu[1] and Elina Zakharchenko[3]

[1]School of Plant Protection and Environment, Henan Institute of Science and Technology, Xinxiang, China
[2]Department of Land Management, Faculty of Agriculture, Universiti Putra Malaysia, Selangor, Malaysia
[3]Faculty of Agrotechnology and Environmental Management, Sumy National Agrarian University, Sumy, Ukraine
*Corresponding author: zhxyzxh@gmail.com

***Keywords**: Biogas slurry, enzymatic activity, sustainable sgronomy, soil*

INTRODUCTION

Sustainable agronomy aims to ensure crop yields while minimizing environmental impacts. Though chemical fertilizers are effective in boosting yields, their long-term excessive use has led to disruptions in the physical, chemical, and biological balance of the soil, resulting in the loss of organic matter, reduced microbial diversity, and increased risks of soil acidification and water eutrophication [1-3].

Against this backdrop, biogas slurry has gained attention as a promising eco-friendly alternative or supplementary resource to chemical fertilizers. Derived from the anaerobic digestion of organic materials such as livestock manure, crop straw, or food waste, biogas slurry is a nutrient-dense organic by-product that aligns with the circular economy principles of sustainable agriculture. Unlike chemical fertilizers, which typically provide only isolated macro-nutrients such as nitrogen (N), phosphorus (P), and potassium (K), biogas slurry offers a comprehensive nutrient profile which contains not only readily available N, P, and K but also abundant dissolved organic carbon (DOC), amino acids, vitamins, and micronutrients. These components work synergistically to nourish soil microbial communities, stimulating the proliferation of beneficial bacteria, fungi, and actinomycetes, and enhancing the synthesis and activity of soil enzymes, which are the "biocatalysts" of soil biochemical processes [4].

Soil enzymes are vital indicators of soil health and fertility because they catalyze key reactions involved in nutrient cycling and organic matter decomposition. Enzymes such as sucrase, urease, acid phosphatase, and catalase reflect the biological potential of soils to mineralize carbon, transform nitrogen, release phosphorus, and regulate oxidative stress, respectively [5]. Consequently, quantifying enzyme activities under different fertilization regimes provides an early

and sensitive assessment of how management practices affect soil quality and long-term productivity.

Incorporating biogas slurry into winter wheat fertilization strategies delivers multiple agronomic and environmental advantages: it allows farmers to reduce reliance on synthetic fertilizers, mitigate greenhouse gas emissions associated with urea production and denitrification, and realize on-farm recycling of agricultural wastes. Furthermore, enhanced soil enzyme activity plays a pivotal role in accelerating nutrient cycling, improving soil aggregate stability, and boosting soil organic carbon sequestration—collectively forming a positive feedback loop that strengthens crop yield resilience amid climate variability. To scale this sustainable practice across the North China Plain and other similar intensive cereal-growing regions worldwide, identifying the optimal biogas slurry substitution ratio is crucial, as this ratio must balance crop nitrogen demands with microbial carbon use efficiency. The findings of this work will help establish optimal substitution rates that maximize soil biological fertility while sustaining crop yields, thereby contributing to the sustainable development of agriculture.

MATERIALS AND METHODS

Experimental site

The field experiment was conducted in Shangshui County, Zhoukou City, Henan Province, China. The soil type is lime concretion black soil, typical of the North China Plain. The region has a temperate monsoon climate, with an annual average temperature of 15°C and precipitation of 785 mm, concentrated mainly in summer. Winter wheat is typically sown in early October and harvested in early June.

Experimental design

Four treatments were established with equal total nitrogen input (180 kg N/ha): CK (No fertilizer), CF (100% chemical fertilizer), BS50 (50% N from biogas slurry and 50% from chemical fertilizer), BS100 (100% N from biogas slurry). Each treatment was replicated three times in a randomized block design. Other management practices followed local wheat cultivation standards. Chemical fertilizer was applied in the form of urea, superphosphate, and potassium chloride. Biogas slurry was sourced from a local pig farm-based anaerobic digester. The slurry was applied uniformly to the soil surface before sowing and incorporated into the topsoil by shallow tillage.

Soil sampling and enzyme activity measurement

At the wheat harvesting stage, topsoil samples were collected from the 0-20 cm soil layer. Activities of sucrase, urease, acid phosphatase, and catalase were determined using standard methods. Urease activity was measured via Indophenol blue colorimetry, which is based on the coloured complex formed by urea hydrolysis products and indophenol blue. Sucrase activity was assayed by 3,5-dinitrosalicylic acid colorimetry, which detects the reducing sugars from sucrose decomposition via a reddish-brown complex. Acid phosphatase activity was determined through

Disodium phenyl phosphate colorimetry, which quantifies the phenol from substrate hydrolysis via a chromogenic reaction. Catalase activity was analyzed by Ultraviolet spectrophotometry, which monitors H_2O_2 decomposition by measuring the absorbance decrease at a UV wavelength. All assays were conducted in triplicate. Data were analyzed using Excel and SPSS, with one-way ANOVA to test for significant differences among treatments.

RESULTS

Sucrase activity

The core role of sucrase in soil is to catalyze the hydrolysis of sucrose in soil into glucose and fructose, converting disaccharides that are difficult for plants to directly utilize into absorbable monosaccharides, which provide key carbon sources and energy for plant growth and soil microbial metabolism. Sucrase activity is an important index to evaluate soil carbon cycle efficiency and biological activity. Higher activity usually means stronger soil organic carbon conversion capacity and higher fertility potential.

The sucrase activities of different treatments in this study are shown in Figure 1. BS50 exhibited the highest sucrase activity (8.53mg•g-1), which was statistically superior to all other groups, it exceeded BS100 by 9.1%, CF by 13.1%, and CK by 61.6%. This indicates that the BS50 treatment most effectively stimulated sucrase synthesis or activated its catalytic site. BS100 and CF showed no significant difference, suggesting that doubling the BS dose (from 50 to 100) did not enhance sucrase activity further, and its effect was comparable to that of CF. The CK had the lowest activity, confirming that both BS and CF can promote sucrase activity, with BS50 being the optimal choice. BS50 may have upregulated the expression of sucrase-encoding genes or provided cofactors (e.g., metal ions) that maximized enzyme activity; higher BS100 might have caused mild feedback inhibition, limiting activity improvement. CF may have supplied nutrients (e.g., nitrogen) to support microbial proliferation in a soil system, thereby increasing total sucrase production, but its effect was weaker than BS50 due to lack of specific enzyme-activating components.

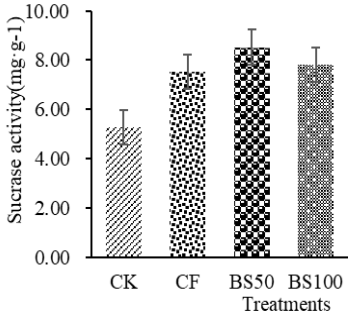

Figure 1: The sucrase activities of different treatments

Urease activity

Urease hydrolyzes urea into ammonia and carbon dioxide, which is the key process for converting organic nitrogen (urea) into inorganic nitrogen (NH_3/NH_4^+) that can be directly utilized by

organisms. As shown in Figure 2, BS50 also had the highest urease activity (219.3 ug•g-1), followed by CF, BS100, and CK. All treatments were significantly different from each other ($p<0.05$). BS50 outperformed CF by 7.3%, demonstrating that BS50 was more effective in promoting urease activity than CF. Notably, BS100 had lower activity than both BS50 and CF, and was only 12.2% higher than CK, indicating that high-dose BS may suppress urease synthesis. Urease-producing microbes may have optimal growth and enzyme secretion under BS50 concentration; excess BS could alter the microenvironment, inhibiting microbial metabolism and thus urease production. CF may provide a stable nitrogen source that sustains moderate urease activity but lacks the microbial-stimulating factors present in BS50, leading to lower activity than BS50.

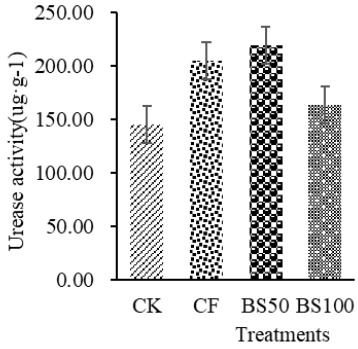

Figure 2: The urease activities of different treatments

Acid phosphatase activity

Acid phosphatase catalyzes the hydrolysis of organic phosphate esters into inorganic phosphate (PO_4^{3-}) under acidic conditions, which is essential for solving phosphorus limitation in acidic soils. The activity of acid phosphatase is shown in Figure 3.

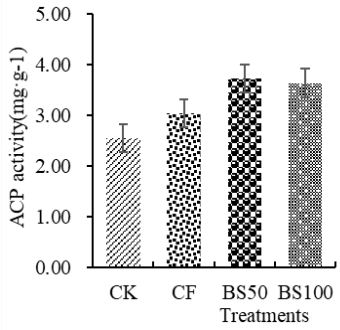

Figure 3: The acid phosphatase activities of different treatments

BS50 (3.73 mg•g^{-1}) and BS100 (3.64 mg•g^{-1}) had the highest activities, with no significant difference between them; they were 22.7%and 19.7% higher than CF, and 45.7% and 42.2% higher than CK. BS may have contained strains that secreted acid phosphatase or induced the expression of phosphatase genes in indigenous microbes; the similar activity of BS50 and BS100 suggests that

the inducing effect of BS reached saturation at BS50, and higher doses did not provide additional benefits. CF showed higher activity than CK but was significantly lower than both BS groups, indicating that BS is a more potent inducer of acid phosphatase than CF.

Catalase activity

Catalase decomposes hydrogen peroxide (H_2O_2) into water and oxygen, which protects organisms from oxidative damage caused by reactive oxygen species (ROS), especially under stress conditions. So, catalase is an intracellular antioxidant; its activity mirrors the rate of intracellular H_2O_2 generation.

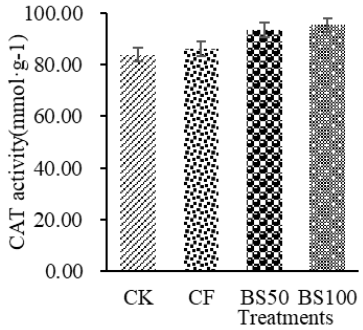

Figure 4: The catalase activities of different treatments

From Figure 4, BS100 and BS50 exhibited the highest activities, with values of 95.3 mmol•g^{-1} and 93.4 mmol•g^{-1} respectively, and there was no significant difference between them ($p>0.05$). Compared with CF, their activities increased by 10.7% and 8.4% respectively; relative to CK, the increases were 13.6% and 11.2% respectively. CF and CK showed no significant difference, indicating that CF has almost no effect on catalase activity, while BS effectively enhances it. BS may have triggered a mild stress response in organisms or supplied antioxidants that induced catalase synthesis to scavenge ROS; the similar activity of BS50 and BS100 suggests that both doses could sufficiently activate the oxidative defense system, with no dose-dependent enhancement. CF does not stimulate the production of ROS-scavenging enzymes, so its catalase activity is indistinguishable from the control group.

Cross-enzyme synergy and system-level efficiency

When the four enzymes were normalized to the CK baseline, BS50 showed the flattest “enzyme profile”, indicating balanced enhancement of C, N, P and redox processes. BS100, by contrast, presented a skewed pattern where C-acquiring and antioxidant enzymes were high, but N-cycling (urease) lagged, a signature of incipient nutrient imbalance. CF exhibited low overall elevation and CK remained uniformly low. Thus, 50 % substitution is the only treatment that simultaneously maximizes nutrient-cycle capacity while maintaining oxidative homeostasis, offering the best trade-off between biological fertility and environmental risk. Overall, the application of biogas slurry, especially in combination with chemical fertilizer (BS50), significantly enhanced most soil enzyme activities.

This was likely due to the input of organic matter and nutrients, which effectively stimulated the activity of microbial communities and promoted enzyme synthesis. Among these enzymes, sucrase and urease, which are involved in carbon and nitrogen cycling, respectively, showed the most significant increases under BS50 treatment, a result that indicates this treatment could substantially improve soil nutrient availability and boost microbial activity.

DISCUSSIONS

In the soil nutrient cycling process, soil enzymes, which are mainly produced by plants, animal, and microbial cells, serve a pivotal role [6]. The observed increases in enzyme activity under BS50 can be attributed to the input of labile organic carbon and micronutrients, which stimulate microbial growth and enzyme synthesis. Biogas slurry contains dissolved organic matter that serves as both a substrate and microbial energy source, enhancing microbial biomass and activity [7]. The balanced nutrient profile in BS50 likely optimized the C:N:P ratio for microbial metabolism, whereas BS100 may have induced nutrient imbalances or mild osmotic stress, suppressing certain microbial functions. Our findings align with previous studies [8]. However, the optimal ratio of biogas slurry to chemical fertilizer application still needs to be discussed based on the specific situation of crops and experimental sites, because different crop varieties and soil conditions also have significant differences in the absorption of nutrients in biogas slurry [9]. Our study uniquely highlights the biological optimum at 50% substitution in a winter wheat monoculture on lime concretion black soil, providing region-specific guidance.

The 50 % rate represents a true “biological optimum” that aligns microbial function with crop nitrogen demand. The BS50 strategy supports China’s “Zero Growth of Chemical Fertilizer Use by 2030” policy. It offers a practical pathway for farmers to reduce fertilizer input without sacrificing yield. Moreover, the use of biogas slurry supports rural waste management and reduces greenhouse gas emissions from both fertilizer production and manure discharge.

CONCLUSIONS

This study concludes that biogas slurry (BS) application significantly enhanced key soil enzyme activities in winter wheat relative to chemical fertilizer (CF) and control (CK) treatments, supporting its potential as a soil amendment to boost biological fertility. BS50 outperformed other treatments overall by comprehensively promoting soil carbon, nitrogen, phosphorus cycling and antioxidant capacity, while BS100 slightly excelled in catalase activity. BS50 is optimal for reducing chemical fertilizer reliance and improving soil health. Future research should explore long-term impacts, microbial dynamics and economic feasibility of BS application, with training and policies needed for scaling—providing scientific basis for its use in sustainable agriculture.

REFERENCES

[1] Xing, Y., Xie, Y., & Wang, X. (2025). Enhancing soil health through balanced fertilization: A pathway to sustainable agriculture and food security. *Frontiers in Microbiology, 16*, 1536524. https://doi.org/10.3389/fmicb.2025.1536524

[2] Pandian, K., Mustaffa, M. R. A. F., Mahalingam, G., Paramasivam, A., Prince, A. J., Gajendiren, M., & Varanasi, S. T. (2024). Synergistic conservation approaches for nurturing soil, food security and human health towards sustainable development goals. *Journal of Hazardous Materials Advances, 16*, 100479. https://doi.org/10.1016/j.hazadv.2024.100479

[3] Osorio-Reyes, J. G., Valenzuela-Amaro, H. M., Pizaña-Aranda, J. J. P., Ramírez-Gamboa, D., Meléndez-Sánchez, E. R., López-Arellanes, M. E., Castañeda-Antonio, M. D., Coronado-Apodaca, K. G., Gomes Araújo, R., Sosa-Hernández, J. E., Melchor-Martínez, E. M., Iqbal, H. M. N., Parra-Saldivar, R., & Martínez-Ruiz, M. (2023). Microalgae-based biotechnology as alternative biofertilizers for soil enhancement and carbon footprint reduction: Advantages and implications. *Marine Drugs, 21*(2), 93. https://doi.org/10.3390/md21020093

[4] Kumar, A., Verma, L. M., Sharma, S., & Singh, N. (2022). Overview on agricultural potentials of biogas slurry (BGS): Applications, challenges, and solutions. *Biomass Conversion and Biorefinery, 13*, 13729–13769. https://doi.org/10.1007/s13399-021-02215-0

[5] Wang, L., Hamel, C., Lu, P., Wang, J., Sun, D., Wang, Y., Lee, S.-J., & Gan, G. Y. (2023). Using enzyme activities as an indicator of soil fertility in grassland—An academic dilemma. *Frontiers in Plant Science, 14*, 1175946. https://doi.org/10.3389/fpls.2023.1175946

[6] Zhang, M., Cui, J., Mi, M., Jin, Z., Wong, M. H., Shan, S., & Ping, L. (2024). Persistent effects of swine manure biochar and biogas slurry application on soil nitrogen content and quality of lotus root. *Frontiers in Plant Science, 15*, 1359911. https://doi.org/10.3389/fpls.2024.1359911

[7] Mukhtiar, A., Mahmood, A., Zia, M. A., Ameen, M., Dong, R., Yang, S., Javaid, M. M., Khan, B. A., & Nadeem, M. A. (2024). Role of biogas slurry to reclaim soil properties providing an eco-friendly approach for crop productivity. *Bioresource Technology Reports, 25*, 101716. https://doi.org/10.1016/j.biteb.2023.101716

[8] Wu, J., Pan, X., Yang, Y., Gao, C., Wang, Y., & Li, M. (2020). Effects of biogas slurry utilization in long-term on soil nutrients and enzyme activities. *Current Investigations in Agriculture and Current Research, 8*(2), 1083–1090. https://doi.org/10.32474/CIACR.2020.08.000286

[9] Zhang, J., Meng, Q., Tang, Y., Zhu, J., Zhang, X., & Gao, L. (2025). Study on the response mechanism of biogas slurry and chemical fertilizer combination application on the physiological characteristics of summer maize leaves. *Archives of Agronomy and Soil Science, 71*(1), 1–15. https://doi.org/10.1080/03650340.2024.2429584

Potential of Lemongrass Essential Oil - Based Nanotechnology in Fungal Phytopathogen Control

M.S. Gandi[1], M.R. Zakaria[1,2], K. Ahmad[3] and M.N. Mokhtar[4]

[1]Institute of Plantation Studies, Universiti Putra Malaysia, 43400, Serdang, Selangor, Malaysia
[2]Department of Bioprocess Technology, Faculty of Biotechnology and Biomolecular Sciences, Universiti Putra Malaysia, 43400, Serdang, Selangor, Malaysia
[3]Department of Plant Protection, Faculty of Agriculture, Universiti Putra Malaysia, 43400, Serdang, Selangor, Malaysia
[4]Department of Process and Food Engineering, Faculty of Engineering, Universiti Putra Malaysia, 43400 Serdang, Selangor, Malaysia

*Corresponding author: mohdrafein@upm.edu.my

***Keywords**: Antifungal, essential oil, fungal pathogen, fungicide, nanoemulsion*

INTRODUCTION

Fungal pathogens pose a major threat to global agriculture, leading to substantial economic losses and compromising food security. Synthetic fungicides remain the primary strategy for controlling the pathogens. However, concerns over the adverse effects on the environment and non-target organisms have driven growing interest in the development of safer and more sustainable fungicide formulations, developed through approaches such as nanotechnology-based interventions. In this context, the development of nanoemulsions as carriers for bioactive compounds and as nanodelivery systems for agrochemicals has garnered considerable attention due to their enhanced efficacy and potential applicability in agricultural systems. Natural products such as plant essential oils are well-documented for their diverse antimicrobial properties, including inhibitory effects against various fungal pathogens. Hence, this study explored the potential of a lemongrass essential oil-loaded nanoemulsion to inhibit the growth of several economically important fungal phytopathogens.

METHODOLOGY

Lemongrass essential oil was extracted from the aerial parts of the fresh plant sample using the hydrodistillation technique employing Clevenger-type apparatus [2]. The percentage of essential oil yield obtained was determined using the formula below:

$$\text{The essential oil yield (\%)} = \frac{\text{weight of oil (g)}}{\text{weight of fresh sample (g)}} \text{ x } 100$$

Subsequently, O/W nanoemulsion formulations were prepared by incorporating the lemongrass essential oil, Tween 80 surfactant and ultrapure water (Table 1). The nanoemulsions were developed through ultrasonication [5]. The resulting nanoformulations were evaluated for their physicochemical properties which include mean droplet diameter, polydispersity index (PDI), zeta potential, pH and viscosity [8]. The selected nanoemulsion was then evaluated for its antifungal activity through disc diffusion assay [3]. Distilled water was used as the negative control. The percentage of mycelial inhibition was determined as follows:

$$Mycelial\ growth\ inhibition\ (\%) = \frac{\text{mycelial growth in control} - \text{mycelial growth in treatment}}{\text{mycelial growth in control}} \text{ x } 100$$

Table 1. Formulation composition of developed nanoemulsion formulations, F1, F2, and F3

Formulation	Lemongrass EO (%) w/w	Tween 80 (%) w/w	Deionized water (%) w/w
F1	10	10	80
F2	10	15	75
F3	10	20	70

RESULTS AND DISCUSSION

Figure 1 shows the essential oil extracted through hydrodistillation. The percentage of essential oil yield obtained was 0.31 – 0.38% (w/w) of fresh plant. This finding is consistent with past studies [11],[3].

Figure 1. Essential oil of *Cymbopogon citratus*

Figure 2 shows nanoemulsoion samples developed through ultrasonication. Ultrasonic emulsification is a suitable approach to produce nanoemulsions with small droplet sizes and long-term stability. The ultrasonic waves released by the sonicator probe produce intense cavitation that leads to the formation of cavitation bubbles. The intense turbulence generated from the collapse of cavitation bubbles leads to droplet deformation [9].

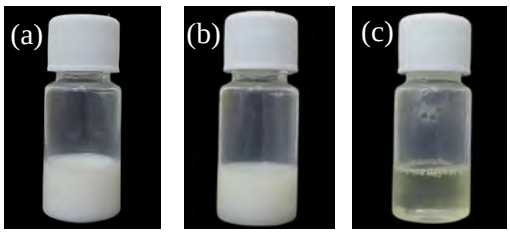

Figure 2. The formation of oil in-water nanoemulsions (a) F1, (b) F2 and (c) F3

Formulations F1 and F2 exhibited a turbid appearance, meanwhile, formulation F3 demonstrated an optically clear appearance. The transparency of formulation F3 signifies a stable dispersion of oil droplets in the aqueous phase, stabilized by the surfactant [3]. Hence, formulation F3 was selected for physicochemical and antifungal activity evaluation.

The physicochemical properties of the selected nanoemulsion formulation were evaluated (Table 2). Formulation F3 demonstrated a mean droplet diameter within the nanometer range, low PDI (<0.5) signifying a uniform particle size, low viscosity and a fair pH.

Table 2. Physicochemical properties of formulation F3

Physicochemical properties of formulation F3				
Mean droplet diameter (nm)	**Polydispersity index**	**Zeta potential (mV)**	**pH**	**Viscosity (mPa/s)**
45.9 ± 1.72	0.244 ± 0.01	-12.955 ± 1.46	5.93 ± 0.21	29.8 ± 1.84

The droplet size of nanoemulsions is influenced by the type and the concentration of the emulsifier and the magnitude of destructive force or energy applied to the liquid sample [10]. Tween 80 is a non-ionic surfactant that reduce interfacial tension and forms a stable nanoemulsion by emulsifying *C. citratus* essential oil in the aqueous medium through its hydrophilic and lipophilic groups [6]. Additionally, the polyoxyethylene chain in Tween 80 provides steric hindrance, preventing particle coalescence. PDI reflects the homogeneity of droplet size within the emulsion. In this study, the PDI value obtained was below 0.5, which indicates a narrow particle size distribution. Zeta potential is an indicator of the degree of repulsion between the charged droplets in an emulsion system, thereby directly denoting the colloidal stability of an emulsion [7]. Emulsion droplets stabilized by Tween 80 showed a negative charge due to the presence of free fatty acids in the non-ionic surfactant [1].

Additionally, nanoemulsion also recorded a low viscosity and a fair pH which is favorable for pesticide applications. The lemongrass essential oil based nanofungicide demonstrated antifungal activity in a dose – dependent manner against all tested phytopathogens (Figure 3).

At 75 µL/ mL, the nanoemulsion completely inhibited the mycelial growth *Pestalotiopsis sp.*, and *P. palmivora*. Meanwhile, at 100 µL/mL, the nanoemulsion inhibited the mycelial growth of *F. oxysporum* and *P. oryzae* by 70.47 % and 84.29 %, respectively. Distilled water showed no inhibition in all tested phytopathogens. This finding is consistent with values reported by [12].

CONCLUSION

This study concludes that O/W nanoemulsion was developed through ultrasonication by employing lemongrass essential oil as the active ingredient. The developed nanoemulsion exhibited favorable physicochemical properties suitable for agricultural applications, such as low mean droplet diameter and PDI, moderate zeta potential, fair pH and low viscosity. The developed nanoemulsion also exhibited good antifungal activity against fungal phytopathogens. The efficacy

highlights its potential as a viable nanofungicide candidate for crop protection.

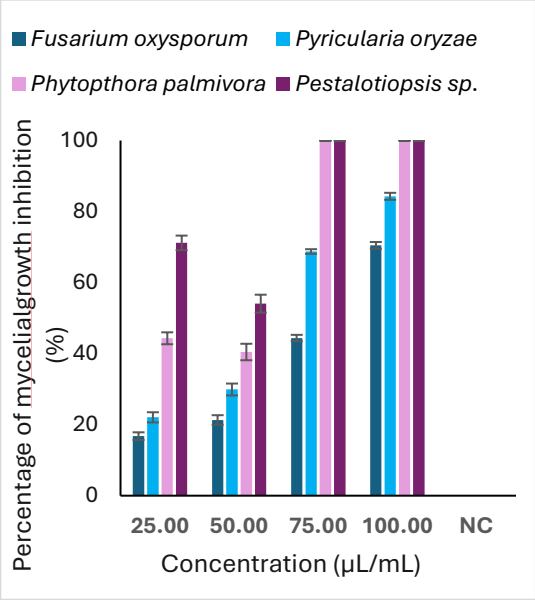

Figure 3. Antifungal activity of lemongrass essential oil based nanofungicide against phytopathogens using disc diffusion assay

REFERENCES

[1] Ahmed, K., Li, Y., McClements, D. J., & Xiao, H. (2011). Nanoemulsion- and emulsion-based delivery systems for curcumin: Encapsulation and release properties. *Food Chemistry*, *132*(2), 799–807. https://doi.org/10.1016/j.foodchem.2011.11.039

[2] Ashaq, B., Rasool, K., Habib, S., Bashir, I., Nisar, N., Mustafa, S., Ayaz, Q., Nayik, G. A., Uddin, J., Ramniwas, S., Mugabi, R., & Wani, S. M. (2024). Insights into chemistry, extraction and industrial application of lemongrass essential oil: A review of recent advances. *Food Chemistry X*, *22*, 101521. https://doi.org/10.1016/j.fochx.2024.101521

[3] Gupta, A., Eral, H. B., Hatton, T. A., & Doyle, P. S. (2016). Nanoemulsions: Formation, properties and applications. *Soft Matter*, *12*(11), 2826–2841. https://doi.org/10.1039/c5sm02958a

[4] Liu, L., Fisher, K. D., Friest, M. A., & Gerard, G. (2023). Characterization and antifungal activity of lemongrass essential oil-loaded nanoemulsion stabilized by carboxylated cellulose nanofibrils. *Polymers*, *15*(19), 3946. https://doi.org/10.3390/polym15193946

[5] Modarres-Gheisari, S. M. M., Gavagsaz-Ghoachani, R., Malaki, M., Safarpour, P., & Zandi, M. (2019). Ultrasonic nano-emulsification: A review. *Ultrasonics Sonochemistry*, *52*, 88–105. https://doi.org/10.1016/j.ultsonch.2018.11.005

[6] Mosa, M. A., Youssef, K., Hamed, S. F., & Hashim, A. F. (2023). Antifungal activity of eco-safe nanoemulsions based on *Nigella sativa* oil against *Penicillium verrucosum* infecting maize seeds: Biochemical and physiological traits. *Frontiers in Microbiology, 13*, 1108733. https://doi.org/10.3389/fmicb.2022.1108733

[7] Singh, I. R., & Pulikkal, A. K. (2022). Preparation, stability and biological activity of essential oil-based nanoemulsions: A comprehensive review. *OpenNano, 8*, 100066. https://doi.org/10.1016/j.onano.2022.100066

[8] Shah, M. A. R., Zhang, Y., Cui, Y., Hu, X., Zhu, F., Kumar, S., Li, G., Kubar, A. A., Mehmood, S., & Huo, S. (2024). Ultrasonic-assisted green extraction and incorporation of *Spirulina platensis* bioactive components into turmeric essential oil-in-water nanoemulsion for enhanced antioxidant and antimicrobial activities. *Food Chemistry, 452*, 139561. https://doi.org/10.1016/j.foodchem.2024.139561

[9] Taha, A., Ahmed, E., Ismaiel, A., Ashokkumar, M., Xu, X., Pan, S., & Hu, H. (2020). Ultrasonic emulsification: An overview on the preparation of different emulsifier-stabilized emulsions. *Trends in Food Science & Technology, 105*, 363–377. https://doi.org/10.1016/j.tifs.2020.09.024

[10] Tran, T. H., Nguyen, D. C., Phu, T. N. N., Ho, V. T. T., Vo, D. V. N., Bach, L. G., & Nguyen, T. D. (2019). Research on lemongrass oil extraction technology (hydrodistillation, microwave-assisted hydrodistillation). *Indonesian Journal of Chemistry, 19*(4), 1000. https://doi.org/10.22146/ijc.40883

[11] Wen, J., Liao, H., Nie, H., Ling, C., Zhang, L., Xu, F., & Dong, X. (2023). Comprehensive transcriptomics and metabolomics revealed the antifungal mechanism of *Cymbopogon citratus* essential oil nanoemulsion against *Fusarium solani*. *Chemical and Biological Technologies in Agriculture, 10*(1). https://doi.org/10.1186/s40538-023-00511-7

Valorisation of Palm Oil Mill Effluent Sludge Oil for Sophorolipids Production by *Starmerella bombicola* DSM 27465

S.J. Chin[1,2], M.N. Mokhtar[1,3], E.K. Bahrin[1,2,4] and M.R. Zakaria[1,2*]

[1]Institute of Plantation Studies, Universiti Putra Malaysia, 43400 Serdang, Selangor, Malaysia
[2]Department of Bioprocess Technology, Faculty of Biotechnology and Biomolecular Sciences, Universiti Putra Malaysia, 43400, UPM Serdang, Selangor, Malaysia
[3]Department of Process and Food Engineering, Faculty of Engineering, Universiti Putra Malaysia, 43400 Serdang, Selangor, Malaysia
[4]Centre for Foundation Studies in Science of Universiti Putra Malaysia, 43400, UPM Serdang, Selangor, Malaysia
*Corresponding author: mohdrafein@upm.edu.my

***Keywords**: Biosurfactant, Sophorolipids, POME sludge oil, Starmerella bombicola, Optimisation*

INTRODUCTION

Environmentally friendly substitutes for synthetic chemicals have gained popularity, especially in the surfactant industry. Because of their high toxicity and poor biodegradability, most chemical surfactants come from petrochemicals, a non-renewable source whose use may have an adverse effect on the environment. Biosurfactants are superior to synthetic surfactants in several ways, including their low toxicity, high biodegradability, biocompatibility, and ability to function in harsh pH, temperature, and salinity environments [5]. Sophorolipids (SLs) are glycolipid biosurfactants made up of a hydrophobic fatty acid tail and a hydrophilic sophorose unit. Crude SLs generally includes both lactonic and acidic forms of SLs, which differ structurally in terms of the length of the fatty acid chains, the degree of saturation of hydroxy fatty acid chains, and the types of acetylation based on the substrates utilized [3].

Although the cost of producing SLs continues to be a barrier to wider usage, recent advancements in fermentation technique and substrate use have started to remove these obstacles. Unconventional feed stocks, such as hydrolyzed food waste and lignocellulosic waste, have been shown in numerous investigations to sustain SLs titters exceeding 100 g/L. For instance, utilizing food waste hydrolysate, the productivity was 1.25 g/L·h and the SLs concentration was 115.2 g/L in 92 hours [10]. During palm oil milling, some oil is lost in waste streams. The industry recovers part of this oil from effluent ponds, classifying it as palm oil mill effluent (POME) sludge oil. It is estimated that about 5% of the crude palm oil produced can be retrieved as POME sludge oil. POME sludge oil is inedible, emits a strong odor, and remains semi-solid at room temperature. POME sludge oil contains a high free fatty acid content, typically ranging from 5% to 80%, and a

water content of 1% to 3% [14].

Research on the use of POME sludge oil especially to produce SLs is still scarce considering these advancements. Its incorporation into *Starmerella bombicola* DSM 27465-based controlled fermentation systems has not yet been thoroughly investigated, despite the substrate's composition suggesting high adaptability. Thus, this study explores the possibility of POME sludge oil as a hydrophobic carbon source for the biosynthesis of SLs, improving the fermentation process using a one-factor-at-a-time (OFAT) strategy.

MATERIALS AND METHODS

Characterisation of POME sludge oil

Gas Chromatography with Flame Ionization Detection (GC-FID) (Agilent, USA) was used to analyse the composition of fatty acids in sludge oil. The fatty acids were transformed into methyl esters (fatty acid methyl ethers) before it undergoes analysis. A DB-23 column was used for the GC-FID analysis. The temperatures of the injector and detector were calibrated to 250°C and 280°C respectively. The oven temperature was first adjusted to 50 °C, and it was then progressively raised to 175 °C. The temperature was then raised to 230 °C. By comparing the chromatogram of a standard fatty acid methyl compound (Supelco, USA) with the chromatographic peaks, the peaks could be recognised [16].

Microorganism and cultivation conditions

The *Starmerella bombicola* DSM 27465 strain was obtained from the German Collection of Microorganisms and Cell Cultures (DSMZ, Leibniz Germany). The strain was kept as a master stock in cryotubes at -80 °C and stored at 4°C on Potato Dextrose Agar (PDA). For seed culture preparation, one loopful of *S. bombicola* DSM 27465 was introduced into Potato Dextrose Broth (PDB). It was incubated at 25°C, 200 rpm for 48 h. 1% (v/v) of the inoculum was inoculated into 50 mL production medium (20 g/L glucose, 2% (v/v) POME sludge oil, 1 g/L KH2PO4, 0.5 g/L MgSO4·7H2O, 0.1 g/L CaCl2·2H2O, 0.1 g/L NaCl, and 5 g/L yeast extract) and incubated at 25°C, pH 6, 200 rpm for 144 h [11]. For optimization, the culture was incubated at different concentrations of glucose, sludge oil, temperature, pH, nitrogen sources and concentration of nitrogen sources. The previously published study served as the basis for the selection of the fermentation parameters [2].

Optimization of culture conditions

To optimize the culture conditions, the effects of glucose concentration, POME sludge oil concentration, nitrogen source and its concentration, as well as pH, were investigated. Glucose was added to the culture medium at five different concentrations (20, 40, 60, 80 and 100 g/L). POME sludge oil was also varied and tested at 2, 4, 6, 8 and 10% (v/v).

Various nitrogen sources, namely yeast extract, sodium nitrate ($NaNO_3$), ammonium chloride (NH_4Cl), ammonium nitrate (NH_4NO_3) and ammonium sulphate ($(NH_4)_2SO_4$), were evaluated as

potential nitrogen supplements. The nitrogen source that gave the best performance was then selected for a concentration study, in which it was added at 2.5, 5.0, 7.5 and 10.0 g/L.
In addition, the effect of initial pH on culture performance was examined by adjusting the medium to pH 4.5, 5.0, 5.5, 6.0 and 6.5 prior to incubation.

Determination of cell optical density

Sample of 1 mL was collected to measure optical density and analyze the composition of the fermentation medium. Each sample was centrifuged at 10,000 xg for 10 minutes. The cell pellet was washed and vortexed with 1 mL of 70% ethanol to remove residual SLs and oil. After a second centrifugation at 10,000 xg for 10 minutes, the supernatant was discarded, and the pellet was resuspended in 1 mL of 0.9% saline solution. This resuspension was used to determine biomass concentration by measuring OD600 with a UV spectrophotometer [8].

Determination of residual sugars

The residual glucose was examined using the supernatant. To determine residual sugars, dinitrosalicylic acid (DNS) method was used. 1 mL of DNS reagent was added to 1 mL of sample. The solution was vortexed for 30 sec. The mixture was heated in boiling water for 5 min and cooled under running tap water. The absorbance was checked at 540 nm. A standard curve with different concentrations of glucose was prepared [7].

Estimation of SLs concentration

0.2 mL of cell-free supernatant was mixed with 1 mL of anthrone reagent in 18 M concentrated sulphuric acid (2 g anthrone in 1 L H_2SO_4). The mixture was heated at 92°C for 30 min and then cooled in water for 5 min. The absorbance at 630 nm was recorded [10]. The values for the concentration of glucose were multiplied by 1.91 to determine the SLs content [21].

RESULTS AND DISCUSSION

POME sludge oil

The composition of fatty acid methyl esters (FAME) was detected by Gas Chromatography-Flame Ionization Detector (GC-FID). As shown in Table 1, majority of the fatty acids present in the POME sludge oil were linoleic acid and palmitic acid at 41.97% and 38.65%, respectively. It was also found that other fatty acids existed in small quantities. This fatty acid composition is different from previous study from [16]. The study shows major fatty acids reported were palmitic acid and oleic acid at 44.39 ± 0.4% and 38.54 ± 0.4%, respectively. The difference may be due to biological transformations brought on by aging, storage, or microbial activity in the sludge that causes oleic acid to degrade preferentially and increases the amount of linoleic acid in the mixture. Fatty acid desaturase is an enzyme found in all living things that can create unsaturated fatty acids by removing hydrogen atoms from the fatty acid's carbon chain [17].

Table 1. Composition of fatty acids from POME sludge oil identified using GC-FID

Fatty acid	Structure	Composition (%)	
		This study	(Mohd Asmadi et al., 2024)
Linoleic acid	C18:2, trans	41.97	-
Linoleic acid	C18:2, cis	10.02	9.22
Palmitic acid	C16:0	38.65	44.39
Oleic acid	C18:1, cis	-	38.54
Oleic acid	C18:1, trans	4.34	-
Stearic acid	C18:0	-	4.29
Lauric acid	C12:0	2.10	-
Myristic acid	C14:0	1.52	1.01
Arachidic acid	C20:0	0.38	-

Note: Values presented are means of duplicate analyses

Optimization of SLs production

In this optimization study, there are 5 main factors include concentration of glucose (20-100 g/L), concentration of POME sludge oil (2-10% (v/v)), type of nitrogen source (yeast extract, sodium nitrate, ammonium chloride, ammonium nitrate and ammonium sulphate), concentration of nitrogen (2.5-10 g/L) and pH (4.5-6.5). Dry cell weight, SLs concentration and residual glucose concentration were measured for each factor.

Concentration of glucose

The results indicated that the highest SLs production of 45.87 g/L was achieved with 80 g/L of glucose, whereas the lowest production, 16.45 g/L, was observed with 20 g/L of glucose. The SLs concentration was increasing as the concentration of glucose used increased from 20 g/L to 80 g/L. As reported by [13], glucose acts as an effective hydrophilic carbon source to support cell growth and metabolism during the initial fermentation phase. This explains the efficient consumption of glucose by *Starmerella bombicola* DSM 27465, resulting in minimal residual glucose in the fermentation broth (ranging from 0.22 g/L to 0.82 g/L). Additionally, the dry cell weight of *Starmerella bombicola* DSM 27465 after 144 h of fermentation time ranged from 3.45 g/L to 3.64 g/L, further indicating active cell growth supported by glucose utilization.

However, the concentration of SLs dropped when 100 g/L of glucose was supplemented in fermentation medium. When glucose concentrations were raised from 100 g/L to 150 g/L, lactonic SLs titres declined significantly [19]. Because of substrate inhibition, any concentration greater than 100 g/L has been demonstrated to have detrimental effects on the production of SLs. In

addition, the growth and synthesis of SLs depend heavily on the oxygen transfer rate. Higher substrate concentrations have an impact on the formation of SLs and biomass because of inefficient oxygen transfer rates [20]. Cell growth was inhibited by a high glucose content [6].

Concentration of POME sludge oil

About 8% POME sludge oil concentration resulted in the highest SLs yield (74.73 g/L), indicating it is the optimal condition for *Starmerella bombicola* DSM 27465 to produce SLs. As the concentration of POME sludge oil increased from 2% to 8%, the SLs production also increased by 66.5%. It is important to create SLs tail through terminal or sub-terminal hydroxylation of fatty acids, which can be provided directly or through lipid precursors. A noticeable reduction in SLs production was observed when oil levels dropped, indicating that the available oil was insufficient to sustain production, resulting in lower final SLs concentrations. Thus, elevated oil levels enhance both SLs production and biomass accumulation [8].

Type of nitrogen source

Different nitrogen sources were tested such as yeast extract, sodium nitrate, ammonium chloride, ammonium nitrate, ammonium sulphate and peptone. The cell growth and SLs production were shown to be affected by various nitrogen sources. To promote cell development and increase the density of cells that can produce SLs, nitrogen can be added to the fermentation media [8]. Due to different nitrogen compounds having varied impacts on microbial metabolism and growth, the choice of nitrogen source can have a major impact on the production of SLs. *Starmerella bombicola* DSM 27465 exhibited optimal growth when supplemented with yeast extract, as indicated by the highest dry cell weight (6.27 g/L) and the highest SLs concentration (85.85 g/L). Higher dry cell weight was achieved with organic nitrogen sources added to the medium.

It was discovered that yeast extract was the most efficient nitrogen source for boosting *S. bombicola*'s biomass production and SLs yield. This is because yeast extract supplies the essential nutrients required such as carbon, nitrogen, vitamins, and trace elements for building cellular components like proteins and nucleic acids. This nutrient profile makes it an effective supplement to support the growth and proliferation of a wide variety of microorganisms [1],[18]. Organic nitrogen sources were more ideal for lactonic SLs synthesis than inorganic nitrogen sources when the nitrogen concentration was fixed [15]. Because organic nitrogen sources are naturally complex, they may also contain carbon within their structure, which can serve as a metabolic precursor that encourages the development of enzymes and cell growth [4].

Concentration of nitrogen

Various yeast extract concentrations (2.5 g/L, 5 g/L, 7.5 g/L and 10 g/L) were investigated during fermentation. It was observed that the dry cell weight showed an increasing trend with a higher yeast extract concentration. Conversely, the residual glucose concentration displayed a decreasing trend when the level of yeast extract was rising. An increased nitrogen level promotes cell proliferation, which in turn enhances the efficient consumption of glucose. The highest dry cell

weight was achieved when the nitrogen concentration was the highest [4],[6].

The highest SLs production (72.97 g/L) was achieved with 0.5 g/L of yeast extract. As reported by [8], nitrogen will be completely depleted when the nitrogen concentration drops below 3 g/L, leading the cells to produce more at lower nitrogen concentrations. Cells must experience stress, which is thought to be brought on by nitrogen deprivation, to begin producing SLs. As a strategy for surviving, the cells may give priority to producing biosurfactants in such nitrogen-limiting circumstances. Biosurfactants can shield cells from harm and help them endure in adverse conditions [16]. When the culture enters the stationary phase, SLs content rises and is independent of growth [4]. Also, [11] found that both cell growth and the production of SLs were improved at the same time by raising the yeast extract concentration to 5 g/L.

Initial medium pH

The initial medium pH is a crucial factor that influences both cell growth and SLs production. The cultures were incubated at 5 different pH values such as 4.5, 5, 5.5, 6 and 6.5. The dry cell weight ranged from 4.24 g/L and 5.08 g/L, indicating that *Starmerella bombicola* DSM 27465 was able to grow well under the tested acidic pH conditions. According to [12], the optimal pH to grow *Starmerella bombicola* DSM 27465 is around pH 6, which is consistent to this study, where the highest biomass was obtained at an initial medium pH of 6. The ideal growth pH is the pH at which growth occurs at the fastest rate. Microbial growth rates fall as the pH of the environment deviates from ideal pH values [9].

When the initial medium pH was 5, the SLs production was the highest (93.61 g/L) and the residual glucose concentration was the lowest (2.78 g/L). On the contrary, the highest residual glucose level (3.53 g/L) was observed at pH 4.5. [9] found that the metabolism of microorganisms may be impacted by pH. The growth rate of a microbe with a pH range of four units can be reduced by almost half if it deviates one unit from its ideal pH, which is assumed to be close to the middle of the pH range. This suggests that pH 4.5 was too acidic for *Starmerella bombicola* DSM 27465, thereby disrupting its metabolism and limiting glucose utilization. On the other hand, at pH 6 and 6.5, the SLs production declined significantly to approximately 55 g/L. This indicates that near-neutral conditions were unfavorable for *Starmerella bombicola* DSM 27465 to synthesise SLs.

CONCLUSIONS

The optimised condition for *Starmerella bombicola* DSM 27465 to produce SLs was using 80 g/L glucose, 8% POME sludge oil, 5 g/L yeast extract at pH 5. The highest concentration SLs achieved was 93.61 g/L. This shows that POME sludge oil could replace purified oil to be an efficient hydrophobic carbon source for *Starmerella bombicola* DSM 27465 to produce SLs. With this approach, cost of substrate and environmental impacts can be reduced. This can lead to environmental sustainability.

REFERENCES

[1] Bajaj, V., Tilay, A., & Annapure, U. (2012). Enhanced production of bioactive sophorolipids by *Starmerella bombicola* NRRL Y-17069 by design of experiment approach with successive purification and characterization. *Journal of Oleo Science, 61*(7), 377–386. https://doi.org/10.5650/jos.61.377

[2] Baskaran, S. M., Zakaria, M. R., Mukhlis Ahmad Sabri, A. S., Mohamed, M. S., Wasoh, H., Toshinari, M., Hassan, M. A., & Banat, I. M. (2021). Valorization of biodiesel side stream waste glycerol for rhamnolipids production by *Pseudomonas aeruginosa* RS6. *Environmental Pollution, 276*, 116742. https://doi.org/10.1016/j.envpol.2021.116742

[3] Cho, W. Y., Ng, J. F., Yap, W. H., & Goh, B. H. (2022). Sophorolipids—bio-based antimicrobial formulating agents for applications in food and health. *Molecules*, *27*(17), 5556. https://doi.org/10.3390/molecules27175556

[4] Eras-Muñoz, E., Wongsirichot, P., Ingham, B., Winterburn, J., Gea, T., & Font, X. (2024). Screening of alternative nitrogen sources for sophorolipid production through submerged fermentation using *Starmerella bombicola*. *Waste Management, 186*, 23–34. https://doi.org/10.1016/j.wasman.2024.05.048

[5] Fonseca, T. C. de S., Rodriguez, D. M., Mendonça, R. de S., Ferreira, I. N. da S., Costa, L. O., & Campos-Takaki, G. M. (2022). Eco-friendly production of thermostable, halotolerant and pH wide-range biosurfactant by *Issatchenkia orientalis* UCP 1603. *Research, Society and Development, 11*(10), e364111032851. https://doi.org/10.33448/rsd-v11i10.32851

[6] Gao, R., Falkeborg, M., Xu, X., & Guo, Z. (2013). Production of sophorolipids with enhanced volumetric productivity by means of high cell density fermentation. *Applied Microbiology and Biotechnology*, *97*(3), 1103–1111. https://doi.org/10.1007/s00253-012-4399-z

[7] Harisha, S. (2007). *Biotechnology procedures and experiments handbook*. Infinity Science Press.

[8] Ingham, B., & Winterburn, J. (2022). Developing an understanding of sophorolipid synthesis through application of a central composite design model. *Microbial Biotechnology*, *15*(6), 1744–1761. https://doi.org/10.1111/1751-7915.14003

[9] Jin, Q., & Kirk, M. F. (2018). pH as a primary control in environmental microbiology: 1. Thermodynamic perspective. *Frontiers in Environmental Science, 6*, 340428. https://doi.org/10.3389/fenvs.2018.00021

[10] Kaur, G., Wang, H, To, M. H., Roelants, S. L. K. W., Soetaert, W., & Lin, C. S. K. (2019).

Efficient sophorolipids production using food waste. *Journal of Cleaner Production, 232*, 1–11. https://doi.org/10.1016/j.jclepro.2019.05.326

[11] Kim, J. H., Oh, Y. R., Hwang, J., Kang, J., Kim, H., Jang, Y. A., Lee, S. S., Hwang, S. Y., Park, J., & Eom, G. T. (2021). Valorization of waste-cooking oil into sophorolipids and application of their methyl hydroxyl branched fatty acid derivatives to produce engineering bioplastics. *Waste Management, 124*. https://doi.org/10.1016/j.wasman.2021.02.003

[12] Leibniz Institute DSMZ–German Collection of Microorganisms and Cell Cultures. (n.d.). *Starmerella bombicola DSM 27465*. Retrieved August 16, 2025, from https://www.dsmz.de/collection/catalogue/details/culture/DSM-27465

[13] Li, Y., Chen, Y., Tian, X., & Chu, J. (2020). Advances in sophorolipid-producing strain performance improvement and fermentation optimization technology. *Applied Microbiology and Biotechnology*, *104*(24), 10325–10337. https://doi.org/10.1007/s00253-020-10964-7

[14] Loh, J. M., Amelia, Gourich, W., Chew, C. L., Song, C. P., & Chan, E.-S. (2021). Improved biodiesel production from sludge palm oil catalyzed by a low-cost liquid lipase under low-input process conditions. *Renewable Energy*, *177*, 348–358. https://doi.org/10.1016/j.renene.2021.05.138

[15] Ma, X. J., Li, H., Shao, L. J., Shen, J., & Song, X. (2011). Effects of nitrogen sources on production and composition of sophorolipids by *Wickerhamiella domercqiae* var. sophorolipid CGMCC 1576. *Applied Microbiology and Biotechnology*, *91*(6), 1623–1632. https://doi.org/10.1007/s00253-011-3327-y

[16] Mohd Asmadi, N. A. N., Zee, K. M., Baskaran, S. M., Ariffin, H., Wasoh, H., Maeda, T., Hassan, M. A., & Zakaria, M. R. (2024). Rhamnolipids production by *Pseudomonas aeruginosa* RW9 using palm oil mill effluent sludge oil as a carbon source. *Biocatalysis and Agricultural Biotechnology*, *57*, 103069. https://doi.org/10.1016/j.bcab.2024.103069

[17] Sudibyo, H., Pradana, Y. S., Budhijanto, & Budhijanto, W. (2018). Bio-synthesis of eicosapentaenoic acid (EPA) from palm oil mill effluent using anaerobic process. *Defect and Diffusion Forum, 382*, 286–291. https://doi.org/10.4028/www.scientific.net/ddf.382.286

[18] Taowkrue, E., Songdech, P., Maneerat, S., & Soontorngun, N. (2024). Enhanced production of yeast biosurfactant sophorolipids using yeast extract or the alternative nitrogen source soybean meal. *Industrial Crops and Products*, *210*, 118089. https://doi.org/10.1016/j.indcrop.2024.118089

[19] To, M. H., Wang, H., Lam, T. N., Kaur, G., Roelants, S. L., & Lin, C. S. K. (2022). Influence of bioprocess parameters on sophorolipid production from bakery waste oil. *Chemical Engineering Journal, 429*, 132246.

[20] Vedaraman, N., & Venkates, N. (2010). The effect of medium composition on the production of sophorolipids and the tensiometric properties by *Starmerella bombicola* MTCC 1910. *Polish Journal of Chemical Technology, 12*(2), 9–13.

[21] Wadekar, S. D., Kale, S. B., Lali, A. M., Bhowmick, D. N., & Pratap, A. P. (2012). Utilization of sweetwater as a cost-effective carbon source for sophorolipids production by *Starmerella bombicola* (ATCC 22214). *Preparative Biochemistry & Biotechnology*, *42*(2), 125–142. https://doi.org/10.1080/10826068.2011.577883

Latex Timber Clone (LTC) Rubber Plantation (*Hevea Brasiliensis*) In Malaysia: Status and Future Prospects

A.F. Mokhtar[1], M.M. Md[2], Z. Khuzaimah[1] and H. Hashim[1]

[1]Institute of Plantation Studies, Universiti Putra Malaysia, 43400 Serdang, Selangor, Malaysia
[2]Institute of Tropical Forestry and Forest Product, Universiti Putra Malaysia, Serdang, Selangor, Malaysia
*Corresponding author: faiz_mokhtar@upm.edu.my

***Keywords**: Rubberwood, latex timber clone (LTC), Hevea brasiliensis, forest plantation, timber supply*

INTRODUCTION

This paper reviews the development of latex timber clone (LTC) rubber forest plantations in Malaysia, with emphasis on log production potential, industrial utilization, and future supply forecasts. LTCs are improved *Hevea brasiliensis* clones bred for both latex and timber, with larger stem girth and good form at falling age.

The world demand for wood is increasing as the population grows, while the natural forest resources are depleting, particularly in the tropical developing countries. In most tropical, large portions of this natural forest have been converted to other alternative land uses, particularly for agriculture development. The conversion of forest lands is also attributed to other activities such as shifting cultivation, development of dams for hydroelectric generation and reservoir, encroachment and illegal logging. These factors led to deforestation, which in turn affect future timber supply and ecological balance.

Traditionally, Malaysia depends on natural forest as its source of timber. Today, we see that there is a decline in resourcing it traditionally as the country is moving towards more sustainable forest management by establishing more forest plantations. The main driver to establish more forest plantations is to ensure there will be sufficient timber supply and at the same time the ecology of the environment is preserved. The Malaysian government is committed in preserving the biodiversity and ecosystems in line with the International Conventions. This move from being dependent on timber from natural forest to forests plantation is seen to be positive. The forest plantations have proven to provide better annual means of increments on average of 5 to 10 higher than those in natural forests. Other than that, the production costs are lower and therefore have an impact on the selling price. This is one of the factors that give Malaysian timbers the competitive advantage.

In the past, most around log timber produced by Malaysia is exported because the processing activities are mostly done by the importing countries. This is shown by the 60 percent export value of primary activities which include harvesting of logs and the processing of sawn timber, plywood, veneer, fiberboard and particle board while 40 percent of export value comes from secondary and tertiary activities such as manufacturing of furniture, moldings, wood flooring and laminated veneer lumber and other related wood products. However, with the changes in policy where there is restriction on logging and export of logs form timber from natural forest, there is a decline in export in primary form and increase in supply to the secondary and tertiary activities locally.

RUBBER FOREST PLANTATION

The rubber tree (*Hevea brasiliensis*) has emerged as a significant alternative to light tropical hardwoods, serving as a major source of timber for furniture and interior components. Since the mid-1980s, Malaysia has pioneered the utilization of rubber wood as a sustainable substitute for natural forest timbers, thereby positioning it as an important raw material to produce furniture, medium-density fiberboard, plywood, particleboard, flooring, and related products [1]. The expansion of value-added industries based on rubber wood has contributed substantially to national income and export earnings [2]. However, the supply of rubber wood from conventional plantations and replanting schemes has declined markedly, largely due to the conversion of rubber-growing areas to oil palm cultivation [3]. An example of a LTC rubber plantation in Bukit Ibam, Pahang is shown in Figure 1.

Figure 1. LTC plantation at Bukit Ibam, Pahang

National statistics indicate that rubber plantation coverage decreased from approximately 2.0 million hectares in the 1980s to 1.2 million hectares by 2007 [4]. In response, the Ministry of Plantation Industries and Commodities (MPIC) introduced a forest plantation programed with the objective of establishing 375,000 hectares of commercial forest plantations, including rubber species, within a 15-year cycle [1]. This initiative reflects a reclassification of rubber from an agricultural crop to a forest plantation species. Two principal models of rubber forest plantations have been identified: (i) latex timber clone plantations, which yield both timber and latex, and (ii) wood-only plantations, which focus exclusively on timber production [5].

In the latex timber clone system, trees are permitted to grow without tapping for eight years, with latex extraction commencing in the ninth year, thereby promoting healthier growth and maximizing stem girth and clear bole length at the felling age of 15 years [6]. In contrast, wood-only plantations forego latex tapping entirely, with trees harvested after 15 years [7]. Despite challenges associated with declining supply and land-use conversion, rubber wood remains integral to Malaysia's plantation forestry strategy and continues to play a vital role in sustaining the nation's timber industry and export economy [8].

PRODUCTION AND SUPPLY OUTLOOK

Rubber wood log production begins when latex yield declines, typically between 15–30 years of the rubber cycle, with the MPIC program mandating felling at 15 years. Harvests average 262 m^3/ha based on a planting density of 524 trees/ha and a saw log yield of 0.5 m^3/tree, compared to earlier yields of 57 m^3/ha from estates and 54 m^3/ha from smallholdings. In the 1990s, Malaysian Timber Council reported annual production of about 971,000 m^3, which fell sharply to 38,000 m^3 in 1997. Key rubber wood production metrics for LTC plantations are summarized in Table 1.

Table 1: Rubber wood production data

Metric	Value
Average Harvest	262 m^3/ha
Planting Density	524 trees/ha
Saw Log Yield	0.5 m^3/tree
Earlier Estate Yield	57 m^3/ha
Earlier Smallholding Yield	54 m^3/ha
1990s Annual Production	971,000 m^3
1997 Annual Production	38,000 m^3

Historically, rubber wood was used for fuel and charcoal in industries such as steel, rubber processing, tobacco curing, and brick manufacturing, but since the 1980s it has become a major timber product, especially for furniture, components, and panels. More recently, it has been used in MDF, particleboard, OSB, and plywood for both construction and decorative purposes. By 2004, Malaysia had 10 MDF mills with a combined capacity of 1.5 million m^3 per year, up from 1.16 million m^3 in 1999. The furniture industry has grown tremendously, with exports rising from RM 214.7 million in 1990 to RM 6,921.1 million in 2008, about 80% of which were rubber wood products in solid, laminated, or reconstituted forms.

Forecasts suggest sustainable harvests of 7.8 million m^3 from 2010–2019 and 10.3 million m^3 from 2020–2030, an increase of 32%, achievable only if the government's target of planting 10–15,000 ha of rubber forest plantations is met alongside the use of improved RRIM-certified planting materials on a 15-year rotation. Current planted areas face low recovery rates (25–30% of large-

diameter logs) due to small and irregular log sizes and forms, underscoring the need for improved practices to secure future supply. Forecasted sustainable harvest volumes of RRIM-certified clones under current planting and recovery assumptions are presented in Table 2.

Table 2. Forecasted sustainable harvest RRIM-certified clones

Year	Output	Planting	Current recovery rate
2010–2019	7.8 million m³	10–15k ha LTC for wood + latex	25–30% due to small/irregular log sizes
2020–2030	10.3 million m³	10–15k ha LTC for wood + latex	25–30% due to small/irregular log sizes
Raising	32%		

UNLOCKING THE POTENTIAL OF RUBBER FOREST PLANTATIONS THROUGH POLICY SUPPORT

Over the past years, rubber forest plantations opportunities have been realized as a new source of raw materials and have given rise to large scale processing industries resulting in downstream processing of high value-added products. However, the high financial risk associated with commercial rubber forest plantation establishment due to its long gestation period, payback period, and uncertainty about future final harvest and revenues which makes it decline rapidly. There are available incentives for the development of commercial forest plantation that have not been addressed for the participation of private sectors due to unattractive incentives. Since, government has long been committed to sustainable forest management (SFM) principles, the ratification of Kyoto Protocols leads to the provision of soft loans to further encourage the development of commercial forest plantation to reduce pressure on native forests.

With this earlier broad argument about unattractive incentives is expected to be addressed. Through RMK-9 government has set up a soft loan program with attractive schemes that encourage the private sectors to participate in forest plantation program. Further through research and development process, based on rubber forest plantation management model such as genetic or tree improvement, silvicultural improvement, continuous monitoring of rubber forest plantation and development of growth and yield model. It is possible to achieve even greater opportunities with rubber forest plantation development. Rubber forest plantation is known to have potential for growers especially in terms of its growth and revenue from latex and timber. Since the latex can be gained at 5 - 8 years of age (to maximize girth), it is proving a boost in overcoming the long gestation period, market risk, physical risk and financial risk when compared with other tree forest plantations.

CONCLUSIONS AND IMPLICATIONS

Rubber forest plantations, especially LTCs, offer viable raw material for high-value products, but private sector participation is constrained by financial risks, long rotations, and weak incentives, prompting government soft loan schemes and commitments to SFM and the Kyoto Protocol to

ease pressure on native forests and foster plantation development.

REFERENCES

[1] Ministry of Plantation Industries and Commodities. (2007). *Forest plantation programme report*. Putrajaya, Malaysia.

[2] Lim, C. H. (2002). Value-added rubber wood products and their contribution to Malaysia's economy. *Forest Products Journal, 52*(4), 15–22.

[3] Department of Statistics Malaysia. (2007). *Agricultural statistics of Malaysia*. Putrajaya, Malaysia.

[4] Ahmad, N. (2008). Conversion of rubber plantations to oil palm in Malaysia: Impacts and trends. *Journal of Tropical Agriculture, 45*(2), 67–75

[5] Chan, F. H. (2010). Rubber forest plantations: Latex timber clones and wood-only systems in Malaysia. *Malaysian Journal of Forestry, 73*(1), 23–34

[6] Ng, T. Y., & Wong, K. L. (2011). Growth performance of latex timber clones in forest plantation systems. *Journal of Rubber Research, 14*(3), 145–158

[7] Rahman, M. S. (2012). Wood-only rubber plantations: Economic viability and silvicultural practices. *International Forestry Review, 14*(2), 89–97

[8] Yusof, Z. (2015). Rubber wood and Malaysia's timber export economy. *Malaysian Timber Bulletin, 19*(1), 33–45.

RNA Interference (RNAi): A Green Revolution for Sustainable Plant Protection

Z.K. Abdullah[1, 2], K. Lihling[1], N. Ariffin[3], J. Hailing[4] and W. Mui-Yun[1,5*]

[1]Institute of Plantation Studies, Universiti Putra Malaysia, 43400 Serdang, Selangor, Malaysia
[2] Department of Plant Protection, Faculty of Agriculture, Helmand University, Peace Watt, Lashkar Gah 3901, Helmand, Afghanistan
[3] Department of Agriculture Technology, Faculty of Agriculture, Universiti Putra Malaysia, 43400 Serdang, Selangor, Malaysia
[4]Department of Microbiology and Plant Pathology, University of California, Riverside, CA, 92521, USA
[5]Department of Plant Protection, Faculty of Agriculture, Universiti Putra Malaysia, 43400, Serdang, Selangor, Malaysia
*Corresponding author: muiyun@upm.edu.my

Keywords*: RNA interference, Plant protection, Gene silencing, dsRNA, Sustainable agriculture*

INTRODUCTION

The challenge to global food security

According to the Food and Agriculture Organization (FAO), food security is the condition in which all people have constant access to sufficient, safe, and nutritious food that meets their dietary needs and preferences for an active and healthy life. While agriculture remains the primary source of food for human beings, however, the current agriculture is undergoing a crucial transformation toward sustainability, aiming to balance the increasing global demand for food with environmental preservation [1].

Historically, approaches such as the Green Revolution significantly increased crop productivity, but it also intensified ecological pressures through the excessive use of synthetic agrochemicals, causing soil degradation, pest resistance, and health concerns [2-3]. Today, farmers face growing challenges from rapidly evolving pests and pathogens, which collectively cause yield losses of 10-40% and over USD 220 billion in annual economic damage [4].

To achieve true sustainability, agriculture needs innovative and precise pest and disease control strategies that break the cycle of chemical dependence. In this context, RNA interference (RNAi) has emerged as a novel, environmentally sustainable approach to crop protection.

This conserved eukaryotic mechanism silences gene expression after transcription by guiding the degradation of target messenger RNA (mRNA) through small RNAs such as small interfering

RNAs (siRNAs) and micro RNAs (miRNAs) [5]. Discovered by Fire and Mello in Caenorhabditis elegans (leading to the 2006 Nobel Prize), this process rapidly established its role across diverse eukaryotic organisms (Figure 1). Its species-specific and non-toxic mode of action offers a precise, safe, and sustainable alternative to traditional chemical control methods [6]. Incorporating RNAi-based technologies into pest breeding for resistance and into the development of eco-friendly crops and protection systems represents a key step in monitoring, aimed at achieving food security and advancing the United Nations Sustainable Development Goals (SDGs).

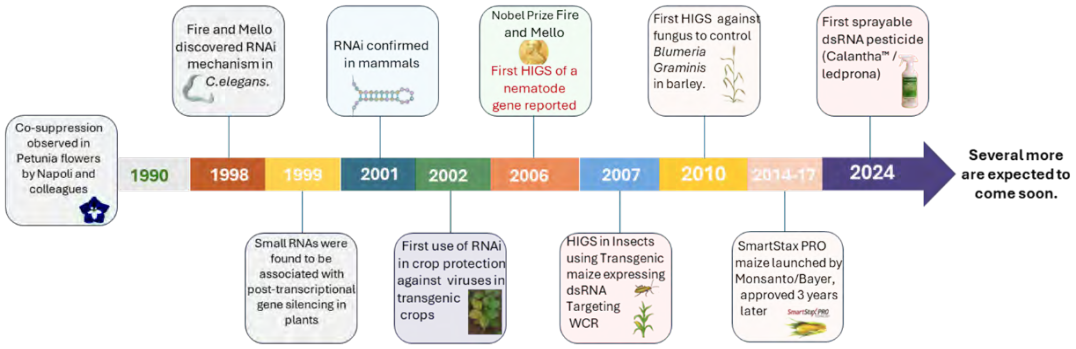

Figure 1. Timeline of key milestones in RNAi, from its discovery in C. elegans (1998) to advances in HIGS, SIGS, nanocarrier delivery, and the commercialization of RNAi-based biopesticides for sustainable crop protection

The core pathway of RNAi

RNAi is a highly conserved biological process that regulates gene expression at the post-transcriptional level through sequence-specific degradation or silencing of mRNA. The mechanism begins when double-stranded RNAs (dsRNA) enter a cell either endogenously from transgenes, viruses, or transcriptional events or exogenously through spraying, soaking, or feeding. Once inside the cytoplasm, the Dicer-like (DCL) proteins recognise and cleave dsRNA into siRNAs, typically 21–24 nucleotides in length. These siRNAs are then incorporated into the RNA-induced silencing complex (RISC), where one strand (guide strand) directs the complex to complementary mRNA targets.

The Argonaute (*AGO*) protein within RISC mediates the cleavage or translational repression of the target mRNA, resulting in gene silencing [7-8]. In some organisms, RNA-dependent RNA polymerases (*RdRPs*) amplify the silencing signal by generating secondary siRNAs, which enhance the durability and spread of RNAi effects [9]. RNAi serves as a natural antiviral defense mechanism in plants, protecting them against viral infections by targeting viral RNA for degradation. It also plays roles in genome stability, developmental regulation, and epigenetic control [10].

RNAi AS A SUSTAINABLE PLANT PROTECTION STRATEGY

RNAi provides a transformative and environmentally sustainable approach to protecting plants by harnessing a natural gene-silencing process to target specific genes in pests and pathogens. In plants, RNAi technology has evolved from creating virus-resistant varieties to more advanced methods such as Host-Induced Gene Silencing (HIGS) and Spray-Induced Gene Silencing (SIGS). HIGS, also known as endogenous expression (Figure 1A), enables plants to produce dsRNA that targets pathogen genes, whereas SIGS involves externally applying dsRNA (Figure 1B) or exogenous application for non-transgenic protection [11].

These methods have shown strong effectiveness against various agricultural pests and diseases [12-14]. For instance, dsRNA targeting virulence genes in Fusarium graminearum and Botrytis cinerea has been shown to decrease fungal growth and mycotoxin levels successfully [15]. Likewise, feeding dsRNA that targets essential genes, such as vATPase and chitin synthase, in Helicoverpa armigera leads to increased larval mortality and decreased feeding [16]. Additionally, developing transgenic plants that express dsRNA sequences targeting viral coat protein genes provide long-lasting resistance against viruses like Tobacco mosaic virus and Potato virus Y [17]. RNAi-based biopesticides target essential genes in pests and plant pathogens, including those involved in feeding, digestion, nervous system function, cuticle formation, virulence, pathogenicity, RNAi pathway, and effector production to achieve high mortality or disease suppression while reducing resistance development.

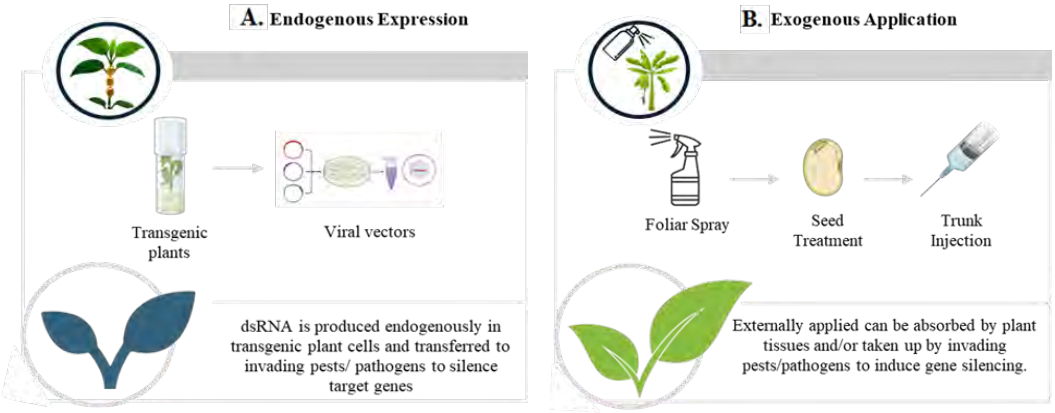

Figure 2. Exogenous dsRNA application (A) and endogenous dsRNA expression (B) pathways in RNAi-based plant protection

FIELD APPLICATION

The deployment of RNAi technology in the field has materialized through two distinct, pioneering commercial models, marking a revolutionary step in crop protection. The first, HIGS, is exemplified by SmartStax Pro (Bayer), a genetically modified maize engineered to internally express a dsRNA targeting an essential gene (*DvSnf7*) in the subterranean pest, the Western Corn Rootworm (*Diabrotica virgifera virgifera*). When the larvae feed on the roots, they ingest dsRNA, triggering RNAi and causing mortality, thereby providing root protection (Figure 3). This

mechanism of action was first characterized in a landmark study detailing dsRNA efficacy and the *Snf7* target [18].

The second model is SIGS, realized in the non-GM biopesticide Calantha. As shown in figure 4, the dsRNA is sprayed directly onto potato foliage. It is then ingested by the highly resistant Colorado Potato Beetle, *Leptinotarsa decemlineata*, where its dsRNA active ingredient, ledprona, silences the beetle's critical proteasome subunit gene (*PSMB5*), a mode of action whose field efficacy has been documented in recent years [19]. While SmartStax Pro utilizes a stable genetic platform for root protection, Calantha introduces a highly selective, rapidly degrading, and environmentally benign topical spray. Together, they demonstrate the flexibility and precision of RNAi to combat major agricultural pests with Novel modes of action.

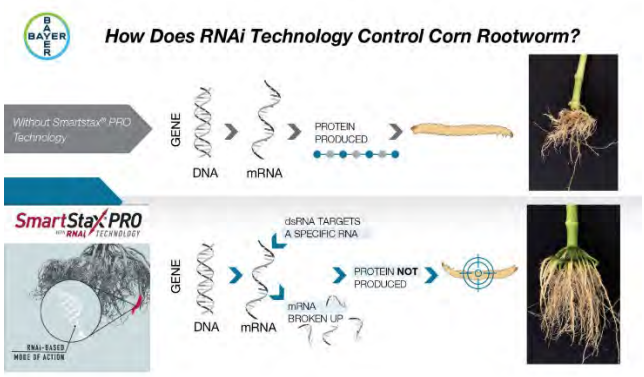

Figure 3. SmartStax Pro Corn (Monsanto, Bayer). The first genetically modified plant produces dsRNA targeting the essential DvSnf7 gene in the Western Corn Rootworm (WCR)

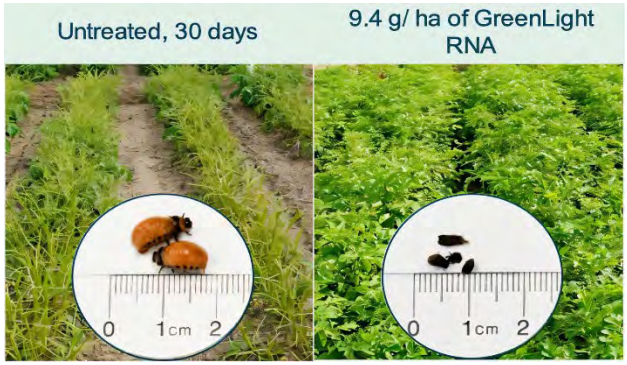

Figure 4. Calantha biopesticide (GreenLight BioScience, 2024). The application of Calantha, the first commercial SIGS product, on the potato (right) and untreated control (left)

CHALLENGES AND FUTURE PERSPECTIVES

RNAi offers a promising approach for sustainable plant protection, owing to its specificity, environmental safety, and targeted action against pests and pathogens, with minimal impact on non-target organisms. However, challenges such as the effective delivery of dsRNA, regulatory

uncertainties, public perception issues, and high production costs hinder its broader application in agriculture. Delivery obstacles can be mitigated using nanoparticle carriers, while varying international regulations complicate the approval process. Additionally, public misunderstandings about RNAi technology must be addressed for better acceptance. Advances in synthesis technologies are helping to reduce production costs, paving the way for broader adoption. Future developments in nanobiotechnology, bioinformatics, and regulatory frameworks are anticipated to enhance the integration of RNAi into pest management, thereby contributing to sustainable agriculture and food security.

Figure 5 summarizes the progression of RNAi technology from conventional gene silencing methods to advanced platforms, including HIGS, SIGS, and nano-enabled delivery systems, which collectively offer species-specific, environmentally friendly, and sustainable strategies for managing plant pests and diseases.

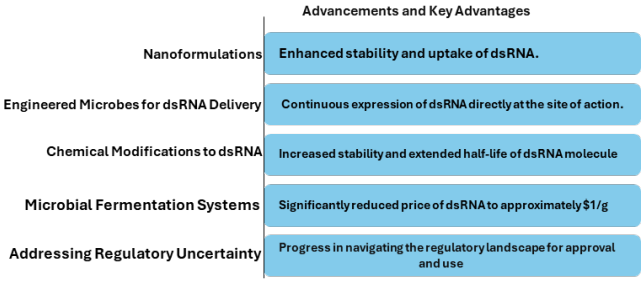

Figure 5. Advancements and advantages of RNAi. This technology has progressed from basic gene silencing to advanced platforms like HIGS, SIGS, and nanoformulations, offering species-specific, eco-friendly, and sustainable crop protection

CONCLUSION

RNA interference (RNAi) represents the next wave of green agricultural innovation, merging molecular precision with environmental stewardship. By enabling highly specific gene silencing in pests and pathogens, RNAi provides a sustainable alternative to broad-spectrum chemical pesticides, which often harm beneficial organisms and degrade ecosystems. Its integration into pest and disease management programs has the potential to substantially reduce chemical inputs, minimize pesticide residues in food and soil, and protect biodiversity. Furthermore, RNAi-based technologies, whether applied through HIGS, SIGS, or nanoparticle-mediated delivery, provide versatile tools adaptable to diverse cropping systems and environmental conditions. Beyond its scientific and practical value, RNAi contributes directly to global objectives such as the United Nations Sustainable Development Goals (SDGs), particularly those addressing zero hunger, responsible production, climate action, and life on land. As agriculture faces intensifying challenges from climate change, evolving pests, and resource limitations, RNAi exemplifies how science-driven, targeted innovation can reshape food production toward a more resilient, eco-friendly, and secure future. Continued interdisciplinary research, regulatory support, and field

validation will be crucial to realizing the full potential of RNAi as a cornerstone of next-generation sustainable agriculture.

REFERENCES

[1] McCarthy, U., Uysal, I., Badia-Melis, R., Mercier, S., O'Donnell, C., & Ktenioudaki, A. (2018). Global food security: Issues, challenges and technological solutions. *Trends in Food Science & Technology, 77,* 11–20.

[2] Boedeker, W., Watts, M., Clausing, P., & Marquez, E. (2020). The global distribution of acute unintentional pesticide poisoning: Estimations based on a systematic review. *BMC Public Health, 20*.

[3] Abdullah, Z. K., Kihara, J., Gondo, Y., Ganphung, R., Yokoyama, Y., & Ueno, M. (2021). Suppressive effect of secondary metabolites from *Streptomyces plumbeus* isolate F31D against *Fusarium oxysporum* f. sp. *lycopersici*, the causal agent of Fusarium wilt of tomato. *Journal of General Plant Pathology, 87,* 335–343.

[4] FAO. (2024). *The state of food and agriculture 2024*. FAO.

[5] Fire, A., Xu, S., Montgomery, M. K., Kostas, S. A., Driver, S. E., & Mello, C. C. (1998). Potent and specific genetic interference by double-stranded RNA in *Caenorhabditis elegans*. *Nature, 391*, 806–811.

[6] Bachman, P. M., Bolognesi, R., Moar, W. J., Mueller, G. M., Paradise, M. S., Ramaseshadri, P., Tan, J., Uffman, J. P., Warren, J. A., Wiggins, B. E., & Levine, S. L. (2013). Characterization of the spectrum of insecticidal activity of a double-stranded RNA with targeted activity against *Diabrotica virgifera virgifera*. *Transgenic Research, 22*, 1207–1222.

[7] Baulcombe, D. C. (2025). The role of viruses in identifying and analyzing RNA silencing. *Annual Review of Virology, 34*.

[8] Dalakouras, A., Wassenegger, M., Dadami, E., Ganopoulos, I., Pappas, M. L., & Papadopoulou, K. (2020). Genetically modified organism-free RNA interference: Exogenous application of RNA molecules in plants. *Plant Physiology, 182*, 38–50.

[9] Mezzetti, B., Smagghe, G., Arpaia, S., Christiaens, O., Dietz-Pfeilstetter, A., Jones, H., Kostov, K., Sabbadini, S., Opsahl-Sorteberg, H. G., Ventura, V., Taning, C. N. T., & Sweet, J. (2020). RNAi: What is its position in agriculture? *Journal of Pest Science, 93,* 1125–1130.

[10] Rank, A. P., & Koch, A. (2021). Lab-to-field transition of RNA spray applications: How far are we? *Frontiers in Plant Science, 12*.

[11] Spada, M., Pugliesi, C., Fambrini, M., Pecchia, S., & Martínez-Gómez, P. (2021). Silencing of the Slt2-type MAP kinase Bmp3 in *Botrytis cinerea* by application of exogenous dsRNA affects fungal growth and virulence on *Lactuca sativa*. *International Journal of Molecular Sciences*.

[12] Werner, B. T., Gaffar, F. Y., Schuemann, J., Biedenkopf, D., & Koch, A. M. (2020). RNA-spray-mediated silencing of *Fusarium graminearum* AGO and DCL genes improves barley disease resistance. *Frontiers in Plant Science, 11*.

[13] Niu, J., Chen, R., & Wang, J. J. (2024). RNA interference in insects: The link between antiviral defense and pest control. *Insect Science, 31*, 2–12.

[14] Koch, A., Biedenkopf, D., Furch, A., Weber, L., Rossbach, O., Abdellatef, E., et al. (2016). An RNAi-based control of *Fusarium graminearum* infections through spraying of long dsRNAs involves a plant passage and is controlled by the fungal silencing machinery. *PLOS Pathogens, 12*.

[15] Jin, S., Singh, N. D., Li, L., Zhang, X., & Daniell, H. (2015). Engineered chloroplast dsRNA silences cytochrome P450 monooxygenase, V-ATPase, and chitin synthase genes in the insect gut and disrupts *Helicoverpa armigera* larval development and pupation. *Plant Biotechnology Journal, 13*, 435–446.

[16] Prins, M., Laimer, M., Noris, E., Schubert, J., Wassenegger, M., & Tepfer, M. (2008). Strategies for antiviral resistance in transgenic plants. *Molecular Plant Pathology, 9*, 73–83.

[17] Bachman, P. M., Bolognesi, R., Moar, W. J., Mueller, G. M., Paradise, M. S., Ramaseshadri, P., et al. (2013). Characterization of the spectrum of insecticidal activity of a double-stranded RNA with targeted activity against Western corn rootworm (*Diabrotica virgifera virgifera*). *Transgenic Research, 22*, 1207–1222.

[18] Pallis, S., Alyokhin, A., Manley, B., Rodrigues, T. B., Buzza, A., Barnes, E., et al. (2022). Toxicity of a novel dsRNA-based insecticide to the Colorado potato beetle in laboratory and field trials. *Pest Management Science, 78*, 3836–3848.

[19] GreenLight Biosciences, I. (2025). Specimen label Bioinsecticide for control of Colorado Potato Beetle on potato plants.

Phenolic Compounds as Antagonists in Altering Mycelial Morphology and Enzyme Activity of *G. Boninense*

D. Ganapathy[1], G. Vadamalai[1], Y. Siddiqui[1], K. Ahmad[2], K.L. Ling[1] and F. Adzmi[1]

[1]Laboratory of Sustainable Agronomy and Crop Protection, Institute of Plantation Studies, Serdang, Malaysia
[2]Department of Plant Protection, Faculty of Agriculture, Serdang, Malaysia
*Corresponding author: ganesanv@upm.edu.my

***Keywords**: Ganoderma boninense, gallic acid, phenolic compounds, basal stem rot disease, oil palm, antimicrobial activity, hydrolytic ang ligninolytic enzymes*

INTRODUCTION

Oil palm (*Elaeis guineensis*) is recognized as the first commercially cultivated and native plantation crop within the economically significant tropical regions and is often referred to as the 'Golden Crop' due to its high economic value and versatility [1]. Globally, palm oil has become the most-sought-after vegetable oil, with its demand continuing to rise steadily due to its wide range of applications, particularly in the food industry.

Indonesia and Malaysia dominate the global palm oil market, collectively accounting for approximately 85% of total production [2]. In Malaysia alone, the oil palm industry is a major pillar of the national economy, contributing 46.6% to the agricultural sector's Gross Domestic Product (GDP) [2]. The widespread cultivation of oil palm and its viral role in international trade underscore its significance not only as a national economic driver but also as a key commodity in global agricultural markets.

Apart from the market dominance and high achievability of oil palm industry, there is a devastating threat occurring which is basal stem rot (BSR) disease caused by white-rot fungus, *Ganoderma boninense* and there were several methods that were opted for such as trunk injection, biocontrol agent, cultural practices, chemical control and application of biofertilizers [3]. Therefore, potential natural inhibitory compounds including gallic acid, thymol, propolis and carvacrol were systematically evaluated for their antagonistic efficacy against *Ganoderma boninense*.

METHODOLOGY

In this study, structural alterations of *Ganoderma boninense* mycelium were investigated under stress conditions induced by selected various phenolic compounds such as gallic acid (GA), thymol (THY), propolis (PRO) and carvacrol (CARV) [4;5]. Both qualitative and quantitative analyses of

hydrolytic and ligninolytic enzyme activities were conducted to evaluate the biochemical responses of the pathogen in the presence of these compounds [6]. Enzymatic profiling aimed to elucidate the potential inhibitory mechanisms associated with phenolic compound exposure. For statistical validation, all data were analyzed using SAS Statistical Software, version 9.4 (English). Mean comparisons were performed using Tukey's Studentized Range (HSD) Test at a 95% confidence level (α=0.05), ensuring the robustness and reliability of the observed differences among treatments [7].

RESULTS

Phenolic compounds caused marked ultrastructural damage to *G. boninense* hyphae. Untreated mycelia showed intact cell walls, well defined membranes and clear organelles. Nonetheless, GA caused irregular membranes, vacuole fusion and rupture and electron-dense inclusions. Moreover, thymol led to severe destruction of cell walls whereas propolis caused organelle disintegration, damaged cell walls and plasma membrane detachment. Carvacrol produced foreshorten nuclear content and irregular, damaged membrane regions. As in broad, phenolic compounds disrupted membrane integrity and organelle structure causing major cytoplasmic and nuclear alterations.

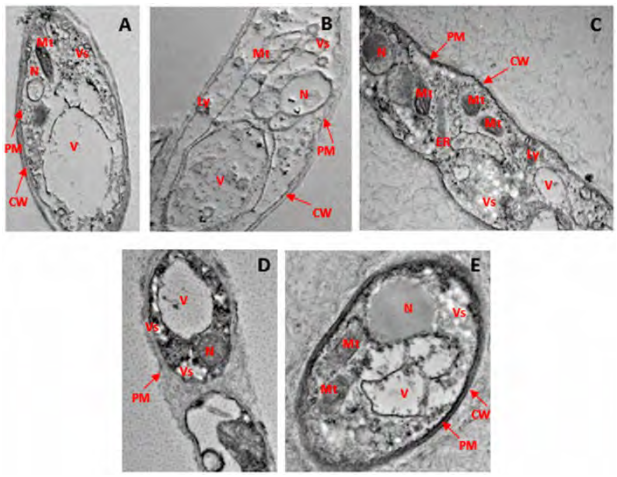

Figure 1. HR-TEM images (6000x) showing ultrastructural changes in *G. boninense* PER 71 hyphae after phenolic compound treatments. (A) Healthy hyphae with intact cell wall, plasma membrane and visible organelles. (B) GA treatment showing disrupted walls and membranes, empty regions, condensed nucleus and deformed mitochondria. (C) Thymol-treated hyphae displaying membrane disruption and cytoplasmic leakage. (D) Propolis-treated hyphae with disrupted membranes and visible organelles. (E) Carvacrol-treated hyphae showing minimal damage and intact structures. Scale: 1 µm

Phenolic compounds caused significant electrolyte leakage in *G. boninense* mycelia ($p<0.05$). GA produced the highest leakage of all concentrations, reaching 100.30µ mhos g^{-1} at 8mg/mL. Thymol caused moderate leakage (61.30µ mhos g^{-1}), while propolis and carvacrol resulted in the lowest leakage across all treatments.

The control sample showed very low cell mortality (0.24%), likely due to sample debris. GA caused highest mortality (45.73%), followed by THY (31.90%), both greatly reducing total cell numbers,

whereas PRO and CARV resulted in lower mortality rates of 20.97% and 5.06% respectively, indicating a higher proportion of surviving fungal cells compared to GA and THY.

Table 1: Electrolyte leakage from the *G. boninense* mycelium under the influence of phenolic compounds

Treatments (mg/mL)	Electrolyte Leakage in *G. boninense* Mycelium
Control	23.83 ± 3.7^{f}
GA-5	79.73 ± 3.82^{ab}
GA-6	79.33 ± 3.82^{ab}
GA-7	92.43 ± 3.82^{a}
GA-8	100.30 ± 3.82^{a}
THY-0.1	42.10 ± 3.72^{d}
THY-0.15	37.77 ± 3.72^{e}
THY-0.2	52.27 ± 3.72^{c}
THY-0.25	61.30 ± 3.72^{b}
PRO-2	43.43 ± 3.72^{d}
PRO- 2.5	44.8 ± 3.72^{d}
PRO-3	31.70 ± 3.72^{e}
PRO-3.5	30.27 ± 3.72^{e}
CARV-0.1	32.47 ± 3.72^{e}
CARV-0.13	22.8 ± 3.72^{f}
CARV-0.15	23.53 ± 3.72^{f}

Means with the same letter are not significantly different within the column. Each value represents a mean of four replicates. ± indicates Standard error. GA = Gallic Acid, THY= Thymol, PRO = Propolis and CARV = Carvacrol.

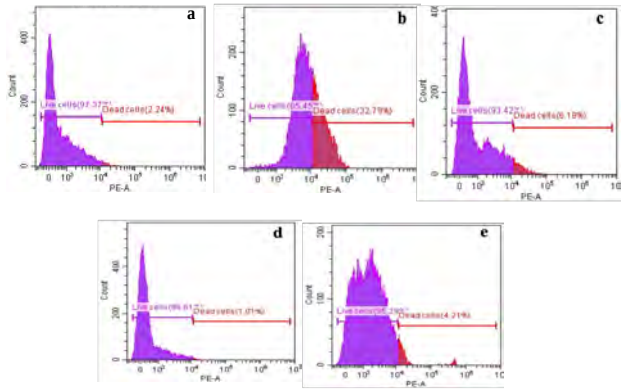

Figure 2. Flow cytometry histogram showing cell viability of *G. boninense* mycelia under control and phenolic compound treatments. Violet indicates live cells and blue indicates dead cells, based on 10000 fluorescence events

Cell membrane permeability analysis using propidium iodide, PI staining showed that control mycelia had very low cell death (2.24%), considered negligible debris. GA caused the greatest membrane damage, with 33% dead cells and strong nuclear staining, indicating severe pore formation. THY resulted in moderate damage (6.18% dead cells), while PRO (1.01%) and CARV (4.21%) caused minimal membrane disruption. Overall, GA induced the most significant cell death and membrane permeability changes, far exceeding the effects of other phenolic compounds.

Phenolic compounds significantly inhibited the radial growth of *G. boninense* mycelia and their enzyme activity, with effectiveness depending on concentration and compound type. Growth was strongly suppressed at 8mg/mL GA, 3.5mg/mL PRO and 0.25mg/mL THY. Higher concentrations generally caused greater inhibition compared to the control. Therefore, GA, PRO and THY were the most effective inhibitors demonstrating a clear impact of phenol concentration on fungal growth.

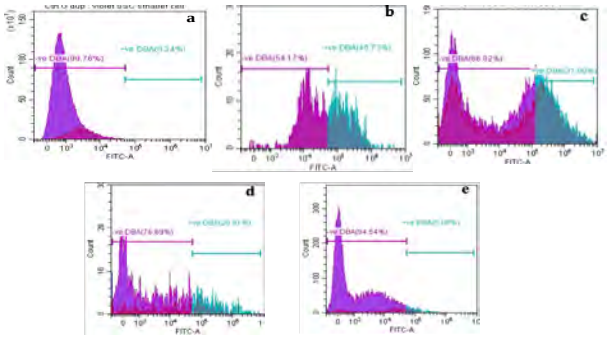

Figure 3. Flow cytometry histogram showing viability of *G. boninense* mycelia under control and phenolic treatments, with live cells in purple and dead cells in red, based on 10000 PI-stained fluorescence events

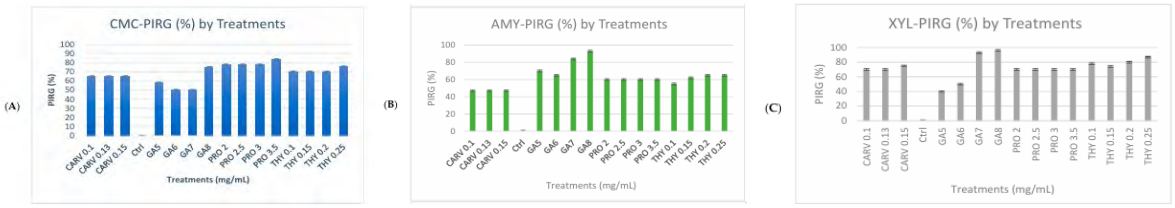

Figure 4. Percentage inhibition of radial growth (PIRG%) and corresponding enzyme production of *G. boninense* PER 71 treated with varying phenolic compound concentrations for cellulase (A), amylase (B) and xylanase (C). Values represent mean ± SE (n=4)

Phenolic compounds significantly affected enzyme production in *G. boninense* PER 71. PIRG values were highest for THY (84% at 0.25mg/mL) and CARC (80% at 0.15mg/mL), while GA (8mg/mL) and PRO (3.5mg/mL) showed lower inhibition (15% and 13.25%) respectively; $p<0.05$, Tukey HSD $p=0.0001$). GA and THY notably reduced lignin peroxidase (LiP) and manganese peroxidase (MnP) production across tested concentrations ($p=0.0055$ and <0.0001) respectively.

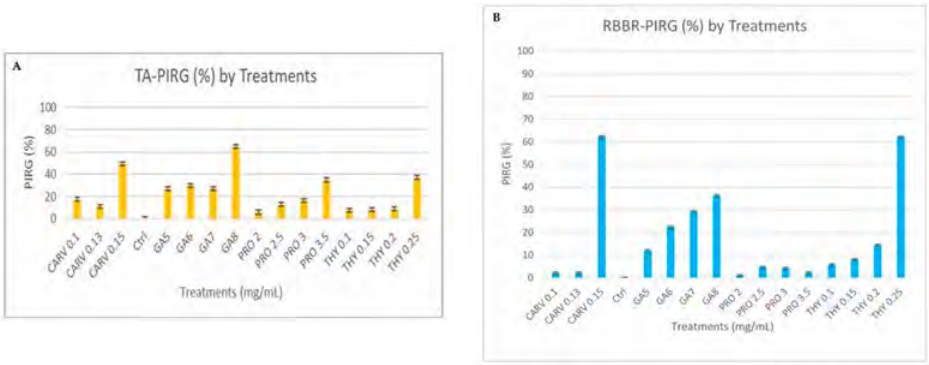

Figure 5. Percentage inhibition of radial growth (PIRG%) enzyme production of *G. boninense* PER71 treated with varying concentrations of phenolic compounds for (A) tannic acid and (B) RBBR. Values are mean ± SE (n=4)

DISCUSSION

Gallic acid (GA) and thymol (THY) demonstrated strong antifungal activity against *Ganoderma boninense*, which was closely associated with causing significant structural damage to the mycelium, including membrane collapse and cytoplasmic leakage and biochemical disruptions in

fungal cells [7]. Moreover, these phenolic compounds exhibited the most pronounced inhibitory effects, causing critical morphological alterations such as mycelial shrinkage, shriveling of the outer membrane, cytoplasmic membrane collapse and detachment of the plasma membrane. These alterations were primarily driven by these phenolic compound's ability to compromise the integrity of the cellular lipoprotein membranes, leading to increased membrane permeability, leakage of intracellular contents and the formation of pores [7]. These effects are largely due to the phenolic compound's hydrophobic nature, which disrupts the fungal cell membrane, increases permeability and leads to loss of cellular contents. Furthermore, it enables them to embed within and disrupt bilayer of the fungal membrane. GA exhibited pro-oxidant behavior, likely generating reactive oxygen species (ROS) such as H2O2 and O2- within fungal cells [8]. This oxidative stress impaired mitochondrial function disrupted intracellular Ca2+ balance and ultimately triggered cell death [9-10].

Furthermore, GA and THY effectively suppressed ligninolytic enzyme production, especially peroxidases, which are crucial for lignin degradation and host tissue colonization [7-11]. The reduction in enzyme secretion, combined with structural disruption, hindered the pathogen's ability to overcome plant defenses. Not only that, but inhibition of enzyme production was also further supported by a marked reduction in enzyme secretion and increased degradation rates, suggesting that the fungal cells were unsuccessful in developing adaptive resistance under phenolic-induced stress [8-12]. Morphological observations supported these findings, showing thin, irregular and stunted mycelial growth under phenolic compounds treatments. These results highlight GA's potential as a natural fungicide for managing basal stem rot disease in oil palm through multiple modes of action such as membrane disruption, oxidative stress and enzymatic inhibition [7; 13]. Overall, the findings suggest that GA and THY exert a multifaceted antifungal effect on *G. boninense* through membrane disruption oxidative stress induction and enzymatic inhibition [14]. These mechanisms collectively hinder fungal growth, metabolism and structural integrity, making GA, in particular, a promising natural antifungal candidate for suppressing basal stem rot (BSR) disease in oil palm plantations.

CONCLUSION

As a conclusion, among the phenolic compounds tested, gallic acid (GA), followed by thymol (THY), emerged as the most effective inhibitors of *Ganoderma boninense*, exhibiting significant antimicrobial activity and causing severe structural damage to the fungal mycelium and cellular components. These compounds, particularly GA, demonstrated strong potential in suppressing hydrolytic and ligninolytic enzyme production, which are critical to the pathogenicity of *G. boninense*. By impairing both structural integrity and enzymatic activity, GA effectively minimizes the impact of BSR disease in oil palms, offering an environmentally friendly alternative to synthetic fungicides. The findings suggest that GA holds strong potential for development as a natural fungicidal agent for the sustainable management and suppression of BSR disease in the oil palm industry.

REFERENCES

[1] Foong, S. Z. Y., Goh, C. K. M., Supramaniam, C. V., & Ng, D. K. S. (2019). Input–output optimisation model for sustainable oil palm plantation development. *Sustainable Production and Consumption, 17,* 31–46. https://doi.org/10.1016/j.spc.2018.08.010

[2] Malaysian Palm Oil Council. (2020). *Malaysian palm oil industry*. Retrieved December 2025, from https://mpoc.org.my/malaysian-palm-oil-industry/

[3] Siddiqui, Y., Surendran, A., Paterson, R. R. M., Ali, A., & Ahmad, K. (2021). Current strategies and perspectives in detection and control of basal stem rot of oil palm. *Saudi Journal of Biological Sciences, 28*(5), 2840–2849. https://doi.org/10.1016/j.sjbs.2021.02.016

[4] Labrada-Delgado, G., Aragón-Piña, A., Campos-Ramos, A., Castro-Romero, T., Amador-Muñoz, O., & Villalobos-Pietrini, R. (2012). Chemical and morphological characterization of PM2.5 collected during MILAGRO campaign using scanning electron microscopy. *Atmospheric Pollution Research, 3,* 289–300

[5] Surendran, A., Siddiqui, Y., Saud, H. M., Ali, N. S., & Manickam, S. (2018). Inhibition and kinetic studies of lignin-degrading enzymes of *Ganoderma boninense* by naturally occurring phenolic compounds. *Journal of Applied Microbiology, 125,* 876–887. https://doi.org/10.1111/jam.13922

[6] Srivastava, N., Rawat, R., Singh Oberoi, H., & Ramteke, P. W. (2015). A review on fuel ethanol production from lignocellulosic biomass. *International Journal of Green Energy, 12,* 949–960. https://doi.org/10.1080/15435075.2014.890104

[7] Ganapathy, D., Siddiqui, Y., Ahmad, K., Adzmi, F., & Ling, K. L. (2021). Alterations in mycelial morphology and flow cytometry assessment of membrane integrity of *Ganoderma boninense* stressed by phenolic compounds. *Biology, 10*(9), 930. https://doi.org/10.3390/biology10090930

[8] Zabka, M., & Pavela, R. (2014). Antifungal efficacy of some natural phenolic compounds against significant pathogenic and toxigenic filamentous fungi. *Chemosphere, 93*, 1051–1056. https://doi.org/10.1016/j.chemosphere.2013.06.084

[9] Chong, K. P., Eldaa, P. A., & Dayou, J. (2014). Relation of *Ganoderma* ergosterol content to basal stem rot disease severity index. *Advances in Environmental Biology, 8,* 14–19

[10] Ramsdale, M. (2008). Programmed cell death in pathogenic fungi. *Biochimica et Biophysica Acta (BBA) – Molecular Cell Research, 1783*(7), 1369–1380. https://doi.org/10.1016/j.bbamcr.2008.01.021

[11] Muniroh, M., Nusaibah, S., Vadamalai, G., & Siddique, Y. (2019). Proficiency of biocontrol agents as plant growth promoters and hydrolytic enzyme producers in *Ganoderma boninense*–infected oil palm seedlings. *Current Plant Biology, 20*, 100116. https://doi.org/10.1016/j.cpb.2019.100116

[12] Surendran, A., Siddiqui, Y., Saud, H. M., Ali, N. S., & Manickam, S. (2017). The antagonistic effect of phenolic compounds on ligninolytic and cellulolytic enzymes of *Ganoderma boninense*, causing basal stem rot in oil palm. *International Journal of Agriculture and Biology*, *19*(6), 1437–1446. https://doi.org/10.17957/IJAB/15.0439

[13] Fernanda, R., Siddiqui, Y., Ganapathy, D., Ahmad, K., & Surendran, A. (2021). Suppression of *Ganoderma boninense* using benzoic acid: Impact on cellular ultrastructure and anatomical changes in oil palm wood. *Forests, 12*(9), 1231. https://doi.org/10.3390/f12091231

[14] Siddiqui, Y., & Ganapathy, D. (2024). Altered cytostructure and lignolytic enzymes of *Ganoderma boninense* in response to phenolic compounds. *Microbiology Research, 15*(2), 550–566. https://doi.org/10.3390/microbiolres15020036

Prediction of MD2 Pineapple Fruit Weight from Fruit and Plant Parameters

S. Siti Nur Ezzati[1], O. Muhammad Faiz[1], K. Norshafiqah[1], G. Norhafizah[2], K.H. Then[3] and M.Y. Muhammad Rashidi[4]

[1]Department of Strategic Crops, FGV R&D Sdn Bhd, Pahang, Malaysia
[2]Unit of Statistics, FGV R&D Sdn Bhd, Negeri Sembilan, Malaysia
[3]Department of Strategic Crops, FGV R&D Sdn Bhd, Kuala Lumpur, Malaysia
[4]FGV Chuping Agro Valley, FGV Integrated Farming Holdings Sdn Bhd, Perlis, Malaysia
*Corresponding author: ezzati.s@fgvholdings.com

***Keywords**: MD2 Pineapple, fruit weight, correlation, morphological traits, yield prediction*

INTRODUCTION

Pineapple (*Ananas comosus L. Merr.*) is famous tropical crop that has significant impact economically. MD2 is one of the famous pineapple varieties in Malaysia. MD2 pineapple gains dominance in Malaysia and internationally due to its sweetness, uniform fruit shape, golden flesh color, low fiber content and high consumer acceptance [1]. Malaysia's fresh pineapple exports increased by 63% between 2011 and 2021, while pineapple-based products contributed RM1.1 billion in 2021 [2]. Therefore, many large-scale producers are trying to grab this opportunity.

International markets have stricter demand specifications as compared to local market. Most international buyers favor fruit within specific weight grades, particularly Grade A (1.40–1.99kg) and Grade B (1.00–1.39kg). These happen to meet optimal size in their local market and portray consistency. However, producers often face problems with inconsistent fruit weights, rejection leads to downgrading and losses. These could lead to worse cases of losing trust from international buyers.

Yield estimation and fruit weight prediction are essential to cater both production planning and market positioning. Accurate and non-destructive prediction of fruit weight are needed to forecast fruit weight prior to harvest.

Previous studies have linked vegetative parameters and fruit quality in pineapple [3,4]. Other recent studies showed the use of morphological traits and plant height for yield estimation in other horticultural crops like tomato, cherry and melon [5,6]. Crop models such as DSSAT Aloha Pineapple [7] provide pineapple yield simulation based on various aspects but are less practical for field use due to its complicity.

Thus, this study was conducted to find reliable traits that could best correlate with fruit weight. This will help to develop practical, field-friendly and data-driven approach prediction model that could support field operations to meet their aim of seizing global market potential by enhancing field management activities in aspect of harvest grading, yield forecasting and export planning.

OBJECTIVES

1. To predict fruit weight and estimate production volume for export purposes based on selected fruit and plant traits in MD2 pineapple
2. To develop prediction models for MD2 pineapple fruit weight using fruit and plant parameters with strong correlation coefficients
3. To identify the most practical and reliable field indicators for estimating fruit weight to support harvest grading, yield forecasting, and export planning

MATERIALS AND METHODOLOGY

The study was carried out in FGV Chuping Agro Valley (FCAV), Perlis, Malaysia. Trial plot was planted in July 2022. Flower induction was carried out in April 2023 which was nine months after planting. Harvest season for trial plot began in September 2023, 145 days after induction. Fruits were categorized based on commercial grades, which are AA (≥2.0kg), A (1.40–1.99kg), B (1.00–1.39kg), C (0.80–0.99kg), and D (≤0.79kg). Grades A–D were sampled as in Figure 1; Grade AA was not sampled due to low availability in field during harvesting season.

Figure 1. MD2 of grade A, B, C and D which had been randomly selected for sampling

Measured parameters for fruit parameters were length, diameter, line of eyes and number of eyes. For plant parameters, height, stem diameter, number of leaves, leaf length and leaf width were measured. Parameter measurements were taken by measuring tapes and digital calipers. Plant height was measured from soil level to apex of longest leaf. Stem diameter was measured at base of plant, located just above soil surface [8,9].

Pearson correlation and quadratic regression were used to assess relationships between fruit and plant traits with fruit weight. Correlation coefficients (r) and coefficient of determination (R^2)

strength was determined as follows: strong (r or $R^2 \geq 0.7$), moderate ($0.3 \geq$ r or $R^2 > 0.7$) and weak (r or $R^2 < 0.3$) [10,11]. R^2 values was used to evaluate model fit [12]. Quadratic regression was chosen here because scatterplots between morphological traits and fruit weight displayed mild curvature characteristics indicating linear models did not represent well the trend. Quadratic models had consistently produced higher R^2 values which provided a better fit to relationship compared to linear models. These models were not cross validated; thus, validation using independent datasets is recommended to assess their robustness.

RESULTS

Correlation analysis

All parameters had Coefficient of Variance (CV) less than 21.4%, except lines of eyes (Mean = 4.880±0.32, CV= 27%) and number of eyes (Mean = 59.350±4.25, CV = 29.5%) which had higher variability. Based on correlation analysis, all fruit parameters had strong positive correlation ($0.752 \leq r \leq 0.951$) which could be referred to in Table 1. Correlation analysis of plant parameters had showed that plant height, leaf width and leaf length possessed strong positive correlation ($0.633 \leq r \leq 0.793$), while number of leaves and stem diameter had moderate positive correlation ($0.513 \leq r \leq 0.516$) as in Table 1.

Table 1. Correlation between multiple variables of fruit and plant parameters with fruit weight (n=17)

Type	Variables	Mean±SE	Pearson Correlation
Fruit	Diameter	10.665±0.34	0.951**
	Length	10.635±0.55	0.934**
	Line of Eyes	4.880±0.32	0.820**
	Number of Eyes	59.350±4.25	0.752**
Plant	Height	88.650±2.40	0.793**
	Leaf Width	4.341±0.11	0.666**
	Leaf Length	81.482±2.37	0.633**
	Number of Leaves	49.710±2.02	0.516*
	Stem Diameter	7.541±0.19	0.513*

Regression models

Regression analysis of fruit and plant parameters had shown that fruit diameter had the highest reliability to be the best predictor among all parameters. Thus, best predictive model was based on fruit diameter and followed by fruit length which model fit by 92% ($R^2 = 0.922$) and 88% ($R^2 = 0.8761$), respectively. Line of eyes ($R^2 = 0.6772$) and number of eyes ($R^2 = 0.5663$) showed moderate association.

The quadratic curve model developed represent pineapple fruit weight indicated that plant height had the highest coefficient of determination among plant parameters ($R^2 = 0.6501$) which fit the model by 65%. Consistent with the model establishment phase, the models predicting stem diameter were unsuitable, with a low coefficient of determination ($R^2 = 0.2651$). In contrast, leaf width, leaf length, and number of leaves demonstrated moderate reliability, with R^2 values of 0.4601, 0.4403, and 0.4012 respectively. Predictive model for fruit diameter was as below while

others could be referred to Figure 2:

$$FW = 0.0294*(FD)^2 - 0.3528*(FD) + 1.3799 \quad (1)$$

where FW is fruit weight in kg and FD is fruit diameter in cm.

DISSCUSSION

Fruit parameters, particularly diameter and length, are highly reliable non-destructive predictors of MD2 fruit weight. Based on Eq. (1) and (2), we could conclude that fruit diameter for AA (≥13.6cm), A (12.1–13.6cm), B (10.8–12.0cm), C (10.1–10.7cm), and D (≤10.0cm). In Physical Science, weight is known as mass, which is the product of density and volume. Thus, this demonstrates fruit weight involvement with both diameter and length. Based on our data, fruit size composed of fruit diameter and length has shown moderate variability ($13.2 \leq CV \leq 21.4$). This indicated that most fruits were uniform, while some variability is important to help with fruit weight estimation. This agrees with findings in other fruit crops where morphological traits able to correlate with yield [5-6]. Both parameters are non-destructive; however, it is non-practical for field supervision.

The strong relationship between plant height and fruit weight highlights the role of vegetative vigor activity in fruit development, consistent with earlier pineapple studies [13]. Unlike fruit parameters which are destructive, plant height serves better as a practical early prediction for estimating yield potential. For commercial plantations, each of these models could be used based on their intended purpose. Diameter and length predictive model could be used for in-field grading during harvesting which makes it able to reduce errors in harvesting fruits that do not meet export grades. This could also help to ensure any miscalculation in yield forecasting could be detected early. With more research studies, this approach could be developed into fruit development simulation and enhance for higher accuracy of yield forecasting in future. On the other hand, plant height predictive models have potential to be used to predict yield before fruit development stages. Plant height predictive model could also help in plantation management decision making.

Compared with simulation-based approaches [7], regression models require only basic field measurements, making them more practical for large-scale applications. However, validation across multiple environments is needed, and integration with digital phenotyping tools may enhance precision [6][14].

CONCLUSION

Fruit weight of MD2 can best predicted using fruit diameter and length, which are practical, efficient, and non-destructive traits for in-field grading. The predictive model of plant height enables early yield estimation. Both functions help reduce grading errors, minimize post-harvest losses, and supports better planning for marketing and export. This approach improves efficiency and profitability in the Malaysian pineapple industry.

ACKNOWLEDGEMENTS

The authors thank FGV R&D Sdn. Bhd. and FGV Integrated Farming Holdings Sdn. Bhd. for funding and support and acknowledge the Strategic Crops Unit and FCAV staff for field data collection.

REFERENCES

[1] Paull, R. E., & Duarte, O. (2025). *Tropical fruits* (Vol. 1, pp. 327–365). CABI

[2] LPNM. (2015–2021). *Laporan tahunan LPNM*. https://www.mpib.gov.my/penerbitan/

[3] Murai, K., Chen, N. J., & Paull, R. E. (2021). Pineapple crown and slip removal on fruit quality and translucency. *Scientia Horticulturae, 283*, 110087

[4] Fassinou Hotegni, V. N., Lommen, W. J., Agbossou, E. K., & Struik, P. C. (2015). Selective pruning in pineapple plants as means to reduce heterogeneity in fruit quality. *SpringerPlus, 4*(1), 129

[5] Johansen, K., Morton, M. J., Malbeteau, Y., Aragon, B., Al-Mashharawi, S., Ziliani, M. G., & McCabe, M. F. (2020). Predicting biomass and yield in a tomato phenotyping experiment using UAV imagery and random forest. *Frontiers in Artificial Intelligence, 3*, 28

[6] Li, B., Lecourt, J., & Bishop, G. (2018). Advances in non-destructive early assessment of fruit ripeness towards defining optimal time of harvest and yield prediction: A review. *Plants, 7*(1), 3

[7] Vásquez Jiménez, J., Bartholomew, D. P., Wilkerson, C. J., Hoogenboom, G., & Vargas Leitón, B. (2024). Predicting growth and development of the pineapple cultivar 'MD-2' with the DSSAT Aloha Pineapple Model. *International Society for Horticultural Science (ISHS), 79*(1), 1–12

[8] Gonzales, J., & Vriesenga, J. (2006). *Pineapple plant named 'P-1972'* (U.S. Plant Patent No. PP16,396 P3). United States Patent and Trademark Office. https://patents.google.com/patent/USPP16396P3/en

[9] Sekiya, F. F. (2012). *Pineapple plant named 'Franklynn'* (U.S. Plant Patent No. PP23,193 P3). United States Patent and Trademark Office. https://patents.google.com/patent/USPP16396P3/en

[10] Jat, M. L., Rana, G. S., Baloda, S., Shivran, J. S., Jat, R. K., Mor, R., & Kumari, S. (2024). Correlation and regression analysis between agronomic and quality attributes of apple (*Malus* × *domestica* Borkh.) cv. Anna. *Journal of Advances in Biology & Biotechnology, 27*(10), 479–490

[11] Cieniawska, B., Pentoś, K., & Szulc, T. (2022). Correlation and regression analysis of spraying process quality indicators. *Applied Sciences, 12*(23), 12034

[12] Chicco, D., Warrens, M. J., & Jurman, G. (2021). The coefficient of determination R-squared is more informative than SMAPE, MAE, MAPE, MSE and RMSE in regression analysis evaluation. *PeerJ Computer Science, 7*, e623

[13] Fassinou Hotegni, V. N., Lommen, W. J., Agbossou, E. K., & Struik, P. C. (2015). Influence of weight and type of planting material on fruit quality and its heterogeneity in pineapple [*Ananas comosus* (L.) Merrill]. *Frontiers in Plant Science, 5*, 798

[14] Putra, A. N., Kristiawati, W., Mumtazydah, D. C., Anggarwati, T., Annisa, R., Sholikah, D. H., & Okiyanto, D. (2021). Pineapple biomass estimation using unmanned aerial vehicle in various forcing stage: Vegetation index approach from ultra-high-resolution image. *Smart Agricultural Technology, 1*, 100025.

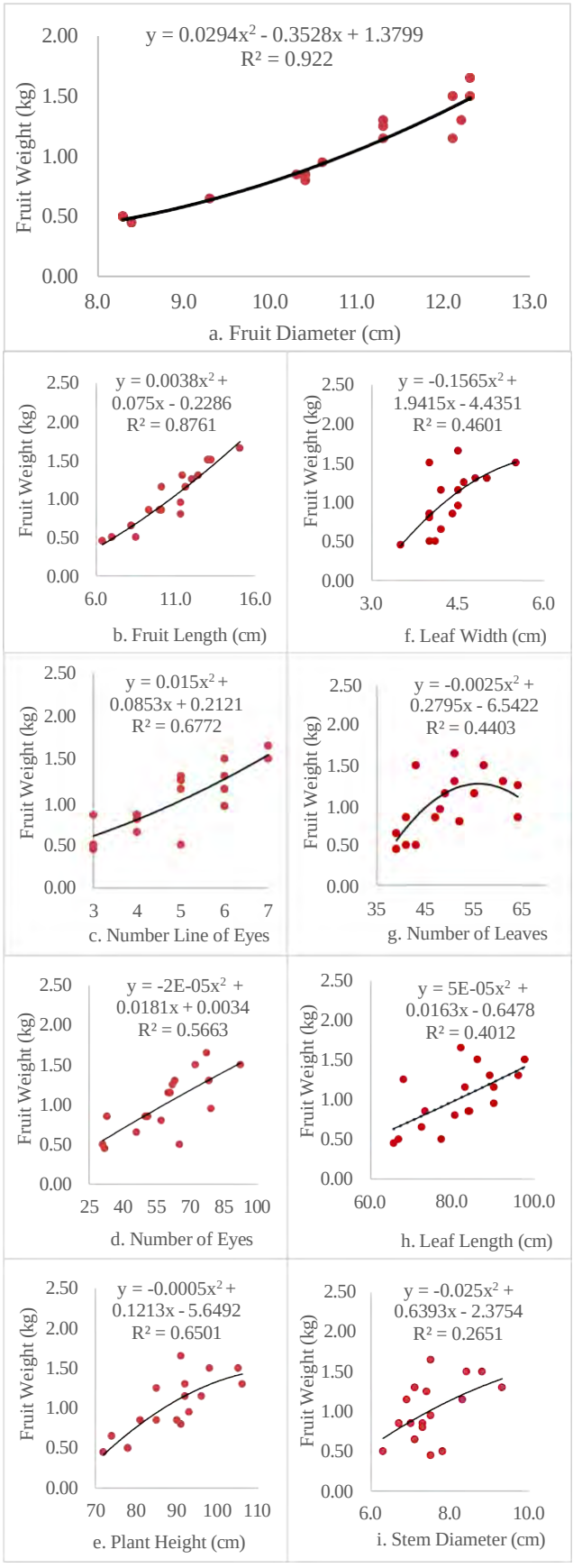

Figure 2. Quadratic regression between fruit weight with fruit diameter (a), fruit length (b), number line of eyes (c), number of eyes (d), plant height (e), leaf width (f), number of leaves (g), leaf length (h) and stem diameter (i)

Detection of Oil Palm Frond Number 17 Using Aerial Imagery and Spiral Angle Modelling

M.F. Abu Muntalib[1,3*], M.S.M. Kassim[1,2], A. Wayayok[2], A.F. Abdullah[2], 'A. Muhadi[2], Z. Khuzaimah[1] and M.Z.S.N.M. Emran[3]

[1]Institute of Plantation Studies, Universiti Putra Malaysia, Serdang, Selangor, Malaysia
[2]Department of Biological and Agricultural Engineering, Faculty of Engineering, Universiti Putra Malaysia, Serdang, Selangor, Malaysia
[3]Putra Agriculture Centre, Universiti Putra Malaysia, Serdang, Selangor, Malaysia
*Corresponding author: m_fitri@upm.edu.my

***Keywords**: Oil palm, frond detection, aerial imaging, phyllotaxis, UAV, spiral modelling, precision agriculture*

INTRODUCTION

Oil palm is the most valuable crop in the industry, contributing significantly to Malaysia's economic sectors [1-4]. Management of Oil Palm Fronds (OPF) in the field is crucial for the effectiveness of bunch productivity [5] and crop health monitoring [6]. Nutrient analysis of frond 17 is crucial for plant nutrient indicators [7-9]. The current practice for frond determination in the field varies among farmers and is only carried out by a competent person [12]. Inaccurate identification of frond can lead to misinterpretation of vital agronomic data, ultimately compromising decision-making processes related to crop productivity and the long-term sustainability of the plantation.

The utilization of Unmanned Aerial Vehicles (UAVs) in the plantation sector is extensive nowadays [15]. Aerial imaging systems are used in many oil palm plantation management systems, vitally for plant health monitoring [16-18]. This approach can facilitate faster frond detection using aerial images compared to traditional methods. However, precise identification of Frond Number 17 (FN17) remains challenging due to overlapping canopies and variations in phyllotactic patterns. Therefore, this study proposes an integrated approach using aerial imagery and spiral angle modelling to accurately locate FN17 based on geometric and phyllotactic relationships among fronds

MATERIALS AND METHODS

The study was conducted at an oil palm plantation under the management of Universiti Putra Malaysia. UAV imagery was collected using a MicaSense RedEdge-MX multispectral sensor mounted on a DJI platform. The flights were conducted at an altitude of 80 m, generating high-resolution orthomosaic and reflectance maps.

Agisoft Metashape Professional (v2.2.0) was used to process UAV images, including alignment, dense cloud generation, and orthomosaic export. A Two-Dimensional Phyllotaxis Image Template (2DPIT) was developed based on the Fibonacci spiral arrangement of fronds (Figure 1), establishing angular positions for each frond. FN1 and FN9 were identified as reference points to compute the divergence angle toward FN17.

An exponential decay model $\theta(n) = A * e \wedge (-kn)$ was applied to describe the angular change along successive fronds. The model parameters A and k were calibrated using ground-measured trunk pseudobark angles and validated using fronds FN2–FN8. Error metrics, including mean absolute error (MAE) and root mean square error (RMSE), were used to assess model performance.

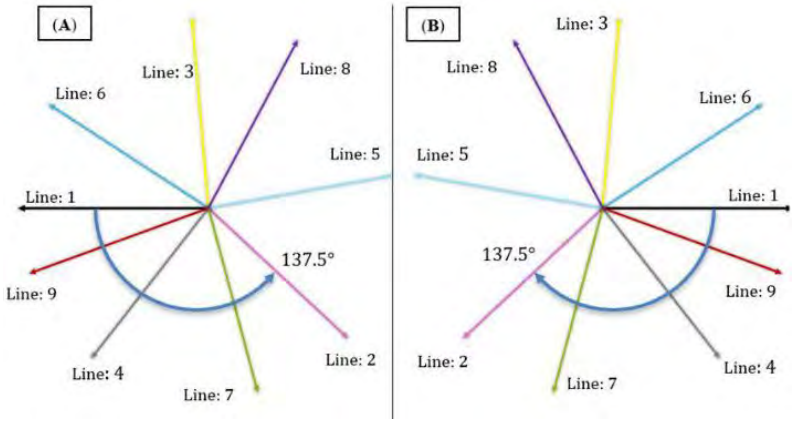

Figure 1. (A) Left-spiral line 1-9 follows a 137.5°, (B) Right-spiral line 1-9 follows a 137.5°

RESULTS AND DISCUSSIONS

Frond angular variability and age influence

Results indicated that FN1 exhibited the greatest variability in angular orientation, particularly in younger palms, suggesting active phyllotactic adjustment during early canopy development. Conversely, FN9 maintained consistent vertical stability, confirming its reliability as a geometric anchor point for subsequent angular calculations.

Table 1 presents comparative deviation angles for aerial and trunk-based frond observations across plantations of varying ages. Although ANOVA revealed no statistically significant differences among blocks, notable interaction effects between block and angle measurements were observed. Block D (18 years after planting) exhibited greater aerial deviation angles, implying structural canopy expansion with age. In contrast, Block B (12 years after planting) showed lower trunk and pseudo bark angular deviations, likely reflecting higher vertical alignment typical of mid-aged palms.

Table 1: Deviation angle of aerial and ground FN1 and FN9 at different blocks with different angle measurement

Item	AAFN 1*	AAFN 9*	TAFN 1*	TAFN 9*
ANOVA				
Block (B)	ns	ns	ns	ns
Angle (A)	ns	ns	ns	ns
B x A	**	ns	**	**
Block				
A (13 YAP)	26.80 b	7.62 a	24.92 ab	12.92 ab
B (12 YAP)	29.55 ab	11.05 a	20.33 b	9.42 b
C (15 YAP)	32.10 a	11.56 a	29.83 ab	14.92 a
D (18 YAP)	32.65 a	12.75 a	25.50 ab	12.92 ab
E (08 YAP)	28.39 ab	7.16 a	33.25 a	13.08 ab
Mean	**29.90**	**10.03**	**26.77**	**12.65**

ANOVA, analysis of variance; no significant difference.

*AAFN1 (Aerial angle frond number one), AAFN9 (Aerial angle frond number nine), TAFN1 (Trunk angle frond number one), TAFN9 (Trunk angle frond number nine), YAP (Years after planting). All the means are presented in degrees.

**Significant at $p < 0.05$, Means with different letters vertically within each age at different blocks are significantly different

Model accuracy and error analysis

The exponential decay model achieved high predictive accuracy for right-handed spirals, with MAE = 3.02° and RMSE = 3.85°. Left-handed spirals showed slightly higher errors (MAE = 3.94°, RMSE = 4.76°), possibly due to canopy asymmetry or image detection noise introduced during orthomosaic alignment.

Frond deviation and canopy implications

Deviation angle analysis across different age groups revealed dynamic patterns of canopy adjustment. These results are consistent with findings by [15], who reported that variations in frond orientation influence canopy interpretation and disease detection accuracy. The aerial angle of FN1 showed the highest mean deviation, indicating substantial angular displacement at the initial frond position. In contrast, FN9 exhibited the lowest mean deviation (10.03°), reflecting reduced variability with increasing frond number.

Overall, frond deviation tended to decrease with palm maturity, with the largest variations occurring at approximately 18 years after planting. This trend suggests structural stabilization of older canopies, contributing to improved light interception and reduced mechanical stress.

Frond 17 (FN17) was observed at an approximate deviation angle of 7°-9°, which corresponds with its physiological function as a structurally stable, mature leaf frequently utilized for nutrient sampling. This modelling approach establishes a robust framework for integrating angular

structure with canopy monitoring and nutrient evaluation in precision agriculture. The combination of UAV imagery and the 2DPIT framework effectively reconstructed the spiral phyllotaxis pattern of the oil palm, enabling accurate predictions of FN17's location. The resulting model enhances automated canopy mapping and presents significant potential for applications in nutrient management and yield forecasting.

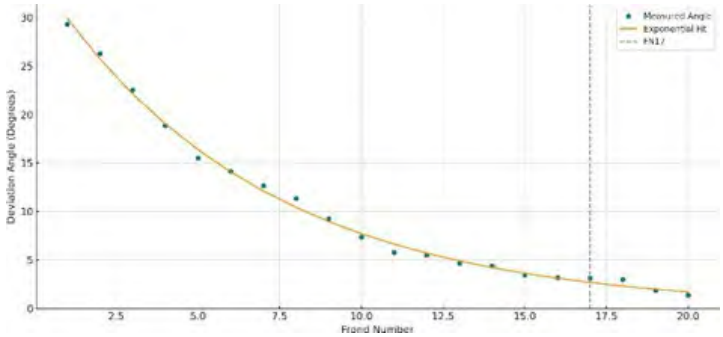

Figure 2. Exponential deviation angle modelling across frond numbers

CONCLUSIONS

A thorough understanding of the phyllotactic arrangement of oil palm and its corresponding frond divergence patterns establishes a solid basis for precise frond detection through aerial imagery. In addition to structural interpretation, the proposed method facilitates the accurate identification of FN17, the standard frond used for nutrient assessment, thereby enhancing the connection between canopy morphology and agronomic decision-making. This framework promotes precision nutrient management, enables spatial monitoring of the physiological status of the palms, and improves sampling consistency across plantations.

The 2DPIT-based frond identification model provides agronomists with a practical and standardized method for accurately locating FN1, FN9, and FN17, offering greater consistency compared to traditional ground-based assessments. By minimizing dependence on subjective visual judgment, agronomists can conduct nutrient sampling, canopy health evaluations, and phenological monitoring with greater precision. When combined with UAV imagery, this model facilitates semi-automated or fully automated detection pipelines, enabling the swift processing of large image datasets through fixed geometric rules instead of complex manual interpretations. This potential for automation significantly reduces labour requirements and allows for timely monitoring across extensive plantation areas. Furthermore, being geometry-driven and not reliant on 3D reconstruction, the model remains lightweight and computationally efficient, making it scalable for large estates and compatible with routine aerial surveys. Consequently, plantation managers can utilize this system to improve decision-making, enhance sampling precision, and support broader precision agriculture initiatives at both the estate and regional levels.

REFERENCES

[1] Kushairi, A., Ong-Abdullah, M., Nambiappan, B., Hishamuddin, E., Bidin, M. N. I. Z., Ghazali, R., ... Parveez, G. K. A. (2019). Oil palm economic performance in Malaysia and R&D progress in 2018. *Journal of Oil Palm Research, 31*(2), 165–194.

[2] Ahmad, M., Ismail, R., Kamarulzaman, N. H., & Ghani, F. (2024). Socio-economic impacts of oil palm plantations in Malaysia: A review of economic and environmental perspectives. *Advanced International Journal of Business, Entrepreneurship and SME's, 6*(20), 319–330.

[3] Ali, M. S., Vaiappuri, S. K. N., & Tariq, S. (2024). *Malaysian oil palm industry* (pp. 268–284). IGI Global. https://doi.org/10.4018/979-8-3693-2149-2.ch014

[4] Zachlod, N., Hudecheck, M., Sirén, C., & George, G. (2025). Sustainable palm oil certification inadvertently affects production efficiency in Malaysia. *Communications Earth & Environment, 6*(1), 200.

[5] Formaglio, G., Veldkamp, E., Damris, M., Tjoa, A., & Corre, M. D. (2021). Mulching with pruned fronds promotes the internal soil N cycling and soil fertility in a large-scale oil palm plantation. *Biogeochemistry, 154*(1), 63–80.

[6] Amirruddin, A. D., Muharam, F. M., Ismail, M. H., Tan, N. P., & Ismail, M. F. (2020). Hyperspectral spectroscopy and imbalance data approaches for classification of oil palm macronutrients observed from frond 9 and 17. *Computers and Electronics in Agriculture, 178*, 105768.

[7] Lundegårdh, H. (1943). Leaf analysis as a guide to soil fertility. *Nature, 151*(3828), 310–311.

[8] De Mello Prado, R., & Rozane, D. E. (2020). Leaf analysis as diagnostic tool for balanced fertilization in tropical fruits. In *Fruit crops* (pp. 131–143).

[9] Janani, M., & Jebakumar, R. (2022, December). Analysis of leaf nutrient concentration in different crop species using image processing techniques. In *2022 Fourth International Conference on Emerging Research in Electronics, Computer Science and Technology (ICERECT)* (pp. 1–7). IEEE.

[10] Ahmad, M. N., Sharif, A. R. M., & Moslim, R. (2024). The functionality and features of AI automated detector and counter, Oto-Bac™ for bagworm census in oil palm plantation. *Indian Journal of Engineering and Materials Sciences, 31*(6), 914–921.

[11] Khuzaimah, Z., Nawi, N. M., Adam, S. N., Kalantar, B., Emeka, O. J., & Ueda, N. (2022). Application and potential of drone technology in oil palm plantation: Potential and limitations. *Journal of Sensors, 2022*, Article 5385505.

[12] Zheng, J., Fu, H., Li, W., Wu, W., Yu, L., Yuan, S., ... Kanniah, K. D. (2021). Growing status observation for oil palm trees using unmanned aerial vehicle (UAV) images. *ISPRS Journal of Photogrammetry and Remote Sensing, 173*, 95–121.

[13] Ahmadi, P., Mansor, S., Farjad, B., & Ghaderpour, E. (2022). Unmanned aerial vehicle (UAV)-based remote sensing for early-stage detection of *Ganoderma*. *Remote Sensing, 14*(5), 1239.

[14] Kouadio, L., El Jarroudi, M., Belabess, Z., Laasli, S. E., Roni, M. Z. K., Amine, I. D. I., ... Lahlali, R. (2023). A review on UAV-based applications for plant disease detection and monitoring. *Remote Sensing, 15*(17), 4273.

[15] Azuan, N. H., Khairunniza-Bejo, S., Abdullah, A. F., Kassim, M. S. M., & Ahmad, D. (2019). Analysis of changes in oil palm canopy architecture from basal stem rot using terrestrial laser scanner. *Plant Disease, 103*(12), 3218–3225.

Soil Microbial Diversity Under Oil Palm Agroforestry

N.J.J. Azleen[1], W.Y. Yeong[1], M.F. Sulaiman[1*], R. Robert[2], M.A. Adibah[1], S.K. Daljit and A. Rival[3]

[1]Department of Land Management, Faculty of Agriculture, Universiti Putra Malaysia, Serdang, Malaysia
[2]Chemistry and Phytochemistry Section, Forest Research Centre, Sabah Forestry Department, Sandakan, Malaysia
[3]UMR Biodiversified Agrosystems (ABSys), CIRAD, Jakarta, Indonesia
*Corresponding author: muhdfirdaus@upm.edu.my

Keywords*: Soil microbiome, agroforestry system, plant-microbe interactions, sustainable land use, 16S rRNA sequencing*

INTRODUCTION

Oil palm (*Elaeis guineensis*) is an important oil crop in Southeast Asian countries, with Indonesia and Malaysia currently in the lead of oil palm land use area for palm oil production [1]. The commercialization of oil palm in this region was initiated as an alternative of another commodity crop which prices are more volatile. Despite its economic benefits, oil palms are often criticized for their role in tropical deforestation which resulted in severe biodiversity losses. Although oil palm industry might have driven deforestation to a certain extent in this region, some plantations might also be established on lands initially deforested for other reasons [2]. Regardless of its role in deforestation, oil palm plantations are typically established as a monoculture, which simplifies the once complex landscape, significantly reducing the biodiversity of an area. For instance, a study in Malaysia revealed almost a 35% decrease in species diversity in oil palm plantations as opposed to forests, with about 80% of species present in the forest absent from the plantation [3]. Thus, this puts the oil palm industry under the global sustainability pressure, which leads to the introduction of expansion caps for oil palm expansion in Malaysia. Malaysia is committed to the existing 6.5 million hectares cap on oil palm land use policy, which was revised by the National Agricommodity Policy (2021-2030). While this effort is promising, it is preventative; thus, it should be complemented by efforts to improve the sustainability of existing plantations.

Agroforestry — agriculture incorporating cultivation of trees — is gaining traction in various agricultural establishments, which are often established by smallholders for income diversification. Apart from income diversification, a meta-analysis found that agroforestry can increase fauna diversity by providing it with a more favorable microclimate and sometimes even food sources [6], allowing it to support native species and used for biodiversity conservation [7]. However, a study from [8] found that study on biodiversity in agroforestry systems in general was heavily focused on trees and wildlife with less attention given to the soil microfauna. Thus,

understanding of agroforestry on soil microbial diversity remains limited.

Soil microbes are the key player in maintaining ecosystem health due to their role in organic matter decomposition, nutrient cycling, disease suppression, etc. However, these microbes are sensitive towards changes in soil properties, with pH being the most important property in shaping soil microbial communities [11], [12]. In oil palm plantation, nitrogen enrichment is particularly crucial to ensure high productivity; yet, excessive and repeated application will reduce soil pH, thus altering its soil microbial diversity. This alteration may affect ecosystem services provided by the microbes, thus affecting the overall ecosystem health. Microbial diversity is positively correlated with an ecosystem's multifunctionality [13]; thus, loss in microbial diversity may reduce the ability of an ecosystem to sustain its ecological functions. Therefore, it may negatively affect the ecosystem health, which is risky given that it is already threatened by climate change.

In the context of oil palm agroforestry, according to [14], it is mostly paired with fruit crops (*Zea mays*, *Arachis hypogaea* and *Musa* sp.) where in this case, oil palm would be considered as a tree species. Meanwhile, combination of oil palm and timber tree for a more permanent agroforestry was found to be the least practiced form of oil palm agroforestry. Although there is some research on oil palm agroforestry, studies are more likely to focus on yield maximization, soil properties and carbon stock [15], [16], [17], [18] rather than biodiversity improvement, particularly at microbial level. Thus, further limiting the understanding on microbial diversity in oil palm agroforestry.

METHODOLOGY

The study was conducted in Melangking Oil Palm Plantation (MOPP) at the vicinity of Kinabatangan River in Sukau, Sabah. A native forest species (*Nauclea subdita*) was incorporated in the agroforestry plot where two trees were interplanted in between two palms as shown in Figure 1. Monoculture plots were established as control. Both monoculture and the agroforestry plots follow the conventional planting density, planting design and upkeep. The establishment of monoculture and agroforestry treatments were done simultaneously in 2022 with five replications for each treatment. A Riparian buffer zone consisting of 30 years old palm stands with mixed forest species which are in the plantation was included in this study. The inclusion of this riparian buffer zone is to serve as a reference site for a less disturbed environment, since the palms in the riparian buffer zone were not harvested since the planting of forest species in 2020.

A composite soil sample consisting of 3 sub-samples was collected from every replicate at two depths, 0-15 cm and 15-30 and immediately stored in a chiller box filled with ice blocks to preserve sample integrity. The samples were transported chill to the laboratory, then stored at - 80°C until DNA extraction. DNA extraction was done using ZymoBIOMICS DNA/RNA Miniprep Kit (Zymo Research, USA), the sent for amplicon library preparation and analysis. Microbial diversity was assessed using 16S rRNA sequencing.

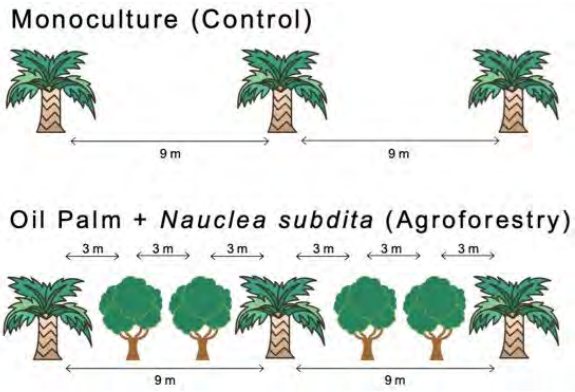

Figure 1. Schematic representation of the monoculture and agroforestry planting design showing the arrangement and spacing of each species

Analyses on microbial community were done using Microbiomenalyst, which includes indicators such as alpha and beta diversity, relative abundance, and microbial taxonomic composition between systems were compared to evaluate the effects of agroforestry on soil microbial diversity. Alpha diversity, which is the measure of within sample diversity was calculated using Shannon-Wiener diversity index, while the difference between samples was assessed using Bray-Curtis index. The dissimilarity pattern was visualized using Principal Coordinate Analysis (PCoA), then assessed using PERMANOVA. The relative abundance analysis across samples were done at the class taxonomic level.

RESULTS AND DISCUSSION

The alpha diversity measured through the Shannon-Wiener index showed no significant difference between treatments after false discovery rate (FDR) correction (q-value=0.201). This indicates comparable microbial species richness and evenness between monoculture, agroforestry, and riparian plots. PERMANOVA analysis for beta diversity revealed that treatment type accounted for 28% of the variation observed in soil microbial community composition across treatments at p-value=0.034. However, similarly, the significant difference was not retained after FDR correction, suggesting overall comparable microbial community composition across treatments. Principal coordinate analysis (PCoA) based on Bray–Curtis dissimilarity showed no clear separation of microbial community across treatments but rather overlapping ellipses, suggesting that the groups are more alike (Figure 2).

Microbial community composition at the class level was also comparable across samples, with some fluctuations in relative abundances, especially for Ktedonobacteria in a sample from the riparian. Nonetheless, no significant difference was found differential abundance of microbial class despite the fluctuations. Overall, these results suggest that the incorporation of native forest species did not alter soil microbial diversity and composition.

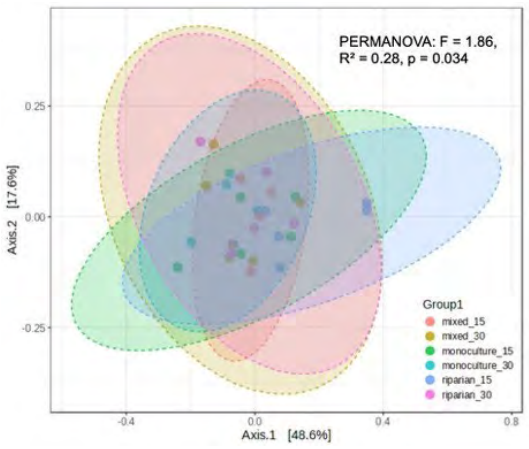

Figure 2. Principal coordinate analysis (PCoA) based on Bray-Curtis dissimilarity where each point represents a sample, colored by treatment. Ellipses represent 95% confidence intervals. “Mixed” represent agroforestry plots

CONCLUSIONS

The comparable microbial diversity and composition observed between different land use only reflected short-term oil palm agroforestry results, as the soil sampling was taken only two years into the experiment, with only one sampling event to date. Thus, this observation suggests that interplanting native forest species within oil palm might need a longer observation period to detect potential patterns or changes in the soil microbial community. The comparable pattern may also indicate that there is a more dominant factor than land use in determining soil microbial diversity, such as management. Thus, a longer observation period might be needed to allow for microbial changes to gradually occur to understand the effect of agroforestry on soil microbial community composition.

REFERENCES

[1] Ritchie, H. (2021). *Palm oil*. Our World in Data. https://ourworldindata.org/palm-oil

[2] Fitzherbert, E. B., Struebig, M. J., Morel, A., Danielsen, F., Brühl, C. A., Donald, P. F., & Phalan, B. (2008). How will oil palm expansion affect biodiversity? *Trends in Ecology & Evolution, 23*(10), 538–545. https://doi.org/10.1016/j.tree.2008.06.012

[3] Dhandapani, S. (2024). *Biodiversity loss associated with oil palm plantations in Malaysia: Serving the need versus saving the nature*. ResearchGate.

[4] Decaëns, T., Santos, A. M. S., Loucougaray, C., Pauli, J. G., & Dubs, R. (2018). Biodiversity loss along a gradient of deforestation in Amazonian agricultural landscapes. *Conservation Biology, 32*(6), 1380–1391.

[5] Vijay, V., Pimm, S. L., Jenkins, C. N., & Smith, S. J. (2016). The impacts of oil palm on recent deforestation and biodiversity loss. *PLOS ONE, 11*(7), e0159668. https://doi.org/10.1371/journal.pone.0159668

[6] Udawatta, R. P., Rankoth, L., & Jose, S. (2019). [Article on agroforestry and sustainability]. *Sustainability, 11*, 2879.

[7] Schroth, G., da Fonseca, G. A. B., Harvey, C. A., Gascon, C., Vasconcelos, H. L., & Izac, A.-M. N. (Eds.). (2004). *Agroforestry and biodiversity conservation in tropical landscapes*. Island Press.

[8] Marsden, C., Martin-Chave, A., Cortet, J., Hedde, M., & Capowiez, Y. (2020). How agroforestry systems influence soil fauna and their functions: A review. *Plant and Soil, 453*(1–2), 29–44.

[9] Wang, W., Li, X., Zhang, L., Chen, Z., Zhang, Y., & He, X. (2022). Effects of plantation type and soil depth on microbial community structure and nutrient cycling function. *Frontiers in Microbiology, 13*, 846468. https://doi.org/10.3389/fmicb.2022.846468

[10] Abadeye, T., Yitbarek, T., Zewide, I., & Adimasu, K. (2023). Assessing soil fertility influenced by land use in Moche, Gurage Zone, Ethiopia. *The Scientific Temper, 14*(1), 80–92. https://doi.org/10.58414/SCIENTIFICTEMPER.2023.14.1.10

[11] Muneer, M. A., Zhang, X., Lin, J., Chen, Y., & Li, C. (2022). Soil pH: A key edaphic factor regulating distribution and functions of bacterial community along vertical soil profiles in red soil of pomelo orchard. *BMC Microbiology, 22*, 38. https://doi.org/10.1186/s12866-022-02452-x

[12] Zhong, Y. Q. W., Yan, W. M., Canisares, L. P., Wang, S., & Brodie, E. L. (2023). Alterations in soil pH emerge as a key driver of the impact of global change on soil microbial nitrogen cycling: Evidence from a global meta-analysis. *Global Ecology and Biogeography, 32*(1), 145–165

[13] Che, Y., & Jin, G. (2024). Plant–soil microbial diversity and structural attributes jointly dominate the multifunctionality of the temperate forest. *Ecological Indicators, 166*, 112282. https://doi.org/10.1016/j.ecolind.2024.112282

[14] Masure, A., Martin, P., Lacan, X., & Rafflegeau, S. (2023). [Article on oil palm-based agroforestry systems]. *Cahiers Agricultures, 32*, 16

[15] Abubakar, A., Kasim, S., Ishak, M. Y., & Uddin, M. K. (2023). Maximizing oil palm yield: Innovative replanting strategies for sustainable productivity. *Journal of Environment and Earth Science, 5*(2), 59–70

[16] Agriani, F., Kaido, B., Syahputri, S. O., Zakaria, A., & Afdhal. (2025). [Article on oil palm-based agroforestry in Indonesia]. *Jurnal Agronomi Tanaman Tropika (JUATIKA), 7*(1), 1–10

[17] Ahirwal, J., Sahoo, U. K., Thangjam, U., & Thong, P. (2022). [Article on agroforestry, ecosystem services and sustainability]. *Sustainable Production and Consumption, 30,* 478–487.

[18] Besar, N. A., Suardi, H., Phua, M.-H., James, D., Mokhtar, M. B., & Ahmed, M. F. (2020). [Article on monitoring oil palm plantations using remote sensing/UAV data]. *Forests, 11*(2), 210.

Development of a Machine Vision System for Automatic Plant Health Levels Evaluation Due to *Ganoderma Boninense* Infection in an *In Vitro* Setup

N.A.H.M Baktiar[1], S. Khairunniza-Bejo[1,2,3*], M. Jahari[1], N.A. Husin[1,2], N.A. Muhadi[1], S. Vetaryan[3], H.W. Yeng[3], A.F.F.A. Wahab[3], S.A. Bakar[3], N.A.M. Zim[3] and L.Y. Ping[3]

[1]Department of Biological and Agricultural Engineering, Faculty of Engineering, Universiti Putra Malaysia, Selangor, Malaysia
[2]Institute of Plantation Studies, Universiti Putra Malaysia, Selangor, Malaysia
[3]Smart Farming Technology Research Centre, Universiti Putra Malaysia, Selangor, Malaysia
[4]FGV R&D Sdn. Bhd., FGV Innovation Centre, Negeri Sembilan, Malaysia
*Corresponding author: skbejo@upm.edu.my

Keywords*: Ganoderma boninense, hue, saturation, value, automatic detection, machine learning*

INTRODUCTION

Ganoderma boninense (*G. boninense*) is a major fungal pathogen responsible for basal stem rot (BSR), a disease that significantly reduces oil palm yield and plantation productivity across Southeast Asia. Early and accurate detection of *G. boninense* infection is crucial to prevent further disease spread and enable timely management interventions. Traditionally, the evaluation of plant health and disease severity has relied on visual observation and expert judgement, which are often subjective, time-consuming, and prone to human error. Hence, there is a need for an automated, reliable, and non-destructive system that can assess infection severity.

Machine vision technology, supported by advanced image processing and machine learning algorithms, offers a promising solution for automated plant health assessment. By analysing visual cues such as colour variation, texture, and morphological changes, machine vision can accurately differentiate between healthy and infected plants. Among various colour models, the hue saturation value (HSV) colour space provides advantages in separating luminance from chromaticity, enhancing the robustness of image analysis under variable lighting conditions.

Prior works have applied machine learning models and deep learning architectures to classify plant diseases or detect *G. boninense* from spectral or imaging data [1-2]. Yet, the application to in vitro oil palm samples under controlled infection with *G. boninense* remains underexplored. Therefore, this study focuses on developing a machine vision system for the automatic evaluation of oil palm plant health levels under in vitro conditions infected by *G. boninense*.

METHODOLOGY

This study aimed to develop a machine vision system for automated evaluation of oil palm health levels due to G. boninense infection under in vitro conditions. The overall process involved four main stages: sample preparation and disease severity classification, image acquisition, image processing, and machine learning classification. Oil palm ramets were categorized into several severity levels based on expert evaluation. Standardized image acquisition was conducted using a fixed camera setup before proceeding with image processing. The analysis was done in the HSV colour space to extract statistical features such as mean intensity and region area. These features were then used as inputs for various machine learning models to classify disease severity levels. Model performance was evaluated using accuracy, precision, recall and F1-score.

Samples distribution

This study utilized 10 varieties of oil palm known as B124, B129, B114, B049, B050, B105, 8784, 8725, 8755 and 8809. Weekly inspections had been conducted throughout 10 weeks to observe the condition of ramets. Evaluation had been done by experts from FGV R&D Sdn. Bhd., and severity level had been classified according to the scoring technique, namely Score 1 and Score 2, by observing the presence of symptoms of BSR disease. The evaluation categorized the ramets based on BSR symptoms into six different classes: healthy (T0), early infection (T1), mild infection (T2), moderate infection (T3), high infection (T4), and severe infection (T5). Standardization had been made by limiting the sample numbers for each severity class. As for Score 1, the sample number was set to 284, while it was 363 for Score 2. Those numbers were chosen following the minimum sample size of T4. Thus, Score 1 had fewer samples compared to Score 2, with 1704 and 2178, respectively. The sample distribution of early evaluation for each severity level is tabulated in Table 1.

Table 1. Sample distribution on early evaluation

Severity Level	Category	Sample Numbers	
		Score 1	Score 2
T0	Healthy	284	363
T1	Early Infection	284	363
T2	Mild Infection	284	363
T3	Moderate Infection	284	363
T4	High Infection	284	363
T5	Severe Infection	284	363
Total		1704	2178

Once conducting classification as mentioned in Section 3.2, using the extracted features for both Score 1 and Score 2, the results revealed that more promising accuracy could be achieved by using Score 2 datasets.

Image acquisition

The setup for image acquisition is visualized as in Figure 1. The distance between the camera and a set of glass vessel holders containing ramets is fixed at about 7.5 cm. During the process, a blank white paper was placed at the back of the glass vessel holders to create background uniformity. Sample images were captured using the camera of a mobile phone with 12 MP and 4000 x 3000 resolution without applying flash. Front and back views for every set of samples were taken and will be used for image processing.

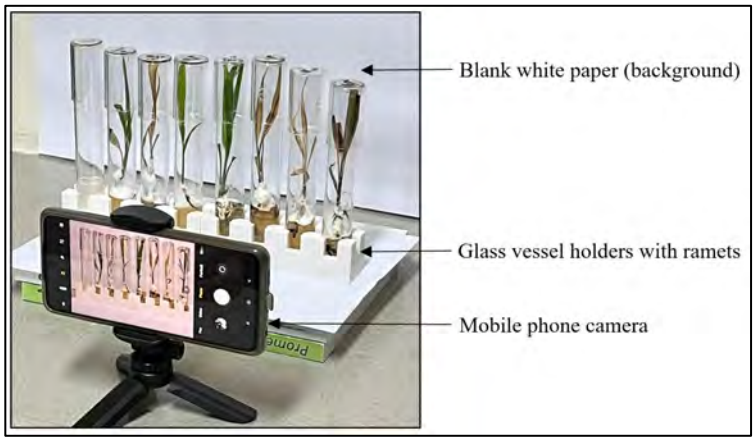

Figure 1. Image acquisition setup

Image processing

The captured images were stored and transferred into MATLAB software (Version R2022b, The Mathworks Inc., Massachusetts, United States) for the image processing step. Initially, every image was uploaded into the Image Segmenter Apps for the segmentation process to separate between sample from background. The generated binary image from segmentation had been standardized into a bitmap image file for further processing. The noise removal stage began with labelling each continuous region in a binary image before calculating the area of the labelled region using the 'regionprops' function. A threshold pixel value was set to isolate the regions and discard small areas prior generating a refined binary mask from selected regions for feature extraction. Subsequently, the original image in RGB format was converted to the Hue Saturation Value (HSV) colour space using the rgb2hsv function. This colour model promotes illumination robustness than RGB model as it separates chromatic content (Hue and Saturation) from luminance (Value). Each colour channel (H, S and V) was analysed independently. The extracted statistical features from those channels including mean intensity, maximum intensity, minimum intensity, and region area. The processed images were shown as in Figure 2.

Machine learning classification

The statistical feature of mean intensity and region area from HSV had been used as inputs for machine learning classifications. The classification had been executed by employing the Classification Learner App from the Statistics and Machine Learning Toolbox, which was available

in the MATLAB software (Version R2022b, The Mathworks Inc., Massachusetts, United States). A total of 29 classification models were trained and tested.

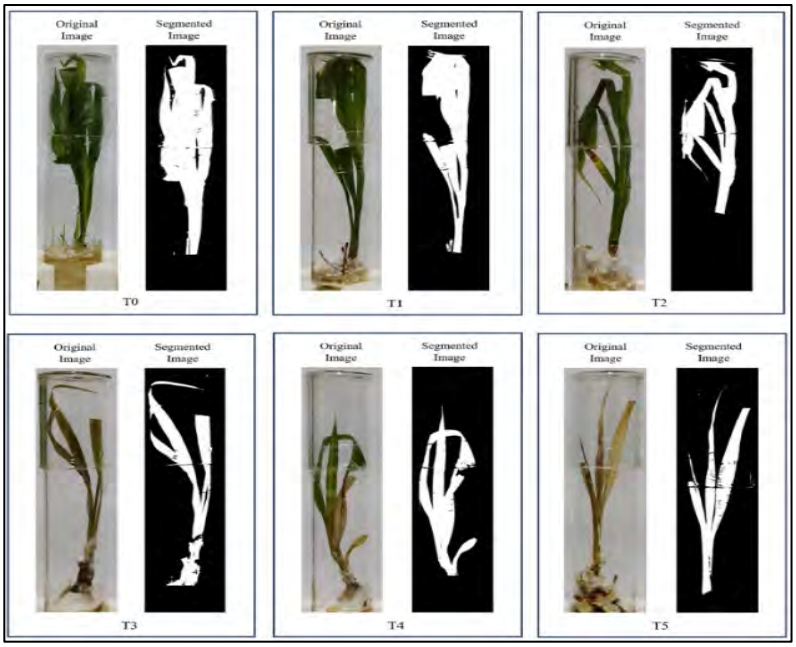

Figure 2. Sample of processed images for each severity level

The classification models' performance was consistently assessed using a 75:25 train-test data split and a 5-fold cross-validation technique. The 75:25 split was chosen to ensure that a substantial portion of the data (75%) is used for training the model, allowing it to learn the underlying patterns and features effectively. Meanwhile, the remaining 25% is reserved for testing, providing an unbiased evaluation of the model's generalization ability on unseen data. This ratio offers a balanced trade-off between learning and validation, particularly in datasets that are moderately sized.

The use of 5-fold cross-validation further enhances the reliability of the evaluation. In this approach, the dataset is divided into five equal subsets or "folds." The model is trained on four folds and tested on the remaining one, repeating the process five times so that each fold is used exactly once as the test set. This approach ensures that all data points are used for both training and validation, leading to a more robust and representative assessment of the classifier's performance.

Model performance evaluation

Once the classification results were obtained, the performance of the best model was evaluated using several key metrics: accuracy, precision, recall, and F1-score. The best model referred to the model with high classification accuracy and consistency of the results. These metrics were calculated individually for each severity level to provide a detailed assessment of the classifier's

ability to distinguish between the different classes. Precision measures the proportion of correctly predicted positive instances out of all instances predicted as positive, reflecting the model's ability to avoid false positives.

RESULTS AND DISCUSSION

Classification model

This research developed a total of 29 classification models using different types of kernels for each score type (Score 1 and Score 2) of each oil palm variety. Table 3 shows the results of accuracy during testing the classification model for Score 1 dataset using three split ratios.

Table 3. Accuracy of the models during testing for Score 1 dataset

Classification Model	Accuracy (%)		
	70:30	75:25	80:20
Fine Tree	46.58	44.37	48.25
Medium Tree	48.14	48.36	52.63
Coarse Tree	48.73	46.24	53.22
Linear Discriminant	34.83	39.2	41.81
Quadratic Discriminant	44.81	48.83	48.83
Gaussian Naïve Bayes	44.81	50.23	47.95
Kernel Naïve Bayes	48.92	50	50
Linear SVM	42.86	42.96	46.78
Quadratic SVM	46.18	47.18	50.58
Cubic SVM	49.12	50.47*	53.51*
Fine Gaussian SVM	46.97	49.06	48.83
Medium Gaussian SVM	43.05	46.24	45.03
Coarse Gaussian SVM	39.53	44.13	43.86
Fine KNN	34.05	46.01	47.37
Medium KNN	44.62	43.43	41.81
Coarse KNN	41.68	39.2	42.4
Cosine KNN	37.18	41.31	41.81
Cubic KNN	45.6	42.02	42.4
Weighted KNN	38.36	44.84	47.37
Ensemble Boosted Trees	50.1	50	52.92
Ensemble Bagged Trees	50.88*	48.59	50.29
Ensemble Subspace Discriminant	38.75	39.91	42.11
Ensemble Subspace KNN	22.11	28.64	17.25
Ensemble RUS Boosted Trees	50.68	48.12	52.34
Narrow Neural Network	50.49	49.06	51.46
Medium Neural Network	49.9	50.23	49.71
Wide Neural Network	48.14	46.24	47.37
Bilayered Neural Network	50.49	49.53	54.09
Trilayered Neural Network	50.49	48.12	50.88

*Note: The highest accuracy across columns

Based on Table 3, it was observed that the range of accuracy for all models is around 30% to 54% except for the Ensemble Subspace KNN that only managed to score between 17% to 29% using three different split ratios. As for Score 1 dataset, the Cubic SVM model performed better than others due to highest accuracy recorded using two different split ratios, 75:25 (50.47%) and 80:20

(53.51%). Table 4 portrays the results of testing classification model for Score 2 dataset using three split ratios.

Classification Model	Accuracy (%)		
	70:30	75:25	80:20
Fine Tree	73.05	72.98	73.1
Medium Tree	74.43	73.53	75.63
Coarse Tree	63.55	62.5	63.91
Linear Discriminant	61.41	63.42	61.84
Quadratic Discriminant	73.05	72.98	71.72
Gaussian Naïve Bayes	72.13	72.79	70.34
Kernel Naïve Bayes	71.36	73.71	73.33
Linear SVM	70.6	72.43	71.95
Quadratic SVM	75.19	75	74.94
Cubic SVM	75.34	75.92	72.41
Fine Gaussian SVM	68.91	73.16	72.64
Medium Gaussian SVM	73.97	72.98	72.41
Coarse Gaussian SVM	69.07	70.77	68.97
Fine KNN	66.31	65.07	64.37
Medium KNN	67.38	69.12	68.51
Coarse KNN	62.79	63.24	65.29
Cosine KNN	61.56	65.81	61.61
Cubic KNN	66.16	68.01	68.74
Weighted KNN	69.37	70.96	71.72
Ensemble Boosted Trees	76.11	75.37	75.86
Ensemble Bagged Trees	75.96	73.71	75.4
Ensemble Subspace Discriminant	60.34	63.79	60.92
Ensemble Subspace KNN	29.1	38.05	29.66
Ensemble RUS Boosted Trees	74.43	73.71	75.63
Narrow Neural Network	74.58	75.74	73.79
Medium Neural Network	77.49*	76.65*	71.26
Wide Neural Network	70.6	72.98	70.8
Bilayered Neural Network	75.34	75	76.09*
Trilayered Neural Network	72.74	71.69	71.49

*Note: The highest accuracy across columns

Based on Table 4, it was observed that classification models performed better by using Score 2 dataset as the accuracy was in the range approximately between 60% to 80% compared to Score 1 dataset. However, the Ensemble Subspace KNN model remained the poorest model as the accuracy ranged only between 29% to 38%. Even the Medium Neural Network model showed two best accuracy values using 70:30 and 75:25 ratios with 77.49% and 76.65%, respectively, the results seem less consistent where at 80:20, it dropped to 71.26%. Therefore, a more consistent model, which is Ensemble Boosted Trees, is chosen as the best model due to its better consistency performance with accuracy of 76.11%, 75.37% and 75.86%

Model performance evaluation

The results indicate that the model performs better in classifying six severity classes by applying Score 2 dataset. Hence, the model performance evaluation is done for the best model with consistent performance which is Ensemble Boosted Trees as shown in Table 5.

Table 5. Results of model performance evaluation for Ensemble Boosted Trees by using Score 2 dataset

Severity Class	Precision	Recall	F1-Score
T0	0.654	0.950	0.783
T1	0.718	0.699	0.708
T2	0.700	0.567	0.625
T3	1.0	1.0	1.0
T4	0.794	0.488	0.605
T5	0.745	0.964	0.840

Based on Table 5, it showed that the Ensemble Boosted Trees model demonstrated generally good performance in classifying six severity classes of oil palm in in vitro setup. The F1-score provides a balanced measure of the model's precision and recall, reflecting its overall classification performance across severity levels. The Ensemble Boosted Trees model achieved the highest F1-Score for T3 (1.000), indicating perfect prediction accuracy for this class. This suggests that the model was highly effective at recognizing and distinguishing T3 samples from others.

Severity levels of T5 (0.840) and T0 (0.783) also recorded relatively high F1-scores, showing that the model performed well in identifying both mild (T0) and severe (T5) conditions. These results imply that the distinguishing features for these classes are well captured by the model. A moderate F1-score was observed for T1 (0.708), suggesting acceptable but not optimal classification performance. Meanwhile, T2 (0.625) and T4 (0.605) showed the lowest F1-scores, indicating that the model struggled with these intermediate severity levels, possibly due to overlapping characteristics between adjacent classes or data imbalance.

Overall, the model performs best at the extreme severity levels (T0, T3, T5) and less effectively at intermediate levels (T2, T4), highlighting areas where feature refinement or data balancing could improve model robustness and class differentiation.

CONCLUSION

The developed machine vision system successfully demonstrated its capability in evaluating oil palm health levels under in vitro conditions infected by *Ganoderma boninense*. Among the tested classification models, the Ensemble Boosted Trees model achieved the most consistent performance using the Score 2 dataset, with F1-scores ranging from 0.605 to 1.000 across six severity levels. The highest F1-score (1.000) for class T3 indicates excellent model precision and recall at moderate infection severity, while high scores for T0 (0.783) and T5 (0.840) suggest reliable identification of healthy and severely infected samples.

However, lower F1-scores for T2 (0.625) and T4 (0.605) reveal that the model had difficulty distinguishing intermediate severity levels, likely due to overlapping visual characteristics and limited feature separation. To address this limitation, future work should consider combining adjacent severity levels (e.g., T1–T2 and T3–T4) to minimize misclassification and improve overall robustness. Expanding the dataset with a more balanced distribution and incorporating additional image features such as texture or multispectral information could also enhance model generalization. Overall, the findings confirm the feasibility of integrating machine vision and machine learning for automatic *G. boninense* infection evaluation. With further refinement, the proposed framework could serve as a foundation for developing a non-destructive, field-deployable diagnostic system to support sustainable oil palm disease management.

REFERENCES

[1] Azmi, A. N. N., Khairunniza-Bejo, S., Jahari, M., Muharram, F. M., & Yule, I. (2021). Identification of a Suitable Machine Learning Model for Detection of Asymptomatic *Ganoderma boninense* Infection in Oil Palm Seedlings Using Hyperspectral Data. *Applied Sciences*, *11*(24), 11798. https://doi.org/10.3390/app112411798

[2] Yong, L. Z., Khairunniza-Bejo, S., Jahari, M., & Muharam, F. M. (2023). Automatic Disease Detection of Basal Stem Rot Using Deep Learning and Hyperspectral Imaging. *Agriculture*, *13*(1), 69. https://doi.org/10.3390/agriculture13010069

Smart Farming for Cocoa: Monitoring Leaf Health Using Remote Sensing Technologies

S.N. Adam[1], Z. Khuzaimah[1], F.M. Taib[2], T.Y. Kheng[3], A.F. Mokhtar[1], H. Hashim[1], A.M. Mustafah[1] and S. Khairunniza-Bejo[1]

[1]Institute of Plantation Studies, Universiti Putra Malaysia, 43400 Serdang, Selangor, Malaysia
[2]FWF International Sdn. Bhd., Taman Melawati, Ulu Klang, 53100 Kuala Lumpur, Malaysia
[3]Malaysian Cocoa Board, Bagan Datuk, Perak, Malaysia
*Corresponding author: snadzah@upm.edu.my

***Keywords**: Cocoa, UAV, ground truthing, portable spectrometer, vegetation indices*

INTRODUCTION

The aerial nutrient mapping initiative was commissioned by the Malaysian Cocoa Board to support precision agriculture and sustainable cocoa cultivation in two strategic plantation sites: PPPK Bagan Datuk in Perak and PPPK Jengka in Pahang. Cocoa production in Malaysia is increasingly challenged by climate variability, soil degradation and labour constraints, creating an urgent need for spatially explicit information on crop condition and nutrient status to guide management decisions. Recent studies have shown how satellite and UAV remote sensing can be used to map cocoa agroforestry systems, classify cocoa stands and characterize climate and management variability in major cocoa regions [1–4].

In this project, Unmanned Aerial Vehicles (UAVs) equipped with optical and active remote sensing payloads were deployed to generate high-resolution geospatial datasets over both plantations. The airborne data included true-colour imagery for detailed mapping of field conditions and multispectral imagery for vegetation index and crop health assessment. These aerial products were designed to be compatible with standard geographic information system (GIS) platforms, enabling integration with existing plantation records.

To link the remotely sensed information with actual plant condition, ground-truth data were collected at both sites. For each location, selected cocoa trees were sampled for leaf-level spectral measurements. Due to logistical constraints, complete ground datasets were obtained only at PPPK Jengka, whereas PPPK Bagan Datuk contributed primarily leaf nutrient analysis. By combining UAV-based observations with field measurements, this study aims to establish a practical framework for monitoring cocoa health, optimising nutrient management and enhancing climate resilience in Malaysian cocoa plantations.

MATERIALS AND METHODS

Study sites

The study was conducted in two cocoa plantation schemes managed under the Malaysian Cocoa Board: PPPK Bagan Datuk (Perak) and PPPK Jengka (Pahang). Both sites consist of mature cocoa blocks under plantation management, but differ in terrain, field layout and management history, providing contrasting conditions for testing the proposed mapping workflow.

Aerial data acquisition and processing

UAV surveys were carried out over both plantations to acquire two main types of geospatial data: RGB imagery for producing high-resolution orthomosaics and visual interpretation of field conditions, and multispectral imagery for calculating vegetation indices (e.g. NDVI, NDRE and related indices) to indicate spatial patterns of crop vigor and potential stress [5]. Table 1 lists the multispectral camera band specifications, showing center wavelengths of 560, 650, 730 and 840 nm, with corresponding bandwidths of ±16 nm for the visible bands and ±26 nm for the near-infrared band.

Table 1. Multispectral camera band specifications

Band	Centre Wavelength ± Bandwidth (nm)
Green	560 ± 16
Red	650 ± 16
Red Edge	730 ± 16
Near-infrared (NIR)	840 ± 26

Ground-truth data collection

A total of 1,500 cocoa leaf samples were collected from 50 cocoa trees. Each tree contributed 30 leaves, comprising 10 leaves from the upper canopy, 10 from the middle, and 10 from the lower canopy. From these, nine representative leaves per tree (three from each canopy level) were selected for spectral measurements. Spectral reflectance data were acquired using the portable spectrometer, which operates in the 200–1200 nm wavelength range with an optical resolution of 0.05 nm. Measurements were taken under controlled dark room conditions using a halogen lamp as a constant light source. The probe was fixed at a 90° angle using a custom holder to maintain a consistent scanning distance. Each leaf was scanned at three different spots, and the average reflectance was used for analysis.

Vegetation indices

Vegetation indices (VIs) were computed from both sensors to evaluate their performance as nutrient indicators, using formulations that have been widely applied in UAV and proximal sensing studies for chlorophyll and nitrogen estimation [6–8]. Equations used in the study include:

- Normalized Difference Vegetation Index (NDVI) = (NIR − Red) / (NIR + Red)
- Green NDVI (GNDVI) = (NIR − Green) / (NIR + Green)
- Leaf Chlorophyll Index (LCI) = (NIR / RedEdge) − 1

- Normalized Difference Red Edge (NDRE) = (NIR − RedEdge) / (NIR + RedEdge)
- Optimized Soil-Adjusted Vegetation Index (OSAVI) = (NIR − Red) / (NIR + Red + 0.16)

RESULTS AND DISCUSSIONS

Among the vegetation indices evaluated, the Leaf Chlorophyll Index (LCI) demonstrated the strongest cross-platform agreement and lowest estimation error. This supports the role of the red-edge region as a reliable indicator of chlorophyll concentration, consistent with recent work highlighting red-edge and narrow-band indices for crop chlorophyll mapping [5,8]. Spectrometer-derived indices consistently exhibited higher sensitivity compared to UAV-based measurements, although UAV imagery offered wider spatial coverage. Together, they form a complementary data stream for precision nutrient monitoring in cocoa plantations, echoing findings from UAV/SPAD (Soil Plant Analysis Development) integration studies in fruit trees and maize [6,7].

Table 2: Statistical comparison of Vegetation Indices

Vegetation Index	Average Difference	Correlation	MAE	RMSE
NDVI	0.1674	-0.1658	0.1674	0.1836
GNDVI	0.0868	-0.1812	0.1029	0.1252
LCI	0.0231	-0.0882	0.0954	0.1164
NDRE	0.0963	-0.2092	0.1085	0.1298
OSAVI	0.1633	-0.1484	0.1670	0.1846

Table 2 summarizes the agreement between different vegetation indices and the reference nutrient or ground data using four statistics: average difference, correlation, mean absolute error (MAE) and root mean square error (RMSE). Overall, all indices show relatively small biases and errors, but their performance differs. LCI exhibits the lowest average difference (0.0231) and the smallest MAE and RMSE (0.0954 and 0.1164), indicating that it provides the closest numerical match to the reference values, although its correlation (-0.0882) is weak.

NDRE shows the strongest correlation in magnitude (-0.2092), suggesting it captures the directional variation in the reference data slightly better than the other indices, but with moderately higher errors. NDVI and OSAVI have the largest average differences and error metrics, implying poorer agreement, while GNDVI performs intermediately with lower errors than NDVI/OSAVI but weaker correlation than NDRE. The consistently negative correlation values indicate that higher index values are associated with lower reference measurements (or vice versa), and this inverse relationship should be considered when interpreting the maps.

CONCLUSIONS

This study successfully evaluated the consistency and reliability of five vegetation indices (NDVI, GNDVI, LCI, NDRE, OSAVI) derived from two different remote sensing platforms: the spectrometer and the multispectral camera. Through statistical comparison, LCI emerged as the most

consistent index across both systems, showing the lowest average difference, MAE, and RMSE, and the weakest negative correlation.

These findings highlight the importance of band matching and spectral resolution in cross-platform vegetation analysis. The results also support the use of LCI and NDRE as robust indicators for monitoring cocoa leaf health and nutrient status, particularly when high-resolution spectral data is available.

REFERENCES

[1] Lammoglia, S.-K., Akpa, Y. L., Danumah, J. H., Assoua Brou, Y. L., & Kassi, J. N. (2024). High-resolution multispectral and RGB dataset from UAV surveys of ten cocoa agroforestry typologies in Côte d'Ivoire. *Data in Brief, 55*, 110664. https://doi.org/10.1016/j.dib.2024.110664

[2] Moraiti, N., Mullissa, A., Rahn, E., Sassen, M., & Reiche, J. (2024). Critical assessment of cocoa classification with limited reference data: A study in Côte d'Ivoire and Ghana using Sentinel-2 and random forest model. *Remote Sensing, 16*(3), 598. https://doi.org/10.3390/rs16030598

[3] Cuellar-Escobar, L. F., & Henao-Céspedes, V. (2025). Remote sensing applied to cocoa crop identification: A thematic review. *International Journal of Electrical and Computer Engineering, 15*(5), 4848–4855. https://doi.org/10.11591/ijece.v15i5.pp4848–4855

[4] Atalaya-Marin, N., et al. (2025). Integrating remote sensing and in-situ data to determine climate diversity and variability in cocoa systems in the provinces of Jaén and San Ignacio, Cajamarca (NW Perú). *Climate Services, 37*, 100569.

[5] Mwinuka, P. R., Mourice, S. K., Mbungu, W. B., Mbilinyi, B. P., Tumbo, S. D., & Schmitter, P. (2022). UAV-based multispectral vegetation indices for assessing the interactive effects of water and nitrogen in irrigated horticultural crops production under tropical sub-humid conditions: A case of African eggplant. *Agricultural Water Management, 266*, 107516. https://doi.org/10.1016/j.agwat.2022.107516

[6] Huang, Y., Li, D., Liu, X., & Ren, Z. (2024). Monitoring canopy SPAD based on UAV and multispectral imaging over fruit tree growth stages and species. *Frontiers in Plant Science, 15*, 1435613. https://doi.org/10.3389/fpls.2024.1435613

[7] Ma, W., et al. (2024). UAV multispectral remote sensing for the estimation of SPAD values at various growth stages of maize under different irrigation levels. *Computers and Electronics in Agriculture, 227*, 109566. https://doi.org/10.1016/j.compag.2024.109566

[8] Li, X., Zhu, B., Li, S., Liu, L., Song, K., & Liu, J. (2025). A comprehensive review of crop chlorophyll mapping using remote sensing approaches: Achievements, limitations, and future perspectives. *Sensors*, *25*(8), 2345. https://doi.org/10.3390/s25082345

Spatial Risk Zoning for Oil Palm Replanting Using UAV Lidar and Topographic Wetness Index (TWI): A Case Study in Tradewinds Plantation Berhad, Malaysia

N.E Ramlan[1], Faris Y[1] and Pupathy U.T[1]

[1]Tradewinds Plantation Berhad (Research & Development), Ampang, Selangor

*Corresponding author: emifad.r@tpb.com.my

***Keywords**: LiDAR, replanting, terrain, topography wetness index (TWI), slope*

INTRODUCTION

Replanting oil palms is a crucial and costly technique that has a direct impact on productivity, sustainability, and long-term estate costs. When the climate and terrain change, traditional planning methods that rely on simple maps and studies by people often aren't accurate enough to handle water and land well. Recent advances in geospatial technology, particularly UAV-based LiDAR, have revolutionized estate replanting. LiDAR provides fast, high-resolution 3D topographical data on micro-topography, drainage patterns, and risk zones. This accuracy improves data-driven design, infrastructure architecture, and replanting hazards.

Topographic wetness index is defined as in equation (1)

$$TWI = ln[A\tan\beta] \qquad (1)$$

Where The slope angle (β) and catchment area (A) indicate the likelihood of water collection in each terrain cell. TWI and other hydrological indicators can help field planners enhance drainage and soil moisture balance using LiDAR-based Digital Terrain Models (DTMs). LiDAR topography modeling and hydrological analysis improve oil palm replanting design in this study. The approach promotes fact-based decision-making, risk management, and estate growth.

METHODOLOGY

Study area

The study was carried out over an area of 2,743 ha in Johor, Malaysia's Sisek Estate. A total of 663 ha in blocks P99A, 99B, 99C, 99D, and 00A will be replanted in the year 2025. Approximately 59% of the slopes in this region range from 6° to 28°, making it both steep and irregular. Terraces and roads become more difficult to construct in such an environment, and

traditional surveying methods fail to adequately reveal topography and elevation changes. Improved topography, better road and terrace design, reduced erosion risk, and assistance with sustainable replanting at Sisek Estate are all outcomes of this study's use of LiDAR-based terrain modeling and high-resolution hydrological analysis to address this issue.

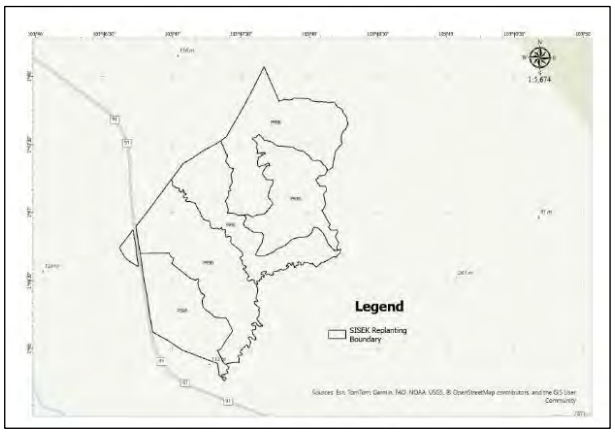

Figure 1. The map of the study area in Sisek, Johor

Acquiring LiDAR data

A DJI Matrice 300 UAV equipped with a LiDAR Z1 sensor was utilized in accordance with standard operating procedures for flight. Terrain-following flights were conducted at an altitude of 100 m AGL, with a 70% overlap in the frontal aspect and a 60% overlap laterally. The PPK method enhanced positioning accuracy, therefore eliminating the use for GCPs.

Data processing

DJI Pilot 2 was utilized for flight mission management, DJI Terra v4.4.0 for data processing, and ArcGIS Pro v3.5.1 for analysis pertaining to DEM creation and spatial evaluation. Figure 2 shows the flow process of this study.

RESULT & ANALYSIS

The elevation of the Sisek Replanting area shown in Figure 3 varies from 10.6 m to 106.6 m. In contrast, the northern and central zones are steeper and more susceptible to erosion, while the southern and southwestern zones are flatter and more susceptible to inundation. Most of the replanting area (approximately 59%) has moderate gradients ranging from 6° to 28°. Straight-line planting is permissible on gentle slopes (<12°) with minimal terracing, whereas areas with slopes exceeding 18° necessitate wider terraces and erosion control measures. In accordance with industry standards:

Zone 1 (<12°): Direct planting, negligible erosion risk
Zone 2 (12–18°): Requires minimal terracing; consistent monitoring is necessary
Zone 3 (>18°): It is advised to implement intensive terracing and erosion barriers

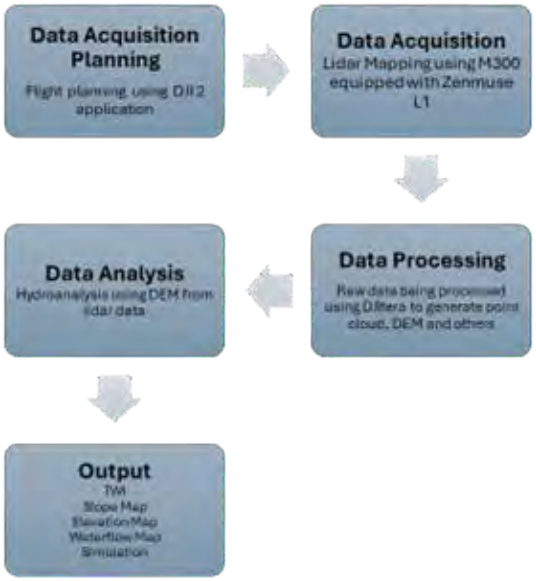

Figure 2. The flow of the methodology

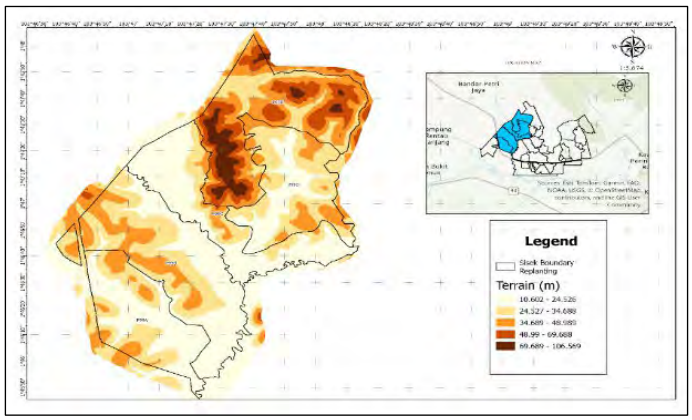

Figure 3. The elevation map for Sisek Estate

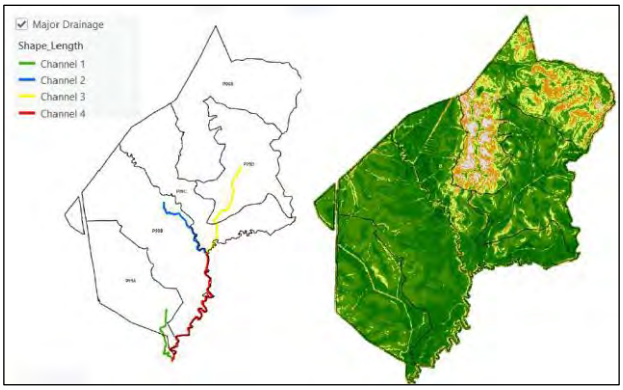

Figure 4. The channel distribution in replanting block Sisek

Figure 4 shows the location of the main channel. Four channels were identified, and the length of each channel is summarized in Table 1. The longest is the main channel (Channel 4), with a total length of 2.3 km, followed by Channel 3 at 1.5 km. The shortest is Channel 1, with a length of 889

m. Superimposing drainage channels with risk zones demonstrate that most drainage lengths are situated within high-risk locations as shown in table 2, signifying a considerable likelihood of water collection, floods, and waterlogging. Channel 4 possesses the most extensive high-risk length at 1,411 m, succeeded by Channels 3, 2, and 1. Extended wet conditions in these areas can obstruct access, harm soil, and diminish palm productivity.

Consequently, efficient drainage management and maintenance are essential. Estate initiatives must include channel expansion, capacity enhancements, and ongoing surveillance to avert waterlogging and facilitate robust oil palm replanting.

Table 1. The length of the channel in replanting block for Sisek Estate

Channel	Length (m)
1	889.8
2	1191.2
3	1597.8
4	2331.3

Table 2. The details of the risk for each channel

Channel	Risk	Length (m)
1	High	334.77
1	Medium	19.38
1	Low	38.80
2	High	1038.82
2	Medium	79.07
2	Low	73.29
3	High	1212.16
3	Medium	143.78
3	Low	123.91
4	High	1411.29
4	Medium	156.11
4	Low	160.68

CONCLUSIONS

These findings demonstrate that the integration of UAV-based LiDAR with spatial analysis efficiently facilitates replanting planning in regions characterized by difficult topography and water-related issues. Estate management must prioritize drainage maintenance, erosion control (such as broader terraces and early cover crops), and synchronizing replanting with infrastructure preparedness.

Nonetheless, constraints encompass the one-time data and restricted ground validation. Subsequent research ought to include multi-temporal data, field validation, and ongoing monitoring to enhance adaptability. This method offers a scalable framework for sustainable, data-driven replanting management.

REFERENCES

[1] Shafri, H., Ismail, M. H., Razi, M., Anuar, I., & Ahmad, A. (2012). Application of LiDAR and optical data for oil palm plantation management in Malaysia. *Proceedings of SPIE, 8526*, 852608. https://doi.org/10.1117/12.979631

[2] Wong, Y. B., Gibbins, C., Azhar, B., Phan, S. S., Scholefield, P., Azmi, R., & Lechner, A. M. (2023). Smallholder oil palm plantation sustainability assessment using multi-criteria analysis and unmanned aerial vehicles. *Environmental Monitoring and Assessment, 195*(5), 577. https://doi.org/10.1007/s10661-023-11113-z

[3] Bretreger, D., Yeo, I.-Y., & Melchers, R. (2021). Terrain wetness indices derived from LiDAR to inform soil moisture and corrosion potential for underground infrastructure. *Science of the Total Environment, 756*, 144138.

[4] Winzeler, H. E., Owens, P. R., Read, Q. D., Libohova, Z., Ashworth, A., & Sauer, T. (2022). Topographic wetness index as a proxy for soil moisture in a hillslope catena: Flow algorithms and map generalization. *Land, 11*, 2018. https://doi.org/10.3390/land11112018

Effect of Golden Apple Snail (GAS) Foliar Biofertilizer Dilution on Leaf Burn Symptoms in Glutinous Rice

N. Abdullah[1,3], N.M. Nawi[1,2], S.R.M. Lazim[2] and N.N.A.R Ismail[1]

[1]Department of Agriculture and Biosystem Engineering, Faculty of Engineering, Universiti Putra Malaysia, 43400, UPM Serdang, Selangor, Malaysia
[2]Institute of Plantation Studies, Universiti Putra Malaysia, 43400, UPM Serdang, Selangor, Malaysia
[3]School of Information and Physical Sciences (Computing and Information Technology), University of Newcastle, Callaghan, NSW 2308, Australia
*Corresponding author: nazmimat@upm.edu.my

***Keywords**: GAS foliar biofertilizer, leaf burn, chlorosis, glutinous rice*

INTRODUCTION

Glutinous rice is defined by its small grain size, which differentiates it from regular white rice. This type of rice is generally referred to as ‘sticky rice’ or ‘waxy rice’, and it is characterized by having a smaller grain size than standard white rice [1]. The increasing demand for glutinous rice among consumers highlights its potential as a profitable crop, leading to a thorough study of sustainability strategies. Therefore, the application of fertilizers to enhance glutinous rice production is essential for increasing yield and sustaining market demand.

Comprehensive studies have demonstrated that applying organic fertilizer to leaves can reduce the total amount of chemical fertilizer used and achieve higher fertilizer efficiency. Considering the advantages of organic foliar fertilization, supplying nutrient elements via foliage fertilization is a good strategy and the trend toward foliar spray application is increasing. Foliar fertilization strategies can achieve higher nutrient use efficiency, reduce the negative impact on the environment, and potentially enhance consumer health benefits [2-3]. Foliar fertilization serves as an alternative method in paddy cultivation, involving the direct spraying of liquid fertilizer onto the leaves [4]. However, due to the comparatively low nutrient content of organic fertilizer, they may not be enough to meet the plant’s needs. Therefore, the application of organic fertilizer integrated with chemical fertilizer increases microbial activity, nutrient usage efficiency, and the availability of native nutrients to plants, resulting in increased nutrient uptake [5].

It should be noted; foliar sprays typically utilize macronutrient concentrations of less than 2% to prevent leaf burn or chlorosis. Therefore, applying organic liquid in excessive quantities without accurate rate assessment may fail to meet the nutritional demands of the rice plant in the field.

However, no one has studied the effect of golden apple snail (GAS) foliar biofertilizer on the crop. Some negative effects of foliar fertilizing have been reported [6], like "foliar burn" or chlorosis on the leaf. As a result, this research objective is to investigate the right dilution of GAS foliar biofertilizer to be applied to minimize the chlorosis symptoms on the glutinous rice leaves. Furthermore, to study the effect of the right concentration of foliar GAS fertilizer integrated with chemical fertilizer on chlorophyll content in glutinous rice, which can later enhance the overall health of the rice plant and produce a better yield.

MATERIALS AND METHODS

The soil was collected from a paddy field, located at Kelantan, Malaysia. Each experimental pot was filled with 12.0 kg of soil. Each pot was saturated with tap water for 10 days and drained to an equilibrium state. Glutinous rice seeds were soaked in water for 24 hours [7] before being placed in the seed tray until germination. The seedlings were planted in a tray, and the germinated seeds were sown until germination for 14 days. The peat moist was used as a medium for the germination process. 90 pots with 6 treatments of GAS foliar biofertilizer (i.e., control and five different concentrations (200, 400, 600, 800, 1000) mL L^{-1} of GAS foliar biofertilizer. The experimental setup followed a random complete block design (RCBD) with three replications per treatment in a net house. This is to ensure the reliability and reproducibility of the results across varying experimental conditions [5].

Fertilizer application

There were four fertilization stages in this experiment. The different chemical fertilizer (CF) application rates were calculated based on the recommended dosage for each of the four fertilization stages, as shown in Table 1. The CF amount was adjusted according to the pot area. The GAS foliar biofertilizer was diluted to (800, 600, 400, and 200) mL L^{-1} per liter of distilled water and sprayed to run-off on each pot in the morning. At the vegetative stage, the GAS foliar biofertilizer (200, 400, 600, 800, and 1000) mL L^{-1} was applied by spraying 1 L per treatment onto the glutinous rice leaves. This application was integrated with the recommended chemical fertilizer (17.5 N: 15.5 P_2O_5: 10 K_2O) at 140 kg/ha, equivalent to 0.8 g per pot, which was broadcast onto the soil during the first fertilization in week 1 after planting (1 DAT).

The second fertilization occurred at the active reproductive stage (week 4 DAT), where 2 L of GAS foliar biofertilizer was applied together with urea (46% N) at 0.46 g per pot, equivalent to 80 kg/ha. At the stem formation (panicle) stage in week 8 DAT, 2 L of GAS foliar biofertilizer (200, 400, 600, 800, and 1000) mL L^{-1}, integrated with chemical fertilizers, was applied. An additional 0.57 g per pot of 17.5 N: 15.5 P_2O_5: 10 K_2O (100 kg/ha) and 0.57 g per pot of 17.5 N: 3.0 P_2O_5: 25 K_2O + MgO (100 kg/ha) were incorporated by applying them to the leaf surface and soil. The final fertilization occurred during the heading stage in week 11 DAT, where 2 L of GAS foliar biofertilizer was sprayed onto the leaves followed by 0.25 g per pot of 17.5 N: 3.0 P_2O_5: 25 K_2O + MgO (equivalent to 50 kg/ha) broadcast onto the soil. Then, effect of GAS foliar biofertilizer on leaves were measured using a ruler. A 10-cm segment from each leaf was measured, and the

chlorosis level of the leaf was subsequently evaluated.

Table 1: Application of chemical fertilizer based on recommendation rate

Fertilization cycle	Maturity period >155 Days after transplanting (DAT)	Growth stage	Type of fertilizer	Fertilizer rate (kg/ha)	Amount of chemical fertilizer (g)/pot	Quantity of GAS foliar biofertilizer (mL L^{-1})/ fertilization					
						Control	200	400	600	800	1000
First fertilzation	5-7	Vegetative (3-leaf stage)	Chemical fertilizer (17:20:10)	140	0.8	-	1	1	1	1	1
Second fertilization	25 - 30	Active Tillering	Urea (46% N)	80	0.46	-	2	2	2	2	2
Third fertilization	55 - 60	Panicle Initiation	Chemical fertilizer (17:20:10)	100	0.57	-	2	2	2	2	2
			Additional Chemical fertilizer (17:3:25+2 MgO)	100	0.57						
Fourth fertilization	75 - 80	Heading and Flowering	Additional Chemical fertilizer (17:3:25+2 MgO)	50	0.29	-	2	2	2	2	2

RESULTS AND DISCUSSIONS

Chlorosis effect on paddy leaves

In this study, the leaves displayed varying degrees of chlorosis affected by different dilutions of GAS foliar biofertilizer. The circumstances are visually presented in Table 2 in this study to detect chlorosis on the glutinous rice leaves. Inadequate nutrition supply could result in chlorosis conditions on leaves, as chlorosis was an indicator of the plant failing to produce the normal quantity of chlorophyll required to support the production of food via photosynthesis.

Applying various dilutions of GAS foliar biofertilizer to leaves showed different percentages of "burn" effects on leaves. The highest concentration of GAS on glutinous rice leaves was 1000 mL L^{-1} causing 85% burn for certain leaves area. The leaves have shown that GAS foliar biofertilizer affected 61% and 35% of the burning symptoms for 800 mL L^{-1} and 600 mL L^{-1}, respectively such as in Table 3. The minimal effect of discoloration on glutinous rice leaves was 10% and 5% for GAS foliar biofertilizer concentrations of 400 mL L^{-1} and 200 mL L^{-1}, respectively. Leaf burn on the plant can be observed after spraying the foliar fertilizer which could indicate high dosage of fertilizer rates used. To avoid burning, lower concentration is usually recommended [8].

No significant differences across the treatments were found in the GAS foliar biofertilizer in glutinous rice leaf, and slightly higher than the control treatment. However, higher concentrations of GAS foliar biofertilizer (1000 mL L^{-1} L^{-1}) caused more severe leaf burn, likely due to the elevated calcium content in the concentration, which can induce phytotoxicity at excessive levels. Therefore, 200 mL L^{-1} and 400 mL L^{-1} were optimum concentrations of GAS foliar biofertilizer for glutinous rice can be applied. Understanding the exact amount of nutrients required by the plant

prior to fertilizer application is essential for avoiding leaf burn incidents caused by inappropriate fertilizer rate application to the plant [9].

Table 2. Chlorosis severity of glutinous rice leaves at different GAS foliar biofertilizer concentrations

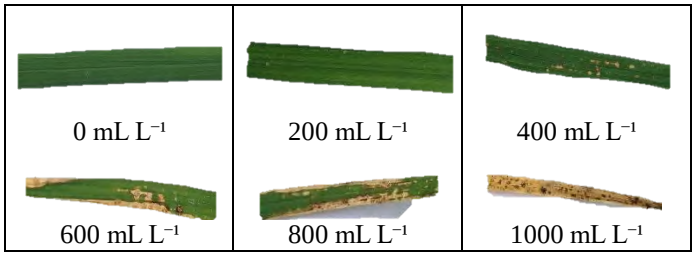

Table 3. Chlorosis severity of glutinous rice leaf treatments versus percentage of leaf burn

GAS foliar biofertilizer Concentration (mL L^{-1})	Chlorosis severity (%)
1000	85
800	61
600	35
400	10
200	5

CONCLUSION

The spraying of foliar fertilizers is a fast, efficient, and targeted fertilization method, which can be combined with soil fertilization to reduce the use of chemical fertilizer and soil salinity accumulation. To maximize the effects of foliar nutrition, attention should be paid to the timing and dilution of the foliar fertilizer to optimum the absorption of foliar through the stomata and avoid the leaf being burned. GAS foliar fertilizer can be safely applied to glutinous rice when diluted to 200–400 mL L^{-1}, with only 5–10% leaf burn observed, whereas higher concentrations up to 1000 mL L^{-1} cause up to 85% chlorosis. Optimizing dilution and timing of GAS foliar fertilizer is essential to avoid leaf damage while benefiting from foliar nutrition for glutinous rice leaves. No significant differences across the treatments were found in the GAS foliar biofertilizer in glutinous rice leaf and minimally slightly high with the control treatment. Further work should quantify effects on chlorophyll (SPAD), yield, and develop NIR–machine learning models for early detection of chlorosis or nutrient status.

REFERENCES

[1] Zainal, N., and Shamsudin, R. (2021). Physical properties of different cultivar local glutinous rice (Susu and Siding) and commercial Thai cultivar. *Advances in Agricultural and Food Research Journal*, 2(1), a0000178. https://doi.org/10.36877/aafrj.a0000178

[2] Otálora, G., Piñero, M. C., López-Marín, J., Varó, P., & del Amor, F. M. (2018). Effects of foliar nitrogen fertilization on the phenolic, mineral, and amino acid composition of escarole

(*Cichorium endivia* L. var. *latifolium*). *Scientia Horticulturae,* 239, 87–92. https://doi.org/10.1016/j.scienta.2018.05.031

[3] Niu, J., Liu, C., Huang, M., Liu, K., & Yan, D. (2021). Effects of foliar fertilization: A review of current status and future perspectives. *Journal of Soil Science and Plant Nutrition*, 21(1), 104–118. https://doi.org/10.1007/s42729-020-00346-3

[4] Alam, M. Z., Sadekuzzaman, M., Sarker, S., & Hafiz, M. H. R. (2015). Reducing soil application of nitrogenous fertilizer as influenced by liquid fertilization on yield and yield traits of Kataribhog rice. *International Journal of Agronomy and Agricultural Research*, 6(1), 63–69.

[5] Anisuzzaman, M., Rafii, M. Y., Jaafar, N. M., Izan, S. R., Ikbal, M. F., & Haque, M. A. (2021). Effect of organic and inorganic fertilizer on the growth and yield components of traditional and improved rice (*Oryza sativa* L.) genotypes in Malaysia. *Agronomy*, 11(9), 1830. https://doi.org/10.3390/agronomy11091830

[6] Phillips, S. B., & Mullins, G. L. (2004). Foliar burn and wheat grain yield responses following topdress-applied nitrogen and sulfur fertilizers. *Journal of Plant Nutrition*, 27(5), 921–930.

[7] Lakitan, B., Jaya, K. K., Ria, R. P., & Morianto, B. (2020). The effects of different NPK fertilization rates and water regimes on ratooned black glutinous rice. *CMU Journal of Natural Sciences*, 19, 350–365.

[8] Krishnasree, R., Raj, S. K., & Chacko, S. R. (2021). Foliar nutrition in vegetables: A review. *Journal of Pharmacognosy and Phytochemistry*, 10(1), 2393–2398. https://doi.org/10.22271/phyto.2021.v10.i1ah.13716

[9] Muhammad, M. N., Wayayok, A., Abdullah, A. F., & Mohamed Shariff, A. R. (2023). Variable rate inorganic foliar fertilization effect on paddy leaves chlorosis, plant growth and yield performance. *Journal of Plant Nutrition*, 46(6), 877–887. https://doi.org/10.1080/01904167.2022.2144363

Soil Microbial Communities Profiling Indicates No Significant Difference Among Genetically Modified (GM) and Non-GM Oil Palms

O.A. Rasid*, F.H. Lim, A.M.Y. Masani, T.M.M Shawal and G.K.A. Parveez

Malaysia palm Oil Board, 6, Persiaran Institusi, Bandar Baru Bangi,
Kajang 43000, Selangor, Malaysia
*Corresponding author: omar@mpob.gov.my

***Keywords**: Metagenomics, oil palm, genetically modified, contained field trial*

INTRODUCTION

Microorganisms in the soil are important to maintain the soil function due to their essential role in soil structure formation, decomposition of organic matter, toxin removal and the cycling of carbon, nitrogen, phosphorus and sulfur [1] as well as suppressing soilborne plant diseases to promote plant growth [2]. Assessing the impact of genetically modified (GM) crops on soil microbial communities is essential for environmental biosafety evaluation. GM oil palms have been produced and planted in a biosafety screenhouse for a contained field trial and assessment of the functionality of the transgenes. Due to the critical roles of soil microorganisms, it is important to evaluate any possible consequences of GM palms to the environment, i.e. the soil microbial community. The possibility of GM plants affecting the surrounding soil microbiomes has been documented in several studies [3]. However, the changes of the soil microbial communities associated with GM plants are usually transient, inconsistent, or indistinguishable from natural soil variations. The findings suggest that GM crops do not pose a significant risk to soil health when compared to other factors like weather and soil type.

The studies on effects of GM crops on the soil microbial communities have been discussed. For example, GM crops have encouraged the widespread use of conservation tillage, in which crops are planted directly into the soil without prior ploughing. This approach helps protect soil microbial communities, preserves soil moisture, and enhances soil carbon retention [4]. However, GM crops may potentially become invasive over time, posing a risk to local wild crop populations. In addition, the reliance on specific chemical herbicides for managing weeds in fields planted with herbicide-tolerant GM crops can drive the emergence of highly resistant weed species that are increasingly difficult to control. The intensified use of these chemicals to manage resistant weeds may further contribute to soil and water degradation; hence affecting the soil microbial communities as well [5].

This study aimed to compare the soil bacterial populations between the GM and control palms

(within and outside the screenhouse) using a metagenomics approach. Soil samples from selected palms have been obtained for soil total DNA extraction. Amplification of the 16S rRNA gene was performed and the V3-V4 region of the 16S rRNA gene was sequenced. The microbial community structure of each soil sample was compared based on the 16S rRNA gene data generated from the amplicon sequencing [6]. The findings of this study provide an important reference for confined field trial or commercial planting of GM palms in future.

MATERIALS AND METHODS

Soil sample collection

A total of 6 GM (Oleic trait: 3 palms; Biodegradable plastic trait: 3 palms) and 3 non-GM (control) oil palms in the screenhouse together with 3 oil palms outside the screenhouse were selected. By using an auger, the soil samples from 15cm in depth were collected and placed in falcon tubes. The soil samples were brought back to laboratory for total DNA extraction.

Total genomic DNA extraction and purification

MOBIO kit (QIAGEN, Germany) was used for soil DNA extraction with some modification on the extraction protocols. Total DNA extractions were performed for each soil sample. The quality and quantity of DNA samples were determined by Nanodrop spectrophotometry and gel electrophoresis.

PCR amplification for 16S rRNA gene

All the purified DNA samples were subjected to PCR amplification of the 16S rRNA gene to ensure that the target gene could be amplified from all the DNA samples. A primer pair, 1392R (5’-GGTTACCTTGTTACGACTT-3’) and 27F (5’-AGAGTTTGATCCTGGCTCAG-3’) was used to amplify the 16s rRNA gene. After amplification, the PCR products were separated by gel electrophoresis and purified.

16S rRNA amplicon sequencing and data statistical Analysis

The 36 soil DNA samples were sent for Amplicon Sequencing targeting the V3-V4 region of the 16S rRNA gene. The sequencing forward primer, 5’CCT ACG GGN GGC WGC AG and reverse primer 5’ GAC TAC HVG GGT ATC TAA TCC were used, and the amplicons were sequenced using the MiSeq platform. After the quality accessment procedure, the reads were clustered de novo into OTUs at 97% similarity using UPARSE v11.0.667. A single representative sequence from each OTU is selected randomly and Pynast was used for OTU alignment and construction of a phylogenetic tree against the SILVA 132 16S rRNA database. Taxonomic assignment of OTU was performed using QIIME V1.9.1 against the Silva database 16S rRNA database (release 132). The Statistic analysis was performed in R package V3.6.1.

RESULTS AND DISCUSSION

PCR amplification of the 16S rRNA gene from the soil DNA samples was carried out and an expected size of 1.5 kb PCR product was successfully amplified from each sample (Figure 1). The

PCR products were excised, purified and sent for sequencing of v3-v4 regions of 16S rDNA gene.

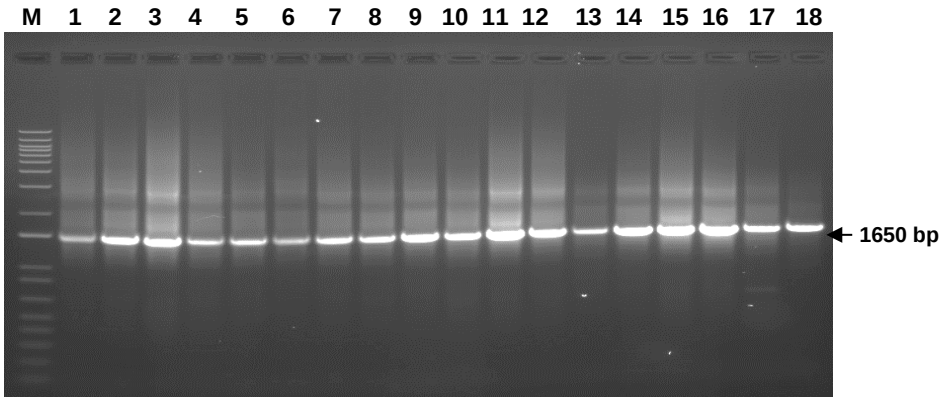

Figure 1. PCR amplification of the 16S rRNA gene

Sequencing yielded 2,280,919 reads, clustered into 65,788 operational taxonomic units (OTUs) at 97% similarity using de novo UPARSE clustering. Alpha-diversity analysis showed high species richness across most samples, with *Proteobacteria* (29.3%), *Acidobacteria* (20.7%), *Actinobacteria* (18.9%), *Chloroflexi* (14.5%), and *Planctomycetes* (4.8%) being the dominant bacterial phyla (Figure 2). Genus-level analysis revealed *Acidothermus*, *Acidibacter*, and *Candidatus Solibacter* as top contributors (Figure 3). The top abundant bacteria at phylum and genus levels in and outside the screenhouse are like the bacterial composition observed in previous reports of soil bacteria study in Malaysia [7].

The Proteobacteria phylum mainly consists of gram-negative bacteria and bacteria that are responsible for nitrogen fixation which are important in soil. The bacterial species under this phylum include *Acidibacter* (the second most abundant genus in soil samples) and *Chujaibacter*. The second abundant phylum is acidobacteria which contains many acidophilic bacteria which are relevant to the acidity pH of the analyzed soil samples (pH 3 to 5) collected from the screenhouse and plantation. The bacteria from the *Acidothermus* genus were found to be the most abundant genus across all the collected soil samples. The bacteria under this genus are heterotrophic, thermophilic and cellulolytic which usually grow in the soil at 37-65°C and pH around 3.5 to 7.

Based on the Venn diagram, the total number of OTU for high oleic, biodegradable plastic, control (Screenhouse) and outdoor control groups is 4,275, 5,116, 6,316 and 4,677, respectively (Figure 4). Majority of the OTUs co-exist in more than 2 groups. A total of 2,449 OTUs were present in all sample groups (both transgenic and control groups).

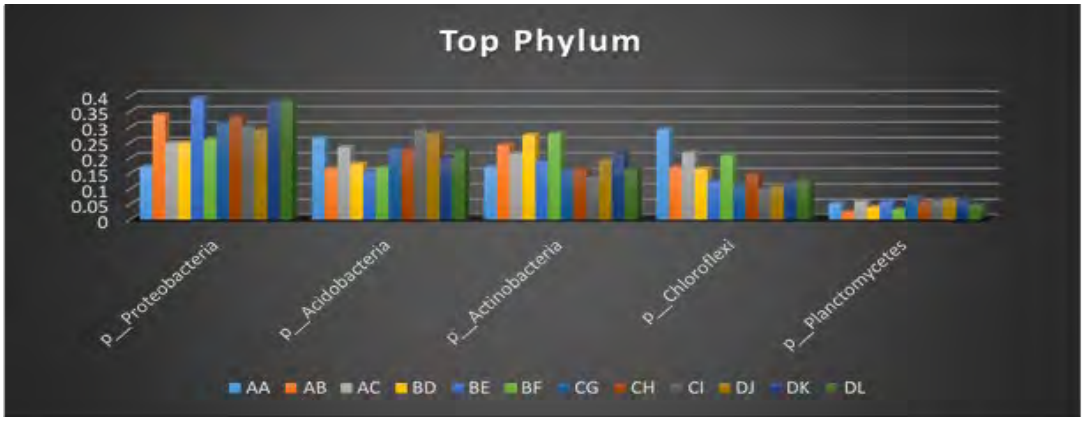

Figure 2. Top 5 most abundant bacterial phylum in the soil samples collected from different oil palms. AA-AC - High Oleic; BD-BF - Biodegradable Plastic; CG-CI - Control (Screenhouse); DJ-DL - Outdoor control

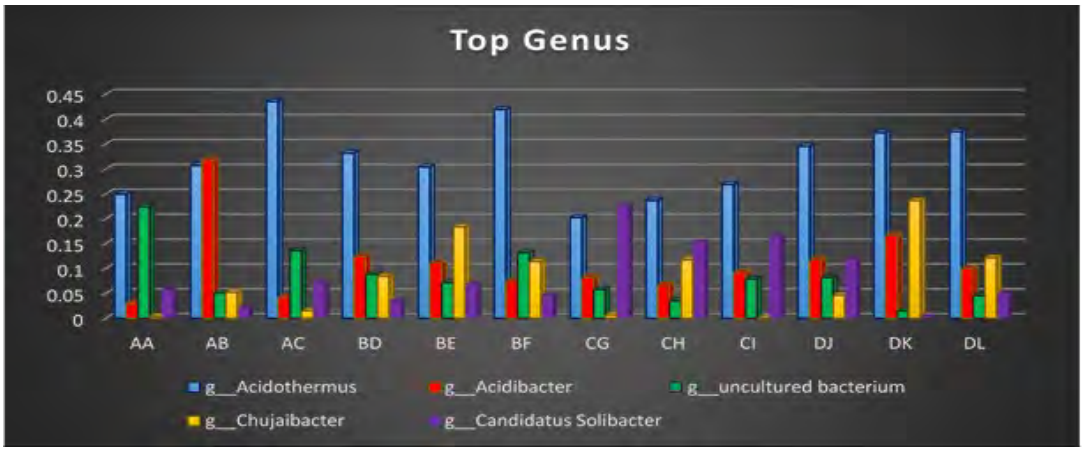

Figure 3. Top 5 most abundant bacterial genus in the soil samples collected from different oil palms. AA-AC - High Oleic; BD-BF - Biodegradable Plastic; CG-CI - Control (Screenhouse); DJ-DL - Outdoor control

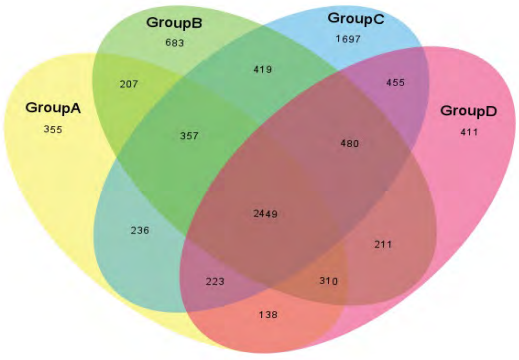

Figure 4. Venn diagram showing the distribution of OTUs across the sample groups. Group A - High Oleic; B - Biodegradable Plastic; C - Control (Screenhouse); D - Outdoor control

CONCLUSION

This study evaluated the soil microbial populations in transgenic and non-transgenic oil palms. The results clearly indicated that the bacterial abundance is relatively similar between transgenic and non-transgenic samples at the Phylum and Genus levels. Nevertheless, slight differences in the abundance were observed at the Genus level between transgenic and non-transgenic samples. This may be caused by several different factors including soil pH and temperature.

REFERENCES

[1] Wang, X., Chi, Y., & Song, S. (2024). Important soil microbiota's effects on plants and soils: A comprehensive 30-year systematic literature review. *Frontiers in Microbiology, 15*, 1347745. https://doi.org/10.3389/fmicb.2024.1347745

[2] Amoo, A. E., Olanrewaju, O. S., Babalola, O. O., Ajilogba, C. F., Chukwuneme, C. F., Ojuederie, O. B., & Omomowo, O. I. (2023). The functionality of plant–microbe interactions in disease suppression. *Journal of King Saud University – Science, 35*(8), 102893. https://doi.org/10.1016/j.jksus.2023.102893

[3] Li, Z., Cui, J., Mi, Z., Tian, D., Wang, J., Ma, Z., Wang, B., Chen, H., & Niu, S. (2019). Responses of soil enzymatic activities to transgenic *Bacillus thuringiensis* (Bt) crops: A global meta-analysis. *Science of the Total Environment, 651*(2), 1830–1838.

[4] Abdul Aziz, M., Brini, F., Rouached, H., & Masmoudi, K. (2022). Genetically engineered crops for sustainably enhanced food production systems. *Frontiers in Plant Science, 13*, 1027828.
[5] Sharma, P., Singh, S., Iqbal, H., Parra-Saldivar, R., Varjani, S., & Tong, Y. (2022). Genetic modifications associated with sustainability aspects for sustainable developments. *Bioengineered, 13*(4), 9508–9520.

[6] Klindworth, A., Pruesse, E., Schweer, T., et al. (2013). Evaluation of general 16S ribosomal RNA gene PCR primers for classical and next-generation sequencing-based diversity studies. *Nucleic Acids Research, 41*(1), e1. https://doi.org/10.1093/nar/gks808

[7] Miyashita, N. T., Iwanaga, H., Charles, S., Diway, B., Sabang, J., & Chong, L. (2013). Soil bacterial community structure in five tropical forests in Malaysia and one temperate forest in Japan revealed by pyrosequencing analyses of 16S rRNA gene sequence variation. *Genes & Genetic Systems, 88*(2), 93–103. https://doi.org/10.1266/ggs.88.93

Plantation Studies Volume 2, 2025—Proceedings of the 3rd International Conference on Plantation Technology (ICPTech2025)

e ISBN 978-629-95253-1-8

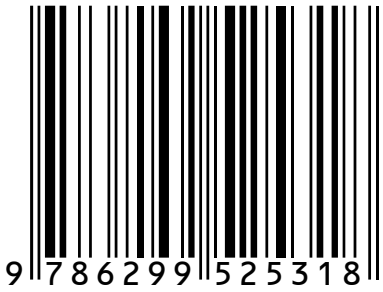

Institut Kajian Perladangan

(online)